5-2013

The Identification of the Mid Transcription Factor Regulatory Network Specifying Cell Fate and Regulating Survival in the *Drosophila* Eye

Sudeshna Das
University of Southern Mississippi

The University of Southern Mississippi

THE IDENTIFICATION OF THE MID TRANSCRIPTION FACTOR REGULATORY NETWORK SPECIFYING CELL FATE AND REGULATING SURVIVAL IN THE *DROSOPHILA* EYE

by

Sudeshna Das

A Thesis
Submitted to the Graduate School
of The University of Southern Mississippi
in Partial Fulfillment of the Requirements
for the Degree of Master of Science

Approved:

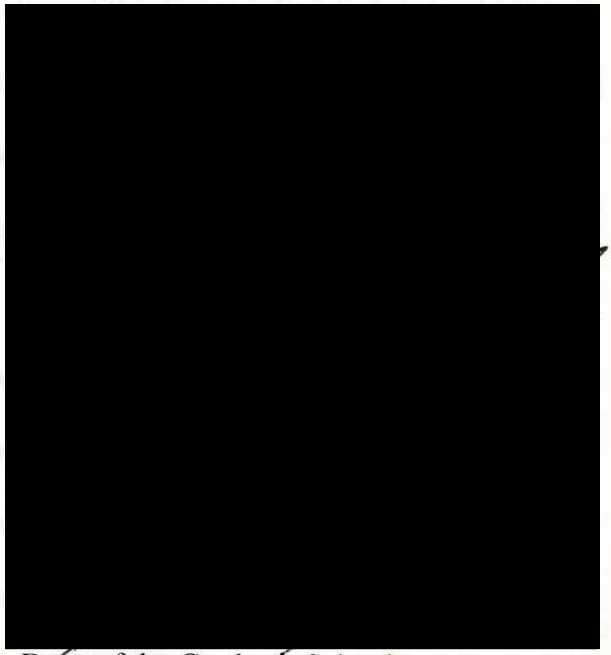

Dean of the Graduate School

May 2013

ABSTRACT

THE IDENTIFICATION OF THE MID TRANSCRIPTION FACTOR REGULATORY NETWORK SPECIFYING CELL FATE AND REGULATING SURVIVAL IN THE *DROSOPHILA* EYE

by Sudeshna Das

May 2013

The *Drosophila melanogaster* T-box transcription factor Midline (Mid) exhibits a high degree of structural and functional conservation with its vertebrate homolog Tbx-20. Both Mid and Tbx-20 regulate cell-fate specification within diverse tissues including the central nervous system (CNS) and heart. Although, some important studies reported that *Tbx-20* transcripts express in a wide range of developing mammalian eye tissues including those of the human fetus, the function of this transcription factor is unknown in the development of eye tissue. This current study is the first attempt to show that Mid and its paralog H15 are expressed within distinct ommatidial cell types including photoreceptor neurons and sensory organ precursor (SOP) cells during early stages of pupal eye imaginal disc morphogensis and also identifies a Mid transcription factor network regulating eye development. Reducing the expression of *mid* transcripts within eye disc tissues using RNA interference (*mid-RNAi*) results in the loss of interommatidial bristles (IOBs) in the adult eye due to the misspecification of sensory organ precursor (SOP) cells and increased levels of apoptosis induced during earlier stages of pupal development. Since the Notch-Delta signaling pathway specifies the SOP cell fate, we sought to place *mid* within the Notch-Delta genetic hierarchy specifying SOP cell fates.

We determined that Mid functions downstream of the Notch receptor and upstream of the *Enhancer of Split gene complex* [*E(Spl)*]. We also discovered *mid* collaborates with two Notch pathway members also implicated in the regulation of cell survival, *extramacrochaetae* (*emc*) and *senseless* (*sens*). Moreover, toward identifying the Mid regulatory transcription factor network specifying cell fate, we found that *mid* collaborates with *dFOXO.* The dFOXO transcription factor is distinct in that it regulates cell proliferation and homeostasis within Insulin regulated stress induced pathway. The culmination of these studies suggests that Mid regulates cell fate specification in collaboration with Notch-Delta signaling pathway and also play important role in cell survival pathways essential for maintaining homeostasis.

ACKNOWLEDGMENTS

I would like to express my gratitude to Dr. Sandra Leal for her continuous support and guidance that helped me to fulfill my studies. Most importantly, I am grateful for the opportunities she offered me to learn and experience science. I benefited from the unconditional help of my colleagues Deepak Kumar, Brandon Drescher, Brent Chen, Joseph Saucier and Randy Toranzo from bench work to improve my writing skill. I am thankful to my committee members Dr. Glenmore Shearer, Dr. Janis O'Donnel, Dr. Yanlin Guo and Dr. Anthony Bell for their helpful suggestions in completion of my thesis projects. I want to thank Baobin Kang for her efforts to teach me confocal microscopy and Dr. Andreas Plagge from Polymer Science Department for teaching me scanning electron microscopy. I want to acknowledge Dr. Graeme Mardon for his helpful recommendations on the dissection and fixation of pupal eye imaginal discs and David Marenda for providing anti-Atonal Antibody, Dr. James Skeath for providing anti-Numb antibody and Dr.Teresa Orenic for providing a supply of anti-Ac monoclonal antibody. I am thankful to Dr. Yuh Nung Jan for anti-Emc antibody and also to Dr. Hugo Bellon for anti-Sens antibody. In addition, I would like to acknowledge Rolf Bodmer, Li Qian, William Brooks, James Skeath, Tanya Wolff and the Bloomington Stock Center (Bloomington, IN) for fly stocks, without these resources my studies would not have been possible.

Confocal microscopy studies were supported by the Mississippi INBRE program funded by grants from the National Center for Research Resources (5P20RR-016476-11) and the National Institute of General Medical Sciences from the National Institutes of

Health (8 P20 GM103476-11) to Glenmore Shearer (Chair, Department of Biological Sciences, University of Southern MS), My research was supported by an NSF Research Initiation Grant awarded to Dr. Leal (ID 920625).

mid Does not Collaborate with *pannier* to Regulate Bristle Complex Formation in the Pupal Eye Disc
A *mid* GOF Mutation Results in Multiple Cellular Defects in the Adult Eye
Reducing *mid* Expression Induces Apoptosis within Early Pupal Stages

V. DISCUSSION 67

Determining the Function of Mid in the Development of *Drosophila* Eye
Mid Functions within the Notch-Delta Regulated Signaling Pathway
Mid Regulates SOP Cell Fate Specification in Collaboration with Members of Notch Delta Signaling Pathway
How to *mid* and *emc* Collaborate to Specify SOP Cell Fate
A Cross Regulatory Induction of Atonal on the Mid-Expressing SOP Cells
Mid Functions as a Pro-survival Factor in Developing Pupal Eye Discs
dFOXO a Member of the *H15/Mid* Regulatory Network Specifying Cell Fate and Survival
The Path toward Deciphering the Mid TF Regulatory Networks

VI. CONCLUSION 77

REFERENCES 78

LIST OF ILLUSTRATIONS

Figure

1. Morphogenetic Gradient Models 5

2. Conservation of T-box Transcription Factor Proteins 7

3. The Drosophila Adult Eye Geometry 13

4. The Third-instar Larval Eye-antennal Disc 14

5. The Retinal Determination Network 16

6. Atonal Expression Pattern 17

7. Development of Sensory Organs 19

8. The Asymmetric Divisions of the SOP Precursor Cell 21

9. Reducing Expression of *mid* during Third-instar Larval and Early Pupal Stages Results in Severe Eye Defects 33

10. The *mid-RNAi* Mutation is Specific and a LOF *H15/mid* Null Mitotic Clone Generated in Developing Eye Tissues Closely Resembles a *Notch* Gain-of-function Phenotype 35

11. Mid, H15, and Elav are Expressed in Photoreceptor Neurons of Third-instar Larval Eye Imaginal Discs 38

12. Mid and H15 are Expressed in Photoreceptor Neurons and Sensory Organ Precursor Cells of Early-staged Pupal Eye Imaginal Discs 39

13. *mid* Regulates the Expression of the Proneural Genes *achaetae* and *senseless* 40

14. *mid* Collaborates with *extramacrochaetae* to Regulate Interommatidial Bristle Generation 42

15. *mid* does not Regulate the Expression of *extramacrochaetae* 44

16. *dFOXO* Collaborates with *mid* to Regulate Interommatidial Bristle Formation 46

17. Loss of *H15/mid* Results in Decreased Delta Expression within Proneural Clusters Posterior of the MF 49

18. Loss of *H15/mid* Results in Decreased *scabrous* Expression 51

19. *mid* Collaborates with *atonal* to Regulate Interommatidial Bristle Generation 54

20. *mid* Collaborates with *senseless* to Regulate Interommatidial Bristle Generation 55

21. Schematics of the Notch-Delta Genetic Pathway of SOP Specification and some Cells of the SOP Lineage 56

22. *mid* does not Appear to Collaborate with *hairless* to Regulate Interommatidal Bristle Generation 57

23. A *mid* Gain-of-function Mutation Exhibits some Features that are Similar to a *Notch* Loss-of-function Phenotype 61

24. Overexpressing a UAS-*mid* Transgene Partially Recovers the *mid-RNAi* Mutation 62

25. Reduced Expression of *mid* Results in Apoptosis within the Pupal Eye Imaginal Disc 65

18. Loss of *H15/mid* Results in Decreased *scabrous* Expression 51

19. *mid* Collaborates with *atonal* to Regulate Interommatidial Bristle Generation 54

20. *mid* Collaborates with *senseless* to Regulate Interommatidial Bristle Generation 55

21. Schematics of the Notch-Delta Genetic Pathway of SOP Specification and some Cells of the SOP Lineage 56

22. *mid* does not Appear to Collaborate with *hairless* to Regulate Interommatidal Bristle Generation 57

23. A *mid* Gain-of-function Mutation Exhibits some Features that are Similar to a *Notch* Loss-of-function Phenotype 61

24. Overexpressing a UAS-*mid* Transgene Partially Recovers the *mid-RNAi* Mutation 62

25. Reduced Expression of *mid* Results in Apoptosis within the Pupal Eye Imaginal Disc 65

CHAPTER I

INTRODUCTION

Drosophila melanogaster is a well studied and genetically tractable model organism. Many basic physiological and developmental mechanisms are conserved between mammals and *Drosophila*. Nearly 75% of human diseases result from mutations in genes with a known functional homolog in *Drosophila*. The complexity of organ systems in higher organisms including the mouse model system makes it difficult to study the underlying mechanisms of developmental processes. Since the development and life cycle of the mouse is slow, it cannot be utilized for high-throughput genetic screening. To develop proper treatments for genetic, metabolic and neurodegenerative diseases, understanding basic cellular processes in development is essential. For example, neurodegenerative diseases are caused by the progressive loss of specific neurons and the late onset of these diseases is asymptomatic during development of the nervous system. Thus, screening for genetic mutations that develop into neurodegenerative phenotypes throughout development and in adulthood can provide insight into the underlying mechanism of the onset of diseases. Since the *Drosophila* genome is sequenced and tools for genetic manipulations are available, this simple model organism is helpful in determining the biochemical and molecular-genetic mechanisms underlying tissue development. The Tbx-20 transcription factor family is well known to regulate a diverse range of developmental mechanisms. Several human limb and heart developmental defects are caused by mutations of genes in this family.

To understand a gene's specific function, genetic studies are undertaken to place that gene within a pathway or hierarchy. In the case of genes encoding transcription factors, functions of these genes are mainly dependent upon their ability to interact with

other transcription factors. The interaction of a set of transcription factors determines the final outcome of a cellular process. Thus, genetic screening is important to identify the interactive partner of a transcription factor leading to the understanding of the functional roles of that gene in developing organisms. The *Tbx-20* transcription factor homologs *mid* and *H15* are essential for heart development and CNS development [1-4]. They were identified in a genetic screen for genes regulating segment polarity and the organization of the embryonic body plan [5]. Although *mid* and *H15* are expressed in a wide range of tissues, very few studies have been undertaken to understand the relevance of *mid* and *H15* function in various developing organ systems. Research on the role of the *mid* vertebrate homolog *Tbx-20* in regulating eye development is limited to two major investigations [6,7]. In the developing mouse visual system, *Tbx-20* transcripts were shown to be expressed in a spatial and temporally-regulated expression pattern in the periphery of the neural retina and within the optic cup [6]. In late-staged embryos, *Tbx-20* mRNA was detected in the neural retina, pigment epithelium, optic nerve and sclera and by 13 weeks of gestation, was broadly detected in the sclera, optic nerve and cornea as well as both the ganglion and neuroblastic layers of the neural retina [6,7]. Although, these studies showed that *mid* is dynamically expressed in eye tissues, they did not address mechanisms of Tbx-20 activity.

The importance of this current study is to elucidate the role of *mid* in regulating the development of specific cell types within the eye. Previous research showed that *mid* and *H15* regulate cell fate specification of many cell types within developing heart and neuronal tissues in cooperation with other transcription factors by working as member of a large transcription factor network [1-4,8].

Thus, in the developing eye tissue it is necessary to identify *mid* collaborating transcription factors to decipher specific regulatory networks guiding cell fate specification and tissue morphogenesis. We are pursuing the first study expanding the *mid*-interacting transcription factor regulatory network in the eye of *Drosophila* toward eventually understanding the evolutionarily conserved developmental mechanisms regulated by the Tbx-20 family of transcription factors.

CHAPTER II

REVIEW OF RELATED LITERATURE

The development of a multicellular organism requires the generation of a diverse array of cells arranged in an organized pattern. The process of generating different cell types with unique identities is known as cellular differentiation. During early embryonic development, cells have to assume a specific position in the growing embryo and once the position is specified, the cells then undergo the differentiation process [9]. Cellular differentiation is initiated by intracellular cues known as transcription factors. These transcription factor DNA binding proteins are first encoded by maternal transcripts stored within the egg cytoplasm. An additional influence upon cellular differentiation is provided by neighboring cells that release paracrine factors referred to as morphogens. The diffusible morphogens establish a concentration gradient with a high concentration beginning near the source of release that gradually decreases over a large distance along the anterior-posterior and dorsal-ventral axes (Figure 1). These morphogenetic gradients span a field of equipotent cells and trigger changes in cell shapes, movements and cell adhesion. The cell's exposure to different concentrations of morphogens determines its fate. To achieve unique fates, every cell needs to differentially regulate gene expression. This is accomplished by transcription factors whose activity is regulated by morphogenetic gradients [10].

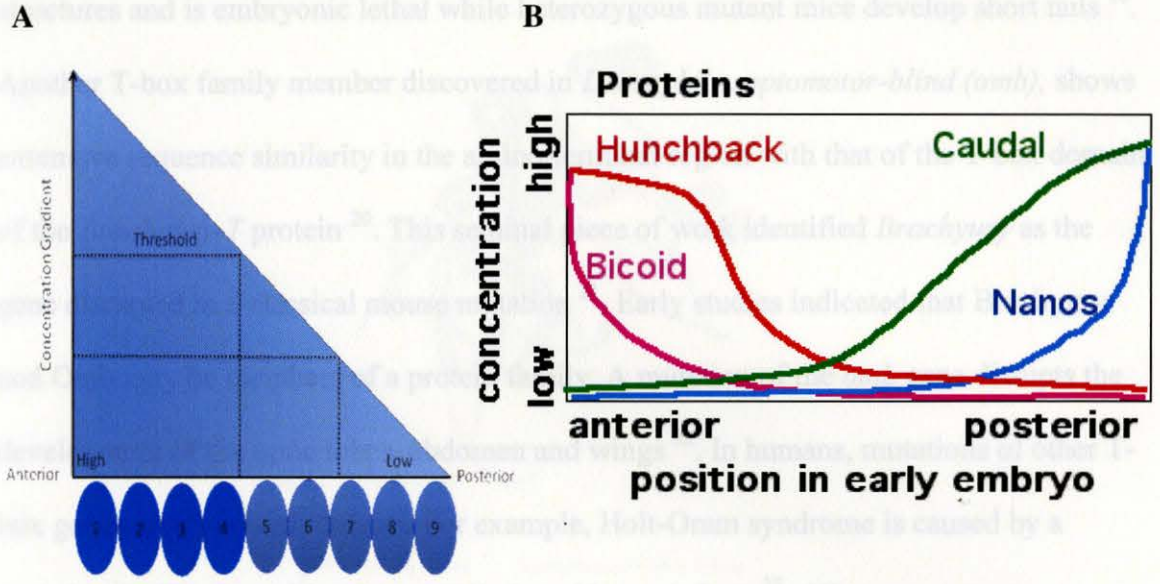

Figure 1. Morphogenetic gradient models. (A) The position of cells located along the anterior-posterior axis of a cellular field is marked by numbers and the blue intensities represent thresholds influencing their cellular differentiation. (B) The anterior-posterior axis in the early *Drosophila* embryo is established by the action of maternally translated proteins Hunchback, Bicoid, Caudal and Nanos which then act as diffusible morphogens and transcriptional regulators ("From gradients to strips in Drosophila embryogenesis: Filling in the gaps". Pomar, R. R., Jackle, H. *Trends Genetics*. 1996. 12; 478-483. The image is adapted from Pomar et al.[11]) (Wikipedia/contains/7/7a/Drosophila_png).

The Role of T-box Transcription Factors as Cell Fate Determinants

The T-box transcription factor family is required for the development of both vertebrate and invertebrate body plans and is critical for heart and limb development [12-14]. The discovery of T-box transcription factors emerged from studies using the mouse model system. The first T-box transcription factor gene mutation of *Brachyury-T* was experimentally created by Dobrovolskaia-Zavadskaia in 1927 by subjecting mice to x-rays.The *Brachyury-T* gene encodes a sequence-specific DNA-binding domain known as a T-box domain. *Brachyury-T* functions both as a transcriptional activator or repressor depending upon its association with other transcription factors [15-19]. A homozygous mutation of the *Brachyury-T* gene disrupts the development of mesoderm-derived

structures and is embryonic lethal while heterozygous mutant mice develop short tails [16]. Another T-box family member discovered in *Drosophila*, *optomotor-blind (omb),* shows extensive sequence similarity in the amino-terminal region with that of the T-box domain of the *Brachyury-T* protein [20]. This seminal piece of work identified *Brachyury* as the gene disrupted in a classical mouse mutation [21]. Early studies indicated that Brachyury and Omb may be members of a protein family. A mutation of the *omb* gene disrupts the development of the optic lobes, abdomen and wings [22]. In humans, mutations of other T-box genes result in birth defects. For example, Holt-Oram syndrome is caused by a mutation in *Tbx-5* resulting in upper limb and heart defects [23]. Ulnar-mammary syndrome is characterized by bone abnormalities in the hand and forearms resulting from a mutation in *Tbx-3* [24].

In *Drosophila,* eight T-box transcription factor genes have been identified including: *Dorsocross-1 (Doc1), Doc2, Doc3, optomotorblind (omb), optomotorblind-related (org1), brachyenteron (Byn), neuromancer1 (nmr1/H15), and neuromancer2 (nmr2/midline)*[25-29]. In 1984, the *Drosophila Tbx-20* homolog *mid* was first identified from a classic genetic screen undertaken by the Nüsslein-Volhard group uncovering segment polarity genes that organize the body plan of the segmented embryo [5] (Figure 2).

A.

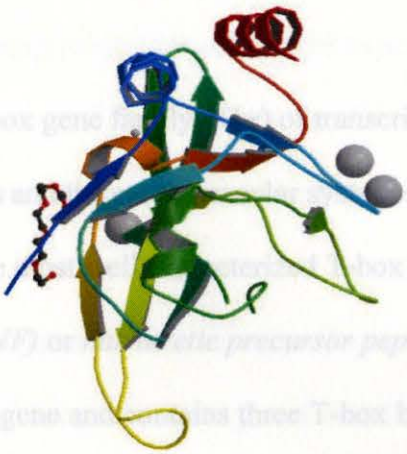

B.

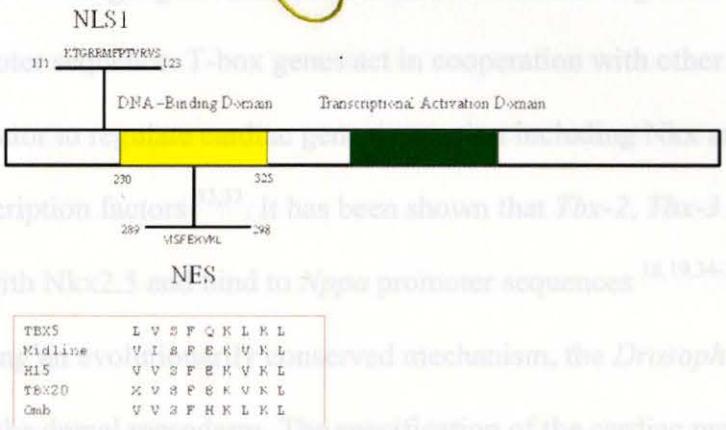

C.

H15	DKFHELGTEMIITKSGRRMFTVRVSFSGPLRQIQPADRYAVLLDVVPLD
Midline	DRFHDLGTEMIITKTGRRMFPTVRVSFSGPLRQIQPADRYAVLMDIIPMD
Tbx2	DQFHKLGTEMVITKSGRRMFPPFKVRVAVSG---LDKKAKYILLMDIVAAD
Tbx20	DKFHELGTEMIITKSGRRMFPTIRVSFSG---VDPEAKYIVLMDIVPVD
Tbx5	LKFHEV- TEMIITKAGRRFMPSYKVKVTTG---INPKTKYILLMDIVPAD

Figure 2. Conservation of T-box transcription factor proteins. (A) The Crystal structure of Human TBX-5 in the DNA-Free-form [30].(B) The functional T-box protein contains a DNA binding domain referred to as a T-box domain (yellow) and a transcriptional activation domain (green) that is required for its association with other transcription factors. Nuclear localization signal (NLS) and Nuclear export signal (NES) are the nuclear localization and nuclear exit signal motifs shared among different species and different members of T-box family proteins. The presence of the NLS and NES motifs indicate that Mid and H15 have the potential to shuttle between cytoplasmic and nuclear compartments. (C) The conservation of T-box sequences in different T-box proteins in various species demonstrates the importance of this domain for function.

Developmental Role of Midline and H15 in Diverse Tissues

Cardiovascular system

Members of the T-box gene family (*Tbx*) of transcription factors are important regulators of organogenesis and the cardiovascular system is highly perturbed by altered T-box gene function [31]. The most well characterized T-box target gene in the heart is *atrial natriuretic factor (ANF)* or *natriuretic precursor peptide A* (*Nppa*). *Nppa* was first identified as a *Tbx-5* target gene and contains three T-box binding elements (TBE) in its proximal promoter sequence. T-box genes act in cooperation with other families of transcription factor to regulate cardiac gene expression including Nkx and the GATA family of transcription factors [32,33]. It has been shown that *Tbx-2*, *Tbx-3* and *Tbx-20* form heterodimers with Nkx2.5 and bind to *Nppa* promoter sequences [18,19,34-36].

Following an evolutionarily conserved mechanism, the *Drosophila* heart tube develops from the dorsal mesoderm. The specification of the cardiac precursor cells from the dorsal mesoderm is governed by a group of homeobox genes. In *Drosophila,* cardiac cell fate is determined by the coordinated action of the homeobox gene *tinman*, the GATA factor *pannier (pnr), even-skipped (eve)* and *ladybird early (lbe).* In addition to these genes two paracrine signaling factors *decapentaplegic (dpp)* and *wingless (wg)* play an essential role in myocardial cell fate specification. To achieve the correct position in a cell cluster, cardiac precursors cells require establishing precise cell-cell contracts. The actions of the Hedgehog (Hh) and RAS/MAP kinase signaling pathways determine the position of each cell in the cluster thereby setting up and establishing a specific pattern. *Drosophila H15* and *mid* genes are both highly expressed in the embryonic cardiac tissue. Mutations of these genes also interfere with cardiac performance and disrupt contractile myofibrillar patterning [1,2,37]. During early developmental stages, mutations of *H15* and

mid in mesodermal tissue cause defects in cardiac cell fate specification characterized by an expansion of *eve*-expressing progenitor cells at the expense of *lbe* expressing cells [1]. As a consequence of defects in cell fate specification, *H15/mid* mutant heart myocardial cells fail to align properly and develop severe polarity defects resulting in lethality.

Central Nervous System

The central nervous system (CNS) consists of a number of interconnected neuronal and glial cell types that generate the greatest cellular diversity compared to all other organ systems. In *Drosophila* the CNS is composed of the brain and ventral nerve cord (VNC). The highly organized three-dimensional VNC develops from a two-dimensional layer of neuroectodermal cells located in the ventral-lateral region of the embryo. During early stages of embryogenesis this uniform neuroectodermal sheet is subdivided along the anterior-posterior (AP) and dorsal-ventral (DV) axes into groups of equivalent neural cells by the sequential action of maternal AP coordinate genes, gap and pair rule genes [38]. The protein products of these genes function as paracrine factors and are secreted from dorsal ectoderm. The cell fates of neurons and glia are specified by the gene products [39-41].

During action of such regulatory gastrulation and germband extension, the developing nervous system exhibits a segmentally repeated striped pattern. The Beuscher research group found that *mid* restricts *wg* expression within narrow domains of odd-numbered abdominal segments to pattern the ventral epidermis and to initiate the sequential expression of genes specifying the fates of neuroblasts (NBs) derived from the neuroectoderm [29]. The expression of segment polarity genes along the AP axis then determines the fate of the each NB whereas the coordinated action of the nuclear NF-kB, bone morphogenetic protein (BMP) and epidermal growth factor receptor (EGFR)

signaling pathways determines the DV borders of the neuroectoderm [42,43]. The Notch-Delta signaling pathway plays a major role in restricting the neural fate to a single cell by regulating the expression of the proneural gene complex *achaete-scute* (*ac-sc*), a basic–helix-loop-helix (bHLH) transcription factor, in the presumptive neural cells.

After segmentation and neuroblast selection, *mid* mRNA and Mid proteins are expressed in a subset of CNS neurons throughout stages 12-16 of embryonic nerve cord [3,4]. In 2009 a forward genetic screen in *Drosophila* identified novel genes essential for embryonic CNS development. The *mid* gene was shown to regulate *even-skipped* (*eve*) expression in specific subsets of terminally differentiated post-mitotic neurons [4]. In order to develop functional neuronal circuitry, different types of neuron and glial cells need to differentiate in a spatial and temporal manner. The precise organization and reiterative pattern formation in the CNS requires highly regulated genetic programs controlled by transcription factors. Initially, different transcription factor families were thought to control certain steps in the differentiation of progenitor cells giving rise to neurons or glia. However, recent findings emphasize the interaction between specific subsets of transcription factors that form a transcription factor code cells utilize to determine their individual fates [44]. For example, genetic epitasis studies showed that *mid* cooperates with the transcription factor *Nkx6* to inhibit *eve* expression [4]. Studies on *H15* and *mid* suggest that they are members of a large transcriptional regulatory network working in collaboration with other transcription factors to regulate neuronal cell fate in the developing CNS.

The *Drosophila* Eye as a Model System

The *Drosophila melanogaster* compound eye provides a unique experimental system in which cellular differentiation and proliferation during development can easily be followed. The *Drosophila melanogaster* compound eye is a highly organized structure comprised of ~800 unit facets arranged in a hexagonal array first described as a neurocrystalline lattice [45-47]. Each facet, referred to as an ommatidium, consists of eight photoreceptor neurons designated R1-R8, four lens-secreting cone cells and two large primary pigment cells [48]. Remaining accessory cells are shared between ommatidia within the lattice. These cells include six secondary and three tertiary pigment cells forming a hexagon surrounding the core as well as three bristle complexes located in alternate vertices between tertiary pigment cells (Figure 3).

An adult eye is composed of ~400 mechanosensory bristle complexes that consist of a shaft cell, socket cell, sheath cell and sensory neuron [49,50]. The shaft cell secrets the bristle. The *Drosophila* eye develops from a simple monolayer of epithelial cells and initiates development within a wave of differentiating cells known as the morphogenetic furrow (MF). The MF is a dorsal-ventral indentation that traverses the eye imaginal disc from the posterior to anterior direction. Within the MF a band of epithelial cells undergoes an apical to basal contraction under the influence of retinal determination transcription factors. The secreted morphogens Dpp and Hh direct the further expression of the genes *eyeless (ey), sineoculis (so)* and *dachshund (dac)* essential for eye morphogenesis (reviewed by Silver and Rebay 2005) [51]. Anterior of the MF, cells do not differentiate and divide in an unsynchronized manner [52]. As the MF moves across the disc, the cells change their shapes and these changes are coordinated with the progression

of the cell cycle. Within the MF, photoreceptor neurons undergo differentiation from a pool of equipotent precursor cells (Figure 4).

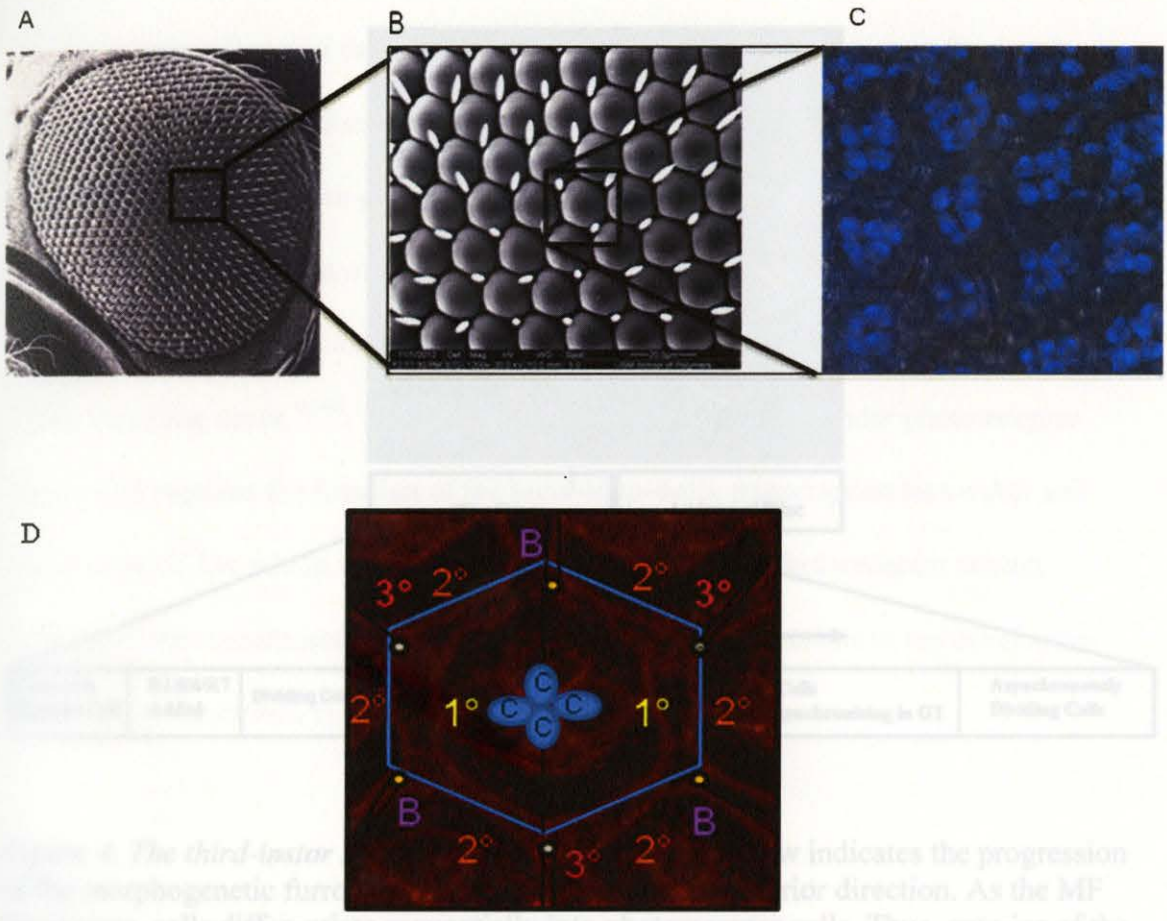

Figure 3. The Drosophila adult eye geometry. (A) A scanning electron micrograph showing the wild-type adult compound eye phenotype. Each eye consists of ~800 ommatidia along with ~ 450 mechanosensory bristles. (B) Magnified section of the boxed area in image (A) depicts the regular hexagonal arrangement of ommatidia. (C) Immunofluoroscent image of the pupal retina labeled with DAPI (blue). DAPI marks the nuclei of photoreceptor neurons in each ommatidium while the surrounding pigment cells form the hexagon around the photoreceptor neurons. (D) An immunofluoroscent image of *Drosophila* pupal eye disc (~40hours APF) was labeled with anti-Numb antibody. This image clearly shows the hexagonal arrangement of primary, secondary, tertiary cells surrounding four cone cells. Bristle complexes are located in alternate vertices of the hexagon.

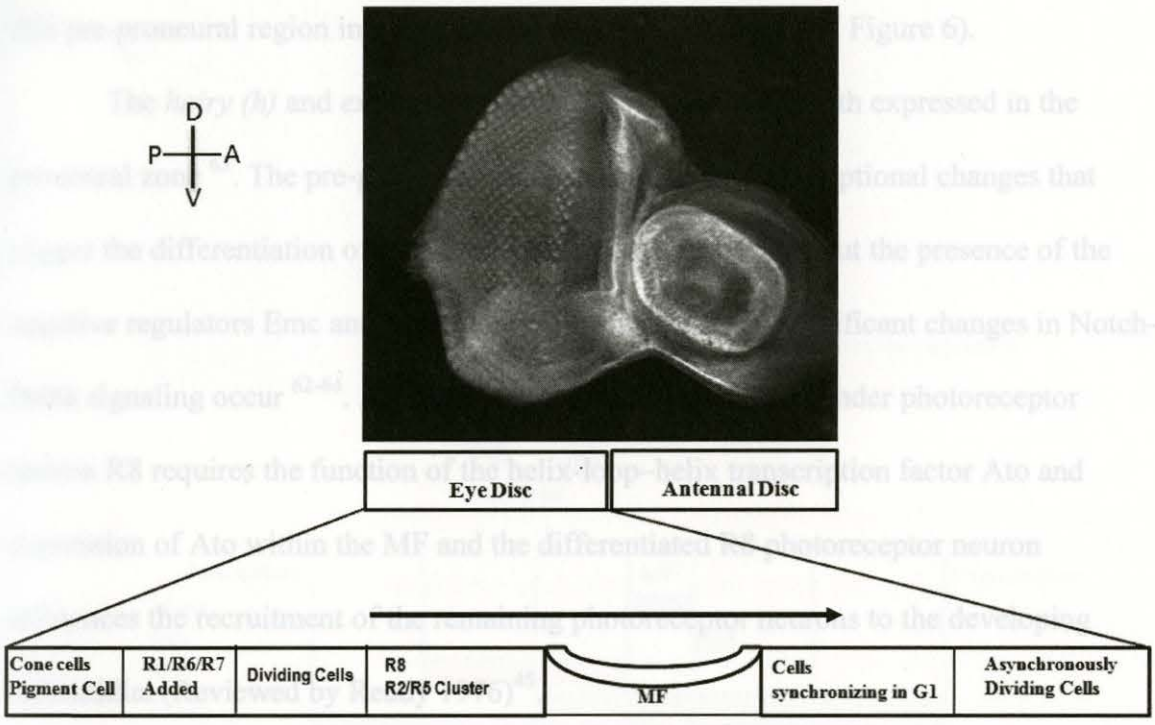

Figure 4. The third-instar larval eye-antennal disc. The arrow indicates the progression of the morphogenetic furrow (MF) from the posterior to anterior direction. As the MF progresses, cells differentiate sequentially into photoreceptor cells. Thus, anterior of the furrow, cells are in undifferentiated dividing stage while posterior of the furrow, cells are differentiated and have acquired specific fates.

The first photoreceptor neuron to be specified is called the R8 or the founder photoreceptor neuron. It is specified by the proneural gene *atonal* (*ato*) [53-55]. Morphogenetic furrow movement also depends on the secreted protein Hedgehog (Hh) [56-58]. Hh is primarily expressed in the photoreceptors behind the furrow and diffuses anteriorly to trigger the initiation of *ato* expression anterior of the furrow [56-60]. The effects of Hh on *ato* expression are partly mediated by secreted Decapentaplegic (Dpp), which is expressed within and ahead of the morphogenetic furrow in response to Hh signaling [56,57,61]. It has been proposed that Dpp acts at a long range to define a 'pre-proneural'

region anterior to the furrow and that shorter range Hh signaling subsequently converts this pre-proneural region into a proneural region [62] (Figure 5 and Figure 6).

The *hairy (h)* and *extramacrochaetae (emc)* genes are both expressed in the proneural zone [63]. The pre-proneural state is acquired by transcriptional changes that trigger the differentiation of proneural cells into neuronal cells but the presence of the negative regulators Emc and h antagonize this process until significant changes in Notch-Delta signaling occur [62-64]. As discussed, the selection of the founder photoreceptor neuron R8 requires the function of the helix-loop–helix transcription factor Ato and expression of Ato within the MF and the differentiated R8 photoreceptor neuron influences the recruitment of the remaining photoreceptor neurons to the developing ommatidia. (Reviewed by Ready 1976)[45].

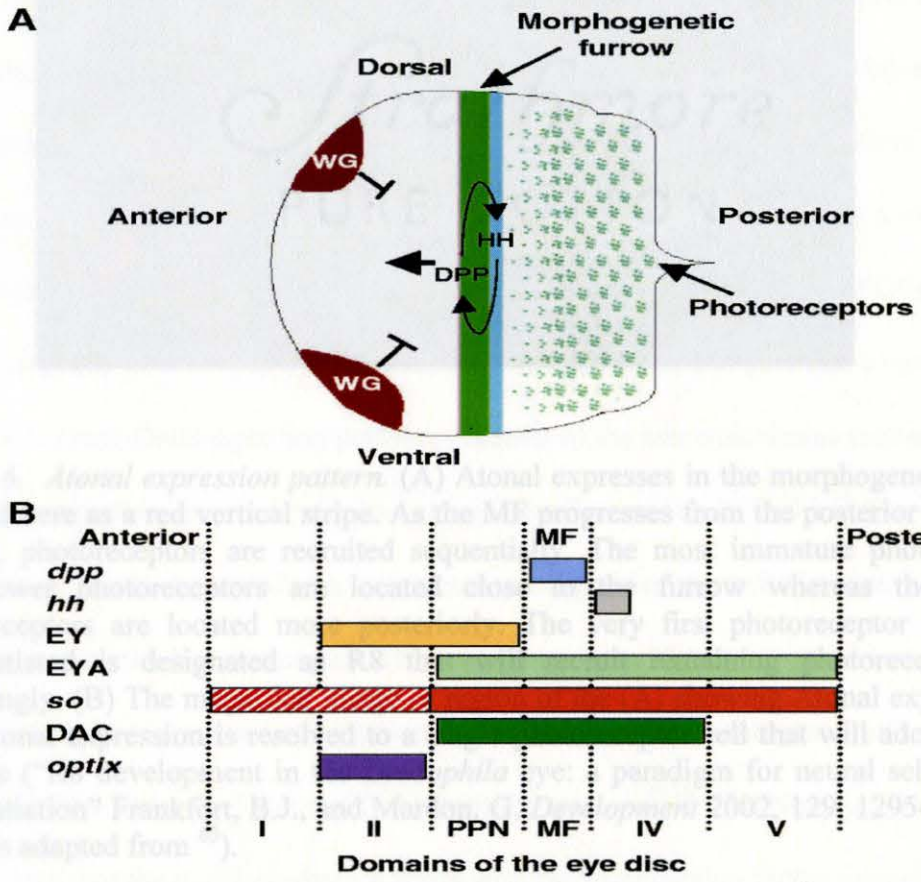

Figure 5. The retinal determination network. (A)The expression of two paracrine signaling molecules Hedgehog and Decapentaplegic in the morphogenetic furrow influences the undifferentiated cells ahead of the furrow to adopt the proneural fate. There is a positive feedback loop between these two signaling factors whereas Wingless expressed anterior of the furrow antagonizes eye tissue formation. (B) A schematic of the expression pattern of retinal determination transcription factors in six different regions of the eye disc, as described by (Bessa et al). EY, Eyeless; EYA, Eyes absent; SO, Sine oculis; DAC, Dachshund; MF, morphogenetic furrow; PPN, preproneural region ("Signaling circuitries in development: insights from retinal determination gene network" Silver, J.S. and Rebay, I. *Development* 2005, 132, 3-13. The image was adapted from [51]).

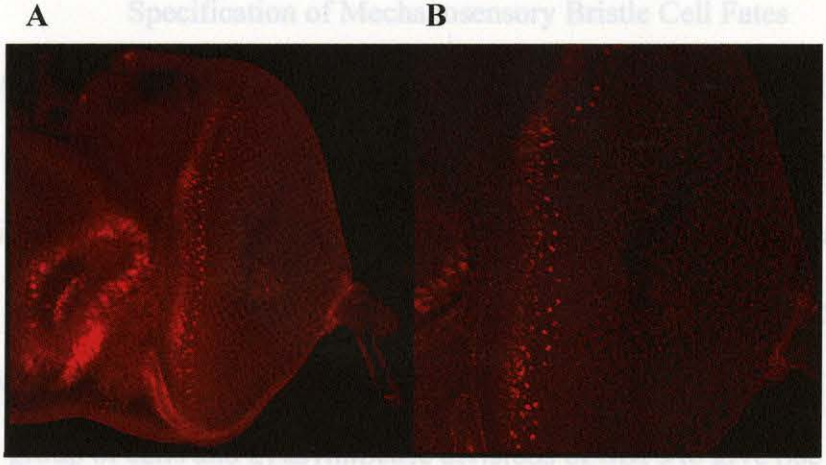

Figure 6. Atonal expression pattern. (A) Atonal expresses in the morphogenetic furrow depicted here as a red vertical stripe. As the MF progresses from the posterior to anterior regions, photoreceptors are recruited sequentially. The most immature photoreceptors with fewer photoreceptors are located close to the furrow whereas the matured photoreceptors are located more posteriorly. The very first photoreceptor cell to be differentiated is designated as R8 that will recruit remaining photoreceptor cells accordingly. (B) The magnified image of region of the (A) showing Atonal expression in MF. Atonal expression is resolved to a single photoreceptor cell that will adopts the R8 cell fate ("R8 development in the *Drosophila* eye: a paradigm for neural selection and differentiation" Frankfort, B.J., and Mardon, G. *Development* 2002, 129, 1295-1306. The image is adapted from [65]).

In a similar fashion, the external sensory organ cells are developed from a single precursor cell known as the sensory organ precursor cell (SOP). The selection of the SOP is dependent upon the action of the proneural gene complex of *ac-sc.* Initially groups of equipotent cells, designated as proneural clusters, are selected by the expression of proteins encoded by *ac-sc* (for reviews see Ghysen and Dambly-Chaudière.1988) [66,67]. Evidence from genetic and *in vitro* studies indicate that basic helix-loop-helix (bHLH) proteins encoded by *ac-sc* form heterodimers with the bHLH transcription factor Daughterless (Da) creating transcriptional activators that can bind the promoters of genes involved in bristle development, including *ac, sca, bearded,* and the *Enhancer of split [E(spl)]* complex genes *m4, m7 and m8* [66-72].

Specification of Mechanosensory Bristle Cell Fates

After the specification of the proneural group of cells which are all competent to adopt the SOP fate, proteins encoded by the neurogenic genes come into play and restrict the adoption of the neural fate to a single cell by a mechanism known as lateral inhibition mediated by the Notch-Delta signaling pathway [73]. Two mechanisms play a role in the development of the external sensory organs: 1) lateral inhibition to select SOPs from the proneural group of cells and 2) asymmetric divisions of SOPs to give rise to daughter cells. The Notch-Delta signaling pathway consists of the transmembrane receptor Notch and a ligand protein from a family known as Delta/Serrate/lag-2 (DSL) [74]. During lateral inhibition, Delta is expressed as a transmembrane ligand on the cells in close proximity to cells expressing the Notch receptor. The activation of the Notch receptor by specific binding of Delta triggers a conformational change in the Notch receptor leading to the cleavage of the intracellular domain of Notch ($Notch_{ICD}$) [75,76]. The $Notch_{ICD}$ then translocates into the nucleus where it binds with the transcription factor Suppressor of Hairless-Su(H)converting Su(H) from a repressor to a co-transcriptional activator of the *Enhancer of Split-E*(*spl*) gene complex [74,77]. E(spl) proteins inhibit the expression of the proneural genes and influence the Notch-activated cell to adopt a non-neuronal, epithelial cell fate (Figure 7).

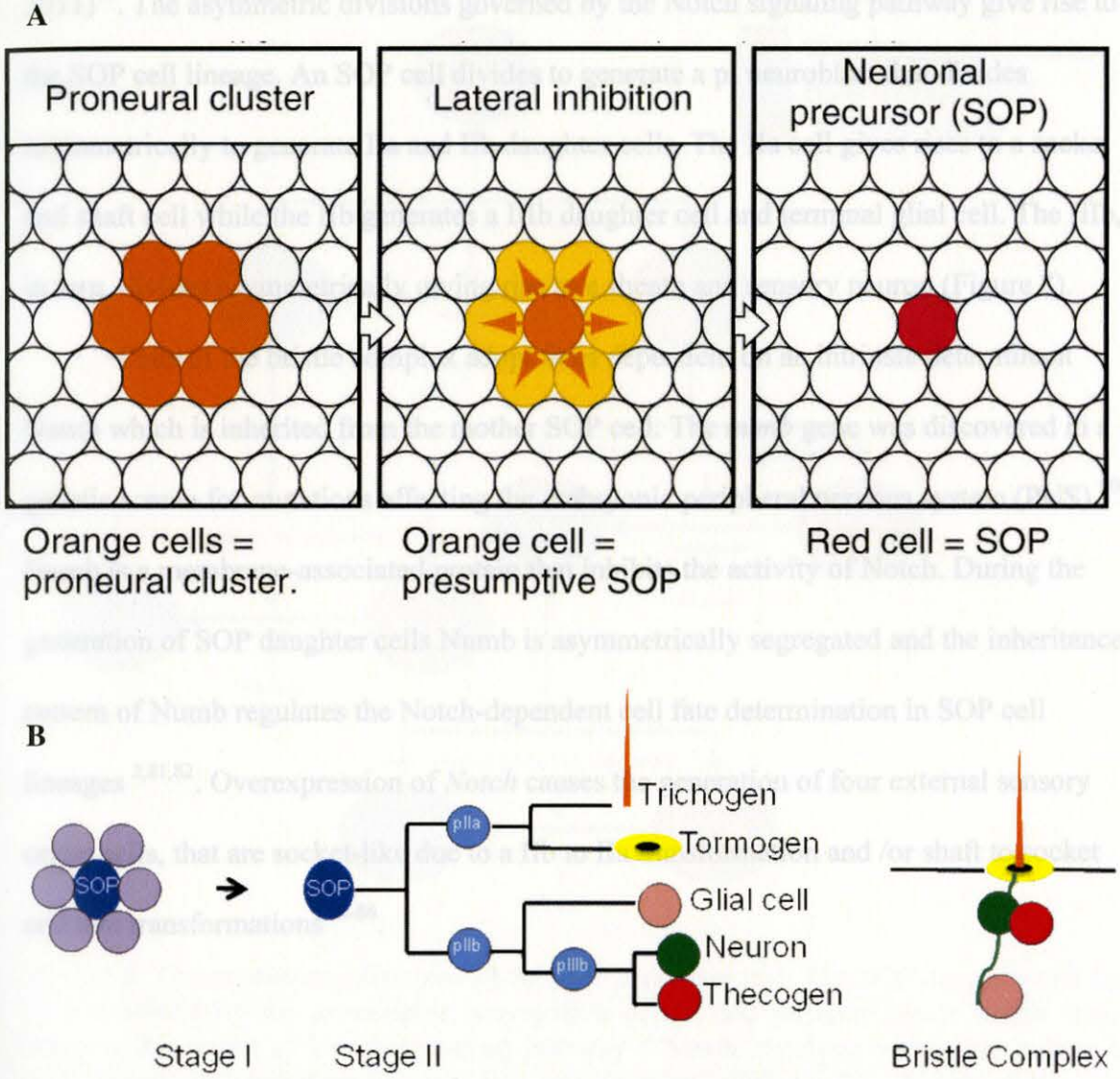

Figure 7. Development of sensory organs. (A) Selection of the SOP cell from a proneural cluster by the lateral inhibitory action of the Notch-Delta signaling pathway. (B) I. Prior to SOP selection, the SOP restricts surrounding cells to adopt the neural cell fate. II. The schematic represents the asymmetric divisions of SOP cells that generate cell diversity. The single mechanosensory bristle complex is composed of the five different cell types: shaft/ trichogen, socket/ tromogen, neuron, glia and sheath cell. Glial cell migrates away later ("Su (H)- independent activity of Hairless during mechano-sensory organ formation in *Drosophila*" Nagel, A.C., Maier, D., and Preiss, A. *Mechanisms of Development* 2000, 94, 3-12 The image was adapted from [78]).

Once this SOP cell is selected, it undergoes asymmetric cell divisions to generate cell diversity in the peripheral nervous system (reviewed by Furman and Bukharina,

2011)[79]. The asymmetric divisions governed by the Notch signaling pathway give rise to the SOP cell lineage. An SOP cell divides to generate a pI neuroblast that divides asymmetrically to generate IIa and IIb daughter cells. The IIa cell gives rises to a socket and shaft cell while the IIb generates a IIIb daughter cell and terminal glial cell. The IIIb, in turn, divides asymmetrically giving rise to a sheath and sensory neuron (Figure 8).

Cells of the bristle complex adopt fates dependent on an intrinsic determinant Numb which is inherited from the mother SOP cell. The *numb* gene was discovered in a genetic screen for mutations affecting the embryonic peripheral nervous system (PNS) [80]. Numb is a membrane-associated protein that inhibits the activity of Notch. During the generation of SOP daughter cells Numb is asymmetrically segregated and the inheritance pattern of Numb regulates the Notch-dependent cell fate determination in SOP cell lineages [2,81,82]. Overexpression of *Notch* causes the generation of four external sensory organ cells, that are socket-like due to a IIb to IIa transformation and /or shaft to socket cell fate transformations [83-86].

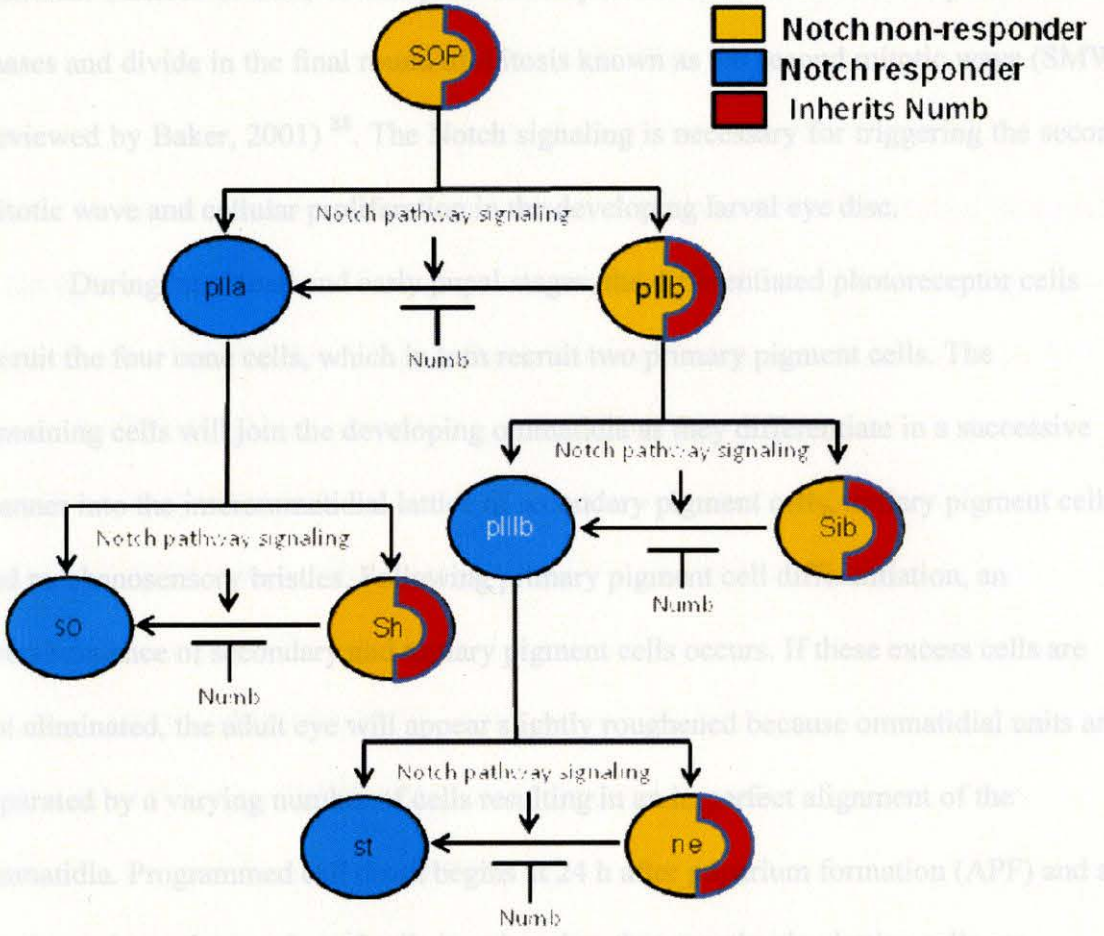

Figure 8. The asymmetric divisions of the SOP precursor cell. The SOP daughter cell fate is determined by the asymmetric segregation of the cell intrinsic factor Numb which inhibits the action of Notch signaling pathway ("Notch regulates *numb*: integration of conditional and autonomous cell fate specification" Rebeiz, M., Miller, S.W., and Posakony, J.W. Development 2011, 138, 215-225 The image was adapted from [87]).

Cell Death Plays an Essential Role in Arranging the Ommatidial Structure

There are two waves of synchronized cell division, referred to as mitotic waves, which increase the cell number in the eye disc during third-instar larval development. As cells enter the morphogenetic furrow, they arrest in G1 phase of the cell cycle in the posterior domain of the furrow. In this zone cells are maintaining two populations: 1) the "preclusters" that initiate differentiation and 2) the undifferentiated surrounding cells. The undifferentiated surrounding cells undergo another round of mitosis, producing a

sufficient number of cells to complete development. These cells enter S phase and G2 phases and divide in the final round of mitosis known as the second mitotic wave (SMW) (reviewed by Baker, 2001) [88]. The Notch signaling is necessary for triggering the second mitotic wave and cellular proliferation in the developing larval eye disc.

During late larval and early pupal stages, the differentiated photoreceptor cells recruit the four cone cells, which in turn recruit two primary pigment cells. The remaining cells will join the developing ommatidia as they differentiate in a successive manner into the interommatidial lattice of secondary pigment cells, tertiary pigment cells and mechanosensory bristles. Following primary pigment cell differentiation, an overabundance of secondary and tertiary pigment cells occurs. If these excess cells are not eliminated, the adult eye will appear slightly roughened because ommatidial units are separated by a varying number of cells resulting in an imperfect alignment of the ommatidia. Programmed cell death begins at 24 h after puparium formation (APF) and a few hours later, the number of cells is reduced so that exactly nine lattice cells are positioned around each ommatidium [89]. The supernumerary secondary and tertiary pigment cells are removed through initiation of the intrinsic apoptotic pathway [90]. Mutations of genes that fail to eliminate cells from the developing eye result in disruptions of the lattice structure and disturb the regular geometry of the eye.

CHAPTER III

METHODOLOGY

Fly Stocks

Drosophila melanogaster strains were maintained at 25°C on standard cornmeal-yeast-agar media. *Oregon-R* flies were used as wild-type (WT) and the following lines were obtained from the Bloomington Stock Center (Bloomington, Indiana):

1. *Df(3L)ED4196*
2. *Df(3R)ED5634*
3. *Df(3L)H99,kni^{rl-1}P^{p}/TM3,Sb^{1}*
4. *mwh^{1}jv^{1}pnr^{D1}/TM2*
5. *82B pnr^{vx6}/TM6B,Tb^{+}*
6. *w$^{1118;}$st^{1}pnr^{vx4}e^{1}/TM3,P{ActGFP}JMR2,Ser^{1}*
7. *w*;emc^{1}P{neoFRT}80B/TM6, Tb^{1}*
8. *H^{1}/In(3R)C e^{1}*
9. *E(spl)m8-HLH^{1}*
10. *w*;ato^{1}/TM6B,Tb^{1}*
11. *h^{1}*
12. *sens^{E2}red^{1}e^{1}/TM6B,Tb^{+}*
13. *da^{1}pr^{1}cn^{1}/SM5*
14. *Su(H)^{1}/ln(2L)Cy,ln(2R)Cy,Cy^{1}pr^{1}*
15. *y^{1}ac^{1}v^{1}*
16. *P{EPgy^{2}}dFOXO^{EY16506}*
17. *P{UAS-N.U}*
18. *y^{1}w*;P{Gal4}54C*

19. *P{UAS-p35.H}BH3,w;+/+;+/+*

20. *UAS-pnr*

We used the *UAS-Gal4* system [91] and the eye-specific driver *GMR-Gal4* balanced on chromosomes II and III (a gift from Tanya Wolff) [90] to express the following transgenes in WT and specific mutant backgrounds: *UAS-mid* and *UAS-mid-RNAi* (provided by Rolf Bodmer) [1]. The *scabrous-gal4;prospero-gal4* transgenic line was used to express *UAS-mid-RNAi* in SOP cells and their daughter cells (provided by James Skeath) [92,93]. Transgenic lines used for the mosaic clonal analyses in Figures 17 and 18 are of the following genotypes: *y w hsFLP;H15^{x4}mid^{1a5}FRT40A/y^{+} ry^{+} 25F FRT40A* and *y w hsFLP; H15X4mid^{1a5} FRT40A/w^{+}GFP FRT 40A* (provided by William Brooks) [94]. *yw; +/+; FRT82dFOXO^{25}/TM6.Tb.Hu* line was provided by Ernst Hafen (Junger et al., 2003) All crosses were performed at 25°C. We followed published procedures for generating mitotic clones within third-instar larvae [94,95].

Preliminary Genetic Modifier Screen

We screened a fraction of isogenized *DrosDel* deficiency lines obtained from the Bloomington Stock Center by crossing each line to *UAS-nmr2-RNAi/CyO*; *GMR-Gal4/TM3* (*mid-RNAi*) flies exhibiting a sensitized genetic mutation for *mid* characterized by an approximate 50% decrease of bristle complexes. Bristles were counted from one-day old female progeny generated from the cross that were maintained at 25°C within a humidified biological incubator under a 12 hr light:dark cycle. Groups of five flies of the genotype *UAS-mid-RNAi/+;GMR-Gal4/Df(3)* were transfixed to a slide with clear nail polish lacquer and submerged in water to prevent light scattering. The complete eye field was viewed under a high-power Leica M165C dissection microscope. A series of images were collected along 10-15 focal planes and digitally recorded using a Leica DFC

camera. These images were flattened to create a final montage using Image Pro Plus software to correct for eye curvature and to digitally tag bristles for accurate quantification (Media Cybernetics Inc., Bethesda, MD).

Using these methods, we identified several deficiency lines that modified the *mid* mutant phenotype (unpublished data). Of these lines, flies heterozygous for *Df(3L)ED207* (61C9-62A6) significantly suppressed the *mid* mutant phenotype while flies heterozygous for *Df(3L)ED4196* (61C7-62A2) did not significantly suppress the phenotype. As a result, we delimited the cytological interval to 61C9-62A2. Upon surveying 71 gene candidates deleted within this interval, we proceeded to a biased genetic modifier assay to determine whether *emc* was a *mid*-interacting gene candidate since this was the only gene reported to regulate SOP formation (flybase.org) and previous research showed that *emc* functioned within the Notch-Delta pathway of SOP cell fate specification [96]. Further studies are underway to complete overlapping deficiency analyses of *Df(3L)ED207* to identify other novel *mid*-interacting gene candidates.

Immunofluorescent Studies

Eye imaginal discs were dissected from developmentally staged third-instar larvae in cold phosphate buffered saline (PBS) and fixed in 3.7% paraformaldehyde in 0.1 M MOPS buffer (pH 7) for 15 min at 25°C followed by two washes of PBS containing 0.1% Triton-X 100 (PTX) and three washes of PTX supplemented with 1% bovine serum albumin (PBT). Discs were incubated in PBT containing 1% goat serum for at least one hour at 25°C and then incubated with primary antibodies for 4 hrs at 25°C or overnight at 4°C. Pupal eye imaginal discs were developmentally staged from either timed collections of embryos laid for a 15-30 minute period from a population cage or by collecting wandering third-instar larvae and staging pupae for unique features characterizing the P0

(0-1 hr APF), P1 (1-3 hrs APF) and P2 stages (3-6 hrs APF) [97]. The P0 and P1 stages were dissected in cold PBS before fixation. The P2-staged pupal eye discs were dissected in PEMF buffer containing 0.1M PIPES (pH 7.0), 1mM MgSO4, 2 mM EGTA and 3.7% paraformaldehyde [98,99]. P0-P2 discs were then fixed in PEMF buffer with 4% paraformaldehyde for 30 minutes on ice under continuous shaking followed by three 10 minute washes with PAXD buffer (PBS supplemented with 1% bovine serum albumin, 0.3% Triton X-100 and 0.3% sodium deoxycholate) [100]. Fixed discs were incubated for 4 hrs at 25°C or overnight at 4°C.

We used the following primary antibodies at the indicated dilutions for this study: anti-Achaetae (1:2; Teresa Orenic, The University of Illinois, Chicago IL) [101], guinea pig anti-Atonal (1:1000; from Dave Marenda, Drexel University, Philadelphia, PA) [102], guinea pig anti-Extramacrochaetae (1:8000; from Yuh Nung Jan, University of California, San Francisco, CA) [103], guinea pig anti-Numb (1:1000; from James Skeath, Washington University School of Medicine, St. Louis MO) [104], anti-Senseless (1:800; from Hugo Bellon, Baylor School of Medicine, Houston, TX) [105], guinea pig anti-H15 (1:2000), rabbit anti-Mid (1:1000) , goat anti-Actin (1:500; Santa Cruz Biotechnology) and rabbit anti-Caspase-3 (1:500 Abcam).

The following monoclonal antibodies were obtained from the Developmental Studies Hybridoma Bank developed under the auspices of the National Institute of Child Health and Development at The University of Iowa: anti-Armadillo (1:10) [106]; anti-DE-Cadherin (1:10) [107], anti-Cut (1:10) [81], anti-Elav (1:10) [108], anti-Delta Extracellular domain (1:10) [109], anti-Notch, extracellular domain, EGF repeats #12-20 (1:10) [110], anti-Notch, intracellular domain (1:1000) [111], anti-Repo (1:10) [112]; and anti-Scabrous (1:10) [113]. We used Alexafluor 488, 594 and 633 secondary antibodies with appropriate species

specificity for immunofluorescent labeling (Molecular Probes). Eye discs were labeled with 4', 6 diamino-2 phenylindole (DAPI) (1 μg/ml in PTX) for 15 min and washed 3 times with PTX for detection of nuclei. Fluorescently labeled tissues were mounted in 50% 1,4-Diazabicyclo [2.2.2]octane (DABCO). Paraformaldehyde was purchased from Fisher Scientific. All other chemicals and goat pre-immune serum were obtained from Sigma-Aldrich (St. Louis, MO).

Confocal Scanning Microscopy

Confocal images were captured by a Zeiss LSM510 META confocal microscope and analyzed using the accompanying Zeiss LSM Image Browser software (version 5). For accurate quantification of H15 and Delta co-expression in WT and *mid-RNAi* mutant tissues reported in figure 17 P from emitted light intensities of respective fluorophores, we focused on imaging proneural cells within the central region of the MF. We generated a Z-stack series comprised of 0.2 μM sections within a 4.9 μm^2 area to analyze the immunofluorescent expression patterns of H15 and Delta in a group of six proneural cells within a single cluster. We recorded the generated histograms from each focal plane representing the mean signal intensities in pixels emitted by the immunofluorescent probes. These studies were repeated with two more independent samples of WT discs and three samples of *mid-RNAi* mutant discs co-immunolabeled with anti-Delta and anti-H15 antibodies. For each immunolabeling experiment of WT and *mid-RNAi* mutant discs performed in triplicate, we calculated the signal intensity of each immunofluorescent probe as a percentage of the total intensity measured for both immunofluors to normalize the data. Immunofluorescent probes were excited at 488 nm (to detect H15) and 594 nm (to detect Delta) of the absorption spectrum. We calculated the means and standard error of the means (SEM) for normalized values (Figure 17P).

Scanning Electron Microscopy

Compound eyes of one-day old adult flies were platinum sputter coated to a thickness of 20 nm. High-resolution images were acquired on an FEI (FEI Company, Hollsboro, OR) Quanta 200 scanning electron microscope with an accelerating voltage of 20 kV (The Department of High Performance Materials and Polymers, USM).

Statistical Analyses

The mean, standard deviation and standard errors of the mean were calculated using Microsoft Excel software. The IOB counts for each genotype were statistically analyzed using Shaprio-Wilk's test for measuring the normal distribution of each data set (JMP10 software, SAS Institute Inc.). We also estimated the equal variance between groups using the Barlett's test. Data sets that met the assumptions of a normal distribution and equal variance were then analyzed using the two-sample, two-tailed pooled Student's t-test. Data sets exhibiting unequal variance were analyzed using the two-sample, two-tailed unpooled Student's t-test. Data sets with an unequal distribution were analyzed by the Wilcoxon rank-sum test. All the probability values were calculated setting the level of significance (α) to 0.05. The data represented in the bar graph of Figure 17P were statistically analyzed using the 'ANOVA Single Factor' function to compare the means between groups. The probability value was calculated setting the level of significance (α) to 0.05 and the degree of freedom (*df*) to 1.

Software Programs

Confocal scanning images were assembled using Adobe Photoshop CS6 software (Adobe Systems, Inc.). We used GraphPad Software, Inc. (La Jolla, CA) to represent data in bar charts. SEM images were cropped and scaled using Image Pro Plus software.

CHAPTER IV

RESULTS

Reducing *mid* Expression within the Eye Epithelial Disc Results in a Significant Loss of Interommatidial Bristles

In order to build a *mid* transcription factor network regulating cell-fate specification, we utilized the advantages of a genetic modifier screen. To greatly facilitate the screen, we chose to use the *Drosophila* eye as a model system. To pursue a successful genetic modifier screen we generated *mid* mutant flies by expressing previously characterized *UAS-mid-RNAi* transgenes [1,4] under the *glass multiple reporter* (*GMR*) *Gal4* driver line [90] and we established a perpetual stock of transgenic flies which reduce *mid* expression within cells undergoing the commitment of neuronal fate during late third-instar larval and early pupal stages of eye imaginal disc development by using the *UAS-Gal4* binary expression system [91].

Using high-resolution scanning electron microscopy (SEM), we closely examined the eye phenotypes from wild-type (WT) and *UAS-mid-RNAi/CyO; GMR-Gal4/TM3* (*mid-RNAi*) one-day old adult female flies. Compared to WT eyes, *mid-RNAi* mutant eyes exhibited multiple cells and tissue defects including decreased bristle numbers, bristle polarity defects, bristle shaft deformations, empty socket cells, abnormally paired bristle complexes and extensive ommatidial fusion (Figure 9A, B). We generated ten SEM images of WT and *mid-RNAi* adult compound eyes for comparing interommatidial bristle (IOBs) counts and observed an approximate 50% decrease of bristles across the entire eye field of *mid-RNAi* mutants compared to WT. We observed a more significant reduction of bristles within the ventral region compared to the dorsal region of the eye field (Figure 9C) and also compared bristle numbers in the posterior versus anterior

regions (Figure 9D). The mutant bristle phenotype of the whole eye field provided an ideal sensitized *mid* LOF phenotype which is required for a genetic modifier screen. In this sensitized background we obtained third chromosomal deficiency lines from the *DrosDel* collection to determine whether the *mid-RNAi* mutant phenotype was enhanced or suppressed. Once a deficiency line is identified by observing a significant modification of the *mid-RNAi* phenotype, we narrowed the cytological region harboring mid-interacting genes undertaking overlapping deficiency mapping analyses.

To increase the efficiency of the screen, we repeated these studies using a high-magnification light microscope to capture and record 10 montage images of WT and *mid-RNAi* mutant eyes (see Methodology). By digitally tagging and counting IOBs from these images, we confirmed that *mid-RNAi* mutant eyes exhibited an approximate 49% decrease of interommatidial bristles compared to WT eyes although we lost a minor degree of resolution in the detection of ventral bristles due to lighting conditions and eye curvature (Figure 9E-H). Despite a small offset in numbers, the mean reduction in bristle numbers of *mid-RNAi* eyes normalized as a percentage of the mean bristle numbers of WT eyes was approximately 50% using either SEM or montage images from the light microscope to quantify them.

In addition to bristle loss and disorganized ommatidia, the light microscope images also revealed altered pigmentation which could be the result of either the loss or misspecification of one or more 1^{o}, 2^{o} and 3^{o} pigment cells (Figure 9F,G). To confirm this observation we used a *54C-Gal4* driver line that targets *mid* reduction in all pigment cells [114] and observed no changes in their pigmentation suggesting that under *mid-RNAi* conditions utilizing the *GMR-Gal4* driver, pigmentation defects must arise as a secondary effect of *mid* reduction in a cell non-autonomous manner (data not shown). In

approximately 20% of the *mid-RNAi* flies screened, reduced *mid* expression resulted in patches of melanized tissue indicative of apoptotic or necrotic cell death as well as some tissue scarring in the eye (Figure 9G). In all studies, mutant *mid-RNAi* eyes exhibiting any degree of scarring were excluded from quantitative and statistical analyses of bristle numbers.

To determine that the *mid* mutant phenotype induced by the *UAS-Gal4* system and *RNAi* method was specific, we examined the individual effects of heterozygous transgenes of *UAS-mid-RNAi* and *GMR-Gal4* by counting the IOB numbers and comparing to Oregon-R (OR) WT fly eyes (Figure 10A, B). We also validated these effects by crossing other transgenes of *UAS-mid-RNAi* driven by a *GMR-Gal4* driver on the second chromosome (data not shown). In order to confirm these observations we further generated mosaic clones null for both *H15* and *mid* (*H15/mid*) and examined the eyes of one-day old flies using SEM. We detected a nearly complete loss of bristles in broad areas of the compound eye characterized by a widespread ommatidial fusion that resembled to the *mid-RNAi* mutant phenotype (Figure 10C). The disrupted *H15/mid* mutant eye tissue also partially phenocopied a *Notch* (N^{full}) gain-of-function (GOF) mutation indicating a possible link to the Notch-Delta pathway that plays a pivotal role in specifying SOP cell fates (Figure 10D) [115]. We also used *scabrous* (*sca*)-*Gal4* and *prospero* (*pros*)-*Gal4* driver line that target the expression of *Gal4* in proneural SOP cells and their pIIb daughter cells, respectively [92,93] , therefore the expression of *UAS-mid-RNAi* transgene under *sca-Gal4;prospero-Gal4* resulted in reduction of *mid* in the proneural SOP cells and their pIIb daughter cells. Under these conditions, we detected an expansion of ommatidial columns within the posterior domain of the eye field lacking IOBs and a small area also located posteriorly devoid of IOBs (Figure 10F). In a few

rows of ommatidia, we also observed a change in the orientation of the bristles suggestive of polarity defects (Figure 10F, inset).

Figure 9: Reducing expression of mid during third-instar larval and early pupal stages results in severe eye defects. Scanning electron micrograph (SEM) images of one-day old adult eyes depict a (A) wild-type Oregon-R (OR) compound (WT) eye with a normal ommatidial array and (B) a *mid-RNAi* eye exhibiting a severe reduction of interommatidial bristles (IOBs) and a rough eye characterized by ommatidial fusion. (A' and B') Enlarged images of the WT pattern of ommatidia (A') and a *mid-RNAi* eye with an arrows pointing to empty sockets (B'). (C and D) The bar charts represent mean IOB numbers and the error bars denote the standard errors of the mean (SEM) quantitated from 10 WT and *mid-RNAi* eyes. (C) Comparisons of dorsal versus ventral and (D) anterior versus posterior fields of WT (white bars) and *mid-RNAi* eyes (black bars) show a significant reduction of IOBs under *mid-RNAi* conditions across all fields. The reduction of IOBs in the ventral field of *mid-RNAi* eyes compared to the ventral region of WT eyes is highly significant ($p^{***} < 0.0001$). Comparisons of data are indicated by brackets linking specific data sets ($p^{*} < 0.01$, $p^{**} < 0.001$) (E-G) Light microscope images taken at 120X magnification of (E) a WT eye exhibiting a precisely patterned ommatidial array and (F) a *mid-RNAi* eye with a loss of IOBs, disorganized ommatidia

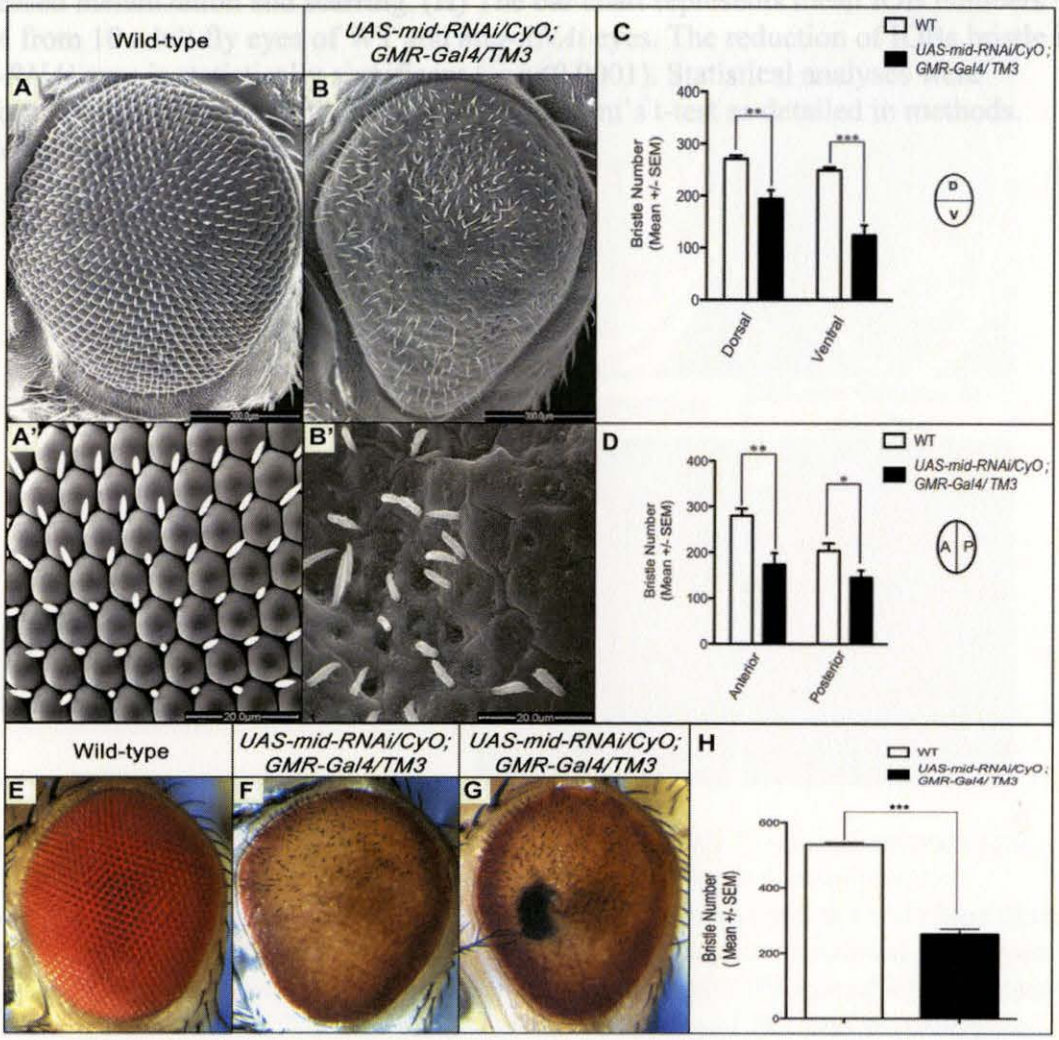

Figure 9: Reducing expression of mid during third-instar larval and early pupal stages results in severe eye defects. Scanning electron micrograph (SEM) images of one-day old adult eyes depict a (A) wild-type Oregon-R (OR) compound (WT) eye with a normal ommatidial array and (B) a *mid-RNAi* eye exhibiting a severe reduction of interommatidial bristles (IOBs) and a rough eye characterized by ommatidial fusion. (A' and B') Enlarged images of the WT pattern of ommatidia (A') and a *mid-RNAi* eye with an arrows pointing to empty sockets (B'). (C and D) The bar charts represent mean IOB numbers and the error bars denote the standard errors of the mean (SEM) quantitated from 10 WT and *mid-RNAi* eyes. (C) Comparisons of dorsal versus ventral and (D) anterior versus posterior fields of WT (white bars) and *mid-RNAi* eyes (black bars) show a significant reduction of IOBs under *mid-RNAi* conditions across all fields. The reduction of IOBs in the ventral field of *mid-RNAi* eyes compared to the ventral region of WT eyes is highly significant ($p^{***} < 0.0001$). Comparisons of data are indicated by brackets linking specific data sets ($p^{*} < 0.01$, $p^{**} < 0.001$) (E-G) Light microscope images taken at 120X magnification of (E) a WT eye exhibiting a precisely patterned ommatidial array and (F) a *mid-RNAi* eye with a loss of IOBs, disorganized ommatidia

and pigmentation defects. (G) An example of a *mid-RNAi* mutant eye exhibiting increased melanization and scarring. (H) The bar chart represents mean IOB numbers +/- SEM from 10 adult fly eyes of WT and *mid-RNAi* eyes. The reduction of IOBs bristle in *mid-RNAi* eyes is statistically significant ($^{***}p<0.0001$). Statistical analyses were performed using Shaprio-Wilk's test and the Student's t-test as detailed in methods. Scale bars measure lengths in micrometers.

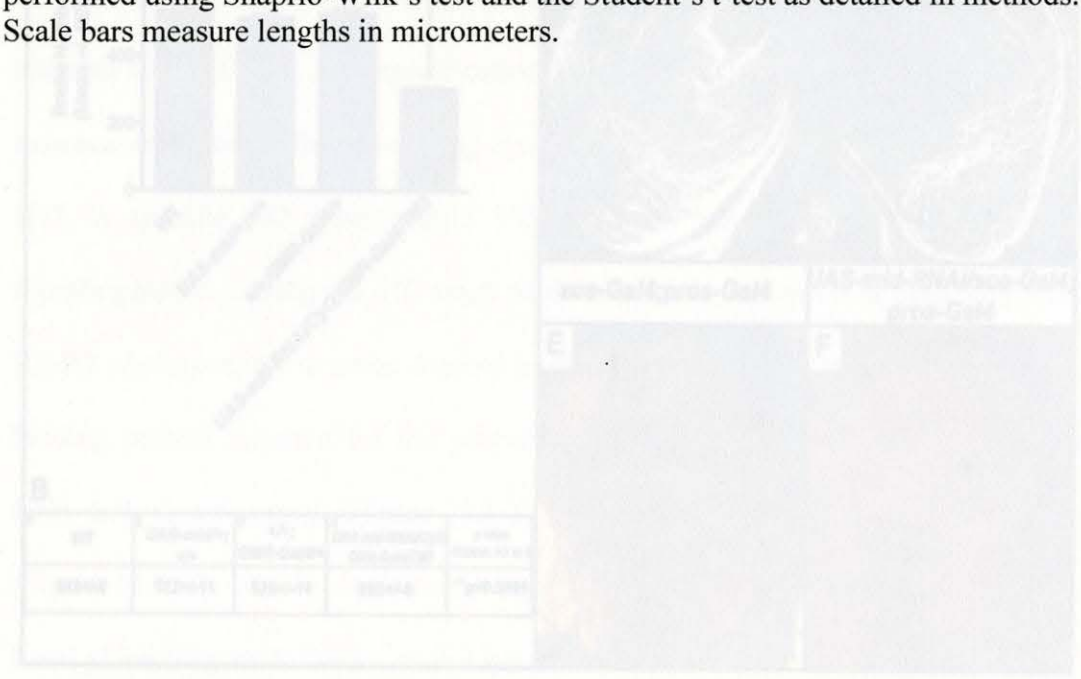

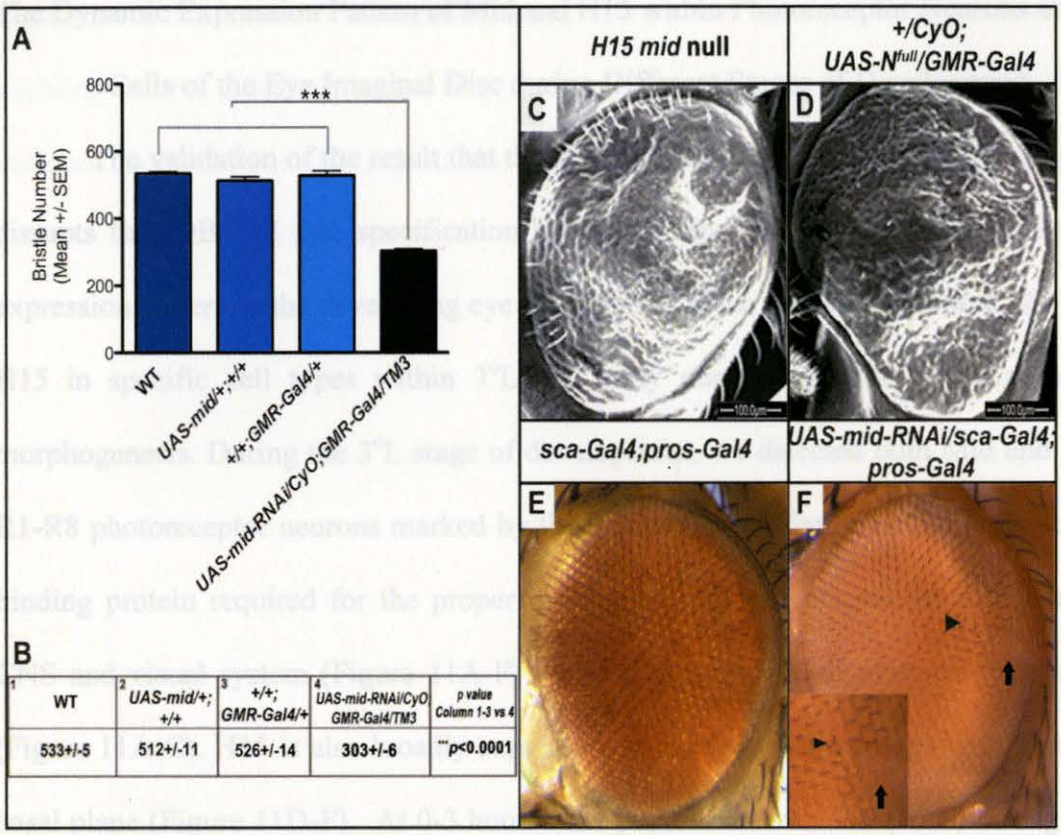

Figure 10 The mid-RNAi mutation is specific and a LOF H15/mid null mitotic clone generated in developing eye tissues closely resembles a Notch gain-of-function phenotype. (A) The bar graph represents mean bristle numbers and the error bars denote standard errors of the mean (SEM) quantitated for 10 eyes per represented genotypes. The WT value is obtained from OR eyes. The inhibition of IOBs in *mid-RNAi* mutants is statistically significant (***$p < 0.0001$). Data comparisons of WT and heterozygous transgenes with the *mid-RNAi* background are indicated by brackets linking data sets. (B) The table represents mean IOB numbers +/- SEM from genotypes represented in the bar graph. (C) A scanning electron micrograph depicts a LOF *H15/mid* null mitotic clone generated during the P0-P2 pupal stages that exhibits similar yet more severe mutant features observed in *mid-RNAi* eyes including the loss of IOBs and ommatidial fusion. (D) Overexpressing *Notch* using the *GMR-Gal4* line (*+/CyO;UAS-N^{full}/GMR-Gal4*) resulted in a mutant phenotype resembling tissues generated from *H15/mid* LOF clones. (E) A light microscope image at 120X of an eye from a *sca-Gal4;pros-Gal4* transgenic line showing a normal pattern of bristle loss in ommatidial columns in the posterior-most region of the eye. (F) An eye from a *UAS-mid-RNAi/sca-Gal4;pros-Gal4/TM3* fly exhibits expanded IOB loss in ommatidial columns in the posterior area, a small region of bristle loss (arrow) and IOBs that have shifted in polarity (inset, arrowhead). Statistical analyses were performed using Shaprio-Wilk's test and the Student's t-test as detailed in methods. (C and D) Scale bars embedded in scanning electron micrographs measure lengths in micrometers.

The Dynamic Expression Pattern of Mid and H15 within Photoreceptor Neurons and SOP Cells of the Eye Imaginal Disc during Different Stages of Development.

The validation of the result that the knock-down of *mid* in the developing eye disc disrupts the IOB cell fate specification requires further analysis of the Mid and H15 expression pattern in the developing eye. We examined the expression pattern of Mid and H15 in specific cell types within 3°L and early pupal stages of eye imaginal disc morphogenesis. During the 3°L stage of development, we detected both Mid and H15 in R1-R8 photoreceptor neurons marked by the expression of Elav, a neural-specific, RNA binding protein required for the proper development of neurons within the developing CNS and visual system (Figure 11A-F) . Mid is detected in all photoreceptor neurons (Figure 11A-C). H15 is also broadly expressed in a pattern that overlaps with Elav at the basal plane (Figure 11D-F). At 0-3 hours after puparium formation (APF) during the P1 stage, we detected H15 and Mid within photoreceptor neuron clusters also marked by Elav (Figure 12A-D). At 3-6 hours APF at the P2 stage when a majority of SOP cells are specified [116], we observed a dramatic shift in the expression pattern of Mid and H15 with respect to Elav. Mid and H15 were co-expressed in a small population of photoreceptor neuron clusters marked by Elav and within a population of SOP cells distinguished by linear arrays of single cells lacking Elav expression (Figure 12G-H). To confirm SOP cell identities directly, we co-immunolabeled P2 staged WT pupal eye discs with anti-Mid antibody and a specific antibody to detect Achaetae (Ac), a basic-helix-loop-helix(bHLH) transcription factor characteristic of SOP cells. These studies revealed an overlapping expression pattern of Mid and Ac within a majority of SOP cells (Figure 13A-C). We then examined the expression pattern of Ac in P2 staged *mid-RNAi* eye discs and observed a significant decrease of Ac in SOP cells suggesting that Mid positively

regulates Ac expression in SOP cells (Figure 13D-F). We validated these studies using an antibody against Senseless, a zinc finger transcription factor marks the SOP cell. We also detected co-expression of Sens and Mid in SOP cells (Figure 13G-I) and under *mid-RNAi* conditions, Sens was also dramatically reduced (Figure 13J-L).

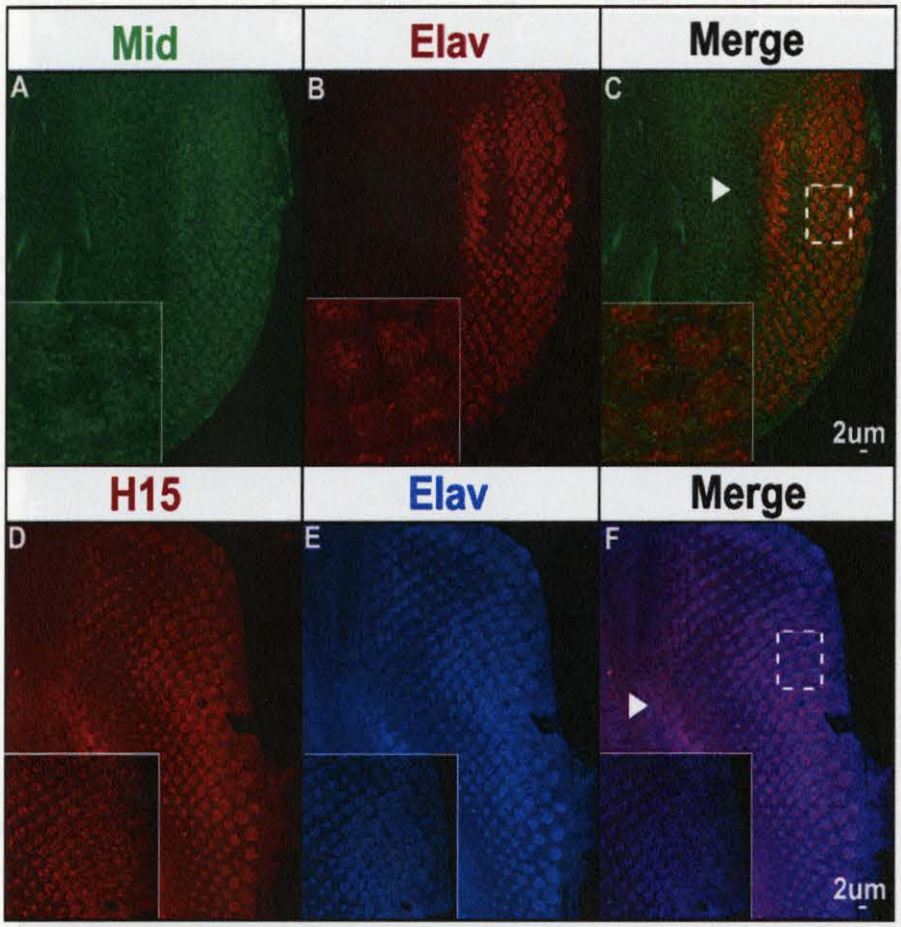

Figure 11. Mid, H15 and Elav are expressed in photoreceptor neurons of third-instar larval eye imaginal discs. Confocal images of WT third-instar larval eye discs co-immunolabeled with (A) Mid (green) and (B) Elav (red) antisera that detect both proteins within photoreceptor neurons. (C) The merged image shows that Mid and Elav are co-expressed within photoreceptor neurons (yellow). (D) A third-instar larval eye disc co- (D) A third-instar larval eye disc co-immunolabeled with H15 (red) and (E) Elav (blue) shows that (F) H15 and Elav are also co-expressed in photoreceptor neurons (merge). The insets within each panel are enlarged images from the boxed regions shown in C and F. The white arrowhead points to the MF. Posterior is right.

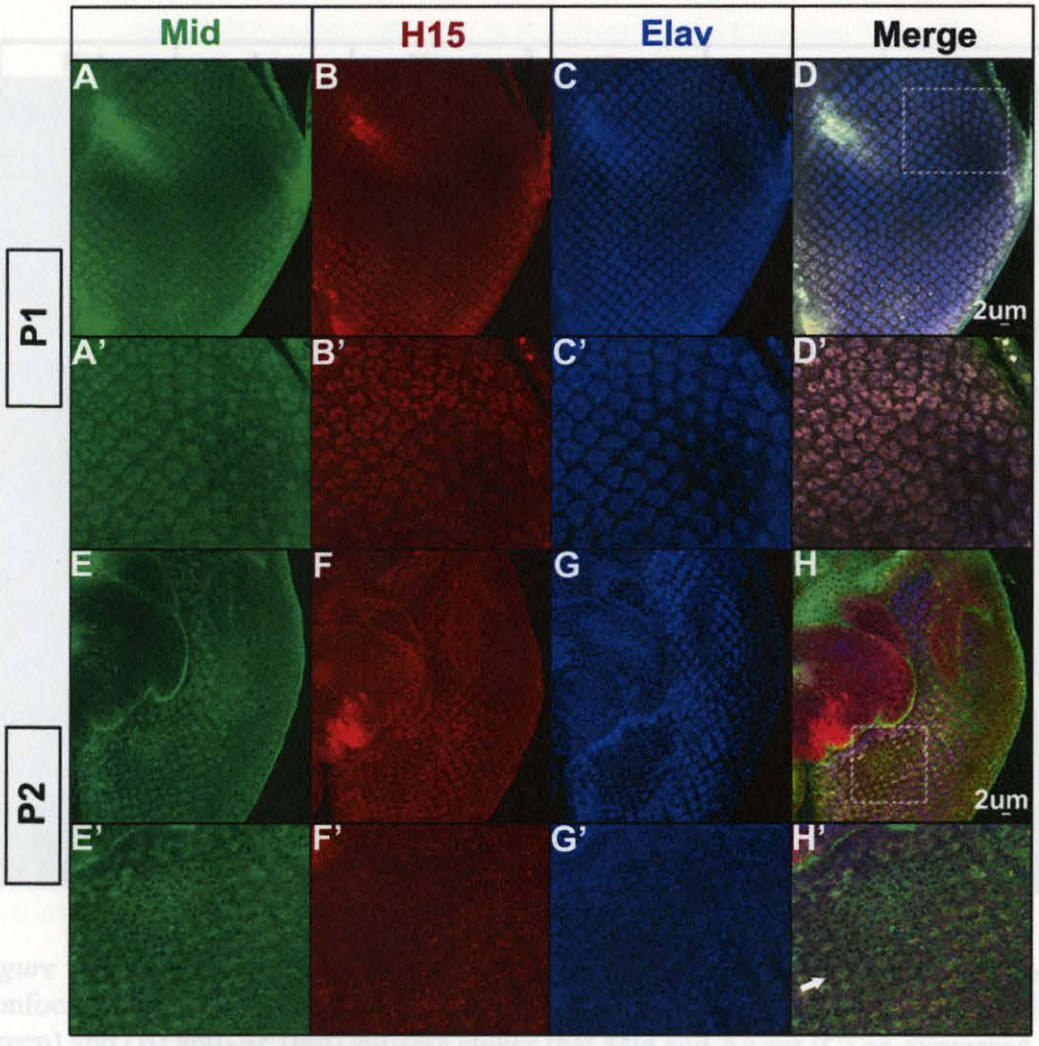

Figure 12. Mid and H15 are expressed in photoreceptor neurons and sensory organ precursor cells of early-staged pupal eye imaginal discs. Confocal images of WT P1-staged pupal eye discs immunolabeled with (A) Mid (green), (B) H15 (red) and (C) Elav (blue) antisera detecting these proteins within photoreceptor neurons during the P1 stage of development. (D) The merged image shows that Mid, H15 and Elav exhibit an overlapping expression pattern within photoreceptor neurons (light magenta). (A'-D') Higher magnification images of panels A-D from the dashed box shown in panel D. (E-H) WT P2-staged pupal eye discs immunolabeled with (E) Mid (green), (F) H15 (red) and (G) Elav (blue) antisera. (H) The orientation of the disc as mounted reveals two unique populations of cells in one focal plane represented by the merged image. (E) Mid(green), (F) H15 (red) and (G) Elav expression is diminishing in photoreceptor neurons that (H, merge) co-express Mid, H15 and Elav (light magenta) while a *mid-* and *H15*-expressing population of SOP cells is detected (arrow). (E'-H') Higher magnification images of panels E-H from the boxed region shown in panel H. Posterior is to the right.

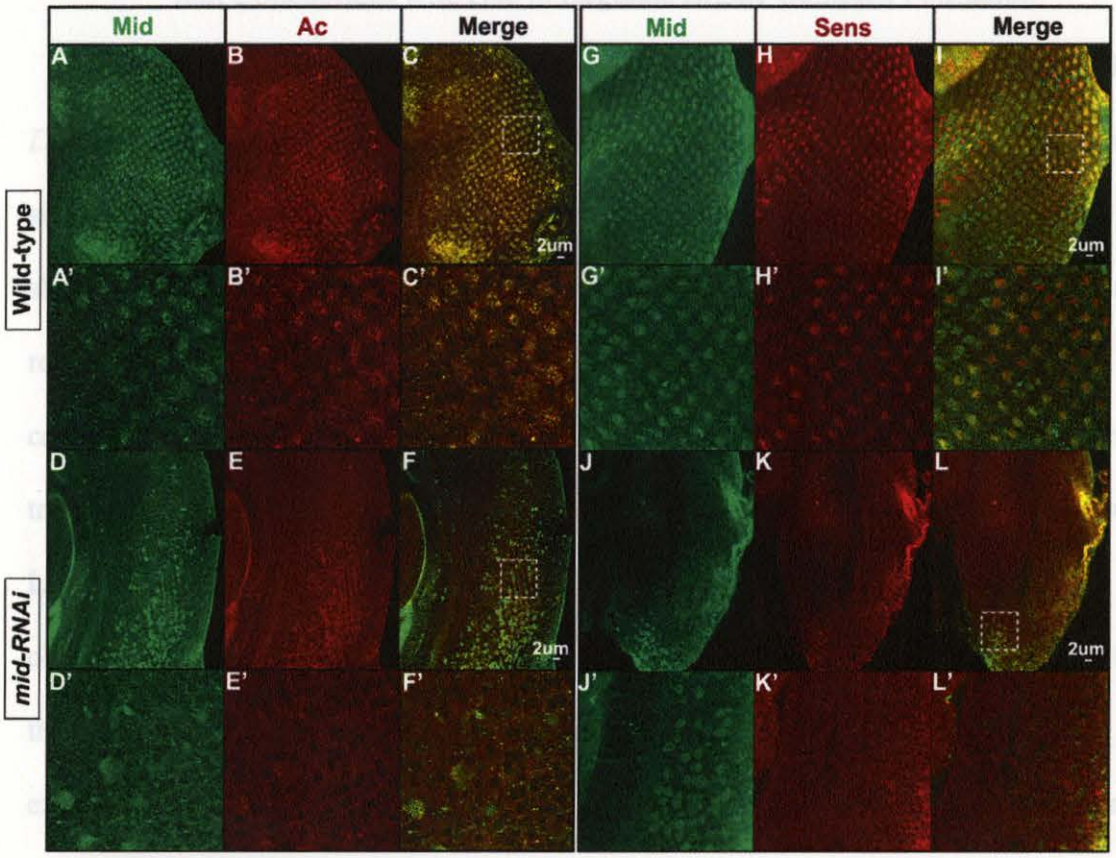

Figure 13 mid regulates the expression of the proneural gene achaetae and senseless. Confocal image of a P2-staged WT pupal eye disc co-immunolabeled with (A) anti-Mid (green) and (B) anti-Ac (red) antisera shows that Mid and Ac are (C) co-expressed in SOP cells (merge). (A'-C') Higher magnification images of panels A-C. (D) A P2-staged *mid-RNAi* pupal eye disc also co-immunolabeled with (D) anti-Mid (green) and (E) anti-Ac antisera (red) depicting reduced Mid and Ac expression (merge) (F). (D'-F') Higher magnification images of panels D-F from the boxed region shown in panel F. (G-I) P2-staged pupal eye discs co-immunolabeled with (G) anti-Mid (green) and (H) anti-Sens (red) antisera. (I) WT discs exhibit an overlapping Mid and Sens expression pattern marking SOPs while (J-L) *mid-RNAi* discs show decreased expression of (J) Mid and (K) Sens where (L) represents the merged image. (J'-L') Higher magnification images of panels J-L from the boxed region shown in panel L. Posterior is to the right.

mid Collaborates with *emc* to Regulate Bristle Complex Formation

From the genetic modifier screen, we uncovered a chromosomal deficiency line *Df(3L)ED207* that when placed in a heterozygous state within the *mid-RNAi* background significantly suppressed the *mid* mutant phenotype and recovered bristles (data not shown). In order to pursue a biased screen for transcription factor genes known to play a role in Notch-Delta signaling pathway, we selected *extramacrochaete* (*emc*) as a candidate from this deficiency line for further characterization. Emc is a helix-loop-helix transcription factor regulates SOP cell fate (Flybase.org) [96]. By placing a heterozygous LOF mutant allele of *emc* (emc^1) in the *UAS-mid-RNAi* sensitized background we observed a significant recovery of IOBs (Figure 14D, F). The F1 progeny generated from the parental cross exhibited normal bristle numbers compared to WT flies with the exception of *+/CyO; GMR-Gal4/*emc^1 flies. These flies exhibited a ~16% decrease in bristles. A high-resolution SEM image of an eye from a *UAS-mid-RNAi/CyO; GMR-Gal4/*emc^1 fly details the significant recovery of bristles and relatively normal ommatidial structures. These results indicate a cell-survival role for Mid as an antagonist of Emc function. A lack of a different species-specificity of antibodies for co-immunolabeling Mid and Emc in disc tissues precluded the examination of their expression patterns. However, we co-immunolabeled P2-staged WT and *mid-RNAi* pupal discs with anti-H15 and anti-Emc antibodies. Although H15 and Emc overlapped in WT discs, we did not detect a significant difference in Emc expression levels between WT or *mid-RNAi* discs (Figure 15). This indicate the Mid may regulate the activity of the Emc protein rather than the transcription of its gene.

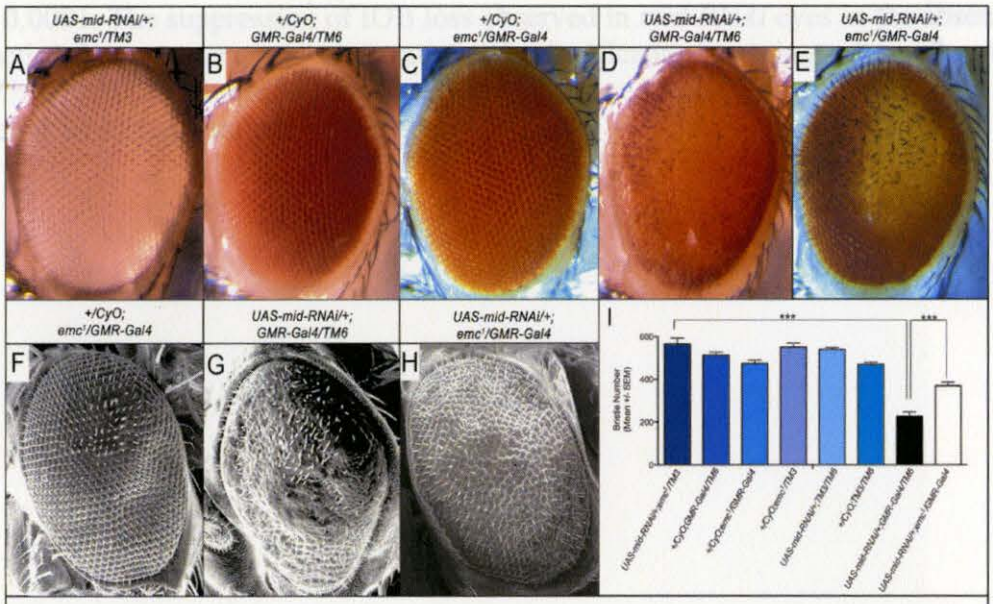

J

1 UAS-mid-RNAi/+; emc¹/TM3	2 +/CyO; GMR-Gal4/TM6	3 +/CyO; emc¹/GMR-Gal4	4 +/CyO; emc¹/TM3	5 UAS-mid-RNAi/+; TM3/TM6	6 +/CyO; TM3/TM6	7 UAS-mid-RNAi/+; GMR-Gal4/TM6	8 UAS-mid-RNAi/+; emc¹/GMR-Gal4	p value Column 1-6 vs 7	p value Column 7 vs 8
564+/-28	512+/-15	473+/-16	550+/-19	539+/-9	469+/-10	226+/-22	369+/-17	$^{***}p<0.0001$	$^{***}p<0.0001$

Figure 14 mid collaborates with extramacrochaetae to regulate interommatidial bristle generation. (A-E) Light microscope images at 120X magnification depict (A) *UAS-mid-RNAi/+;emc^{1}/TM3*, (B) *+/CyO;GMR-Gal4/TM6* and (C) *+/CyO;GMR-Gal4/emc^{1}* eyes of F1 progeny exhibiting a well-organized ommatidial array and numbers of IOBs that are nearly equivalent to the WT OR eye phenotype. (D) A *UAS-mid-RNAi/+;GMR-Gal4/TM6* (*mid-RNAi*) eye exhibits a ~60% loss of IOBs and disorganized ommatidia. (E) Placing the heterozygous *emc^{1}* mutant allele in the *mid-RNAi* background to generate a *UAS-mid-RNAi/+;GMR-Gal4/emc^{1}* eye partially suppresses the mutant IOB phenotype observed by a ~25% increase in IOBs, partially recovers the integrity of the ommatidial array and partially restores pigmentation. (F-H) scanning electron micrograph images of eyes from selected F1 progeny show greater details of IOBs and ommatidial arrangements. (F) The *+/CyO;GMR-Gal4/emc^{1}* eye depicts a few duplicated bristles within the center. (G) The *mid-RNAi* eye exhibits large regions of IOB loss, ommatidial fusion and remaining IOBs are disorganized. (H) Although a few ommatidia are fused (inset) and there appear to be size differences among them, the *UAS-mid-RNAi/+;GMR-Gal4/emc^{1}* eye exhibits a significant recovery of IOBs throughout the eye field. The ommatidia of the *UAS-mid-RNAi/+;GMR-Gal4/emc^{1}* represented in (H) were counted and were approximately equal in number (701 counted) to ommatidia of WT OR eyes (750 counted). (I) The bar graph represents mean bristle numbers +/- SEM quantitated for 10 eyes for each F1 genotype shown in panels A-E as well as additional genotypes generated from the cross including *+/CyO;emc^{1}/TM3*, *UAS-mid-RNAi/+;TM3/TM6* and *+/CyO;TM3/TM6*. Comparisons of data are indicated by *brackets* linking specific data sets. The full genotype of the mutant *emc^{1}* allele is *emc^{1}P{neoFRT}80B*. (J) A table with columns labeled 1-8 in the left top corners represents the mean IOB numbers +/- the SEM

for each genotype represented in the bar graph. The inhibition of bristle numbers in *mid*-RNAi mutants was statistically significant comparing columns 1-6 versus (vs) 7 where ***$p < 0.0001$. The suppression of IOB loss observed in *mid-RNAi* eyes in the absence of one functional copy of *emc* was also statistically significant comparing column 7 vs 8 where ***$p < 0.0001$. Statistical analyses were performed using Shaprio-Wilk's test and the Student's t-test as detailed in methods.

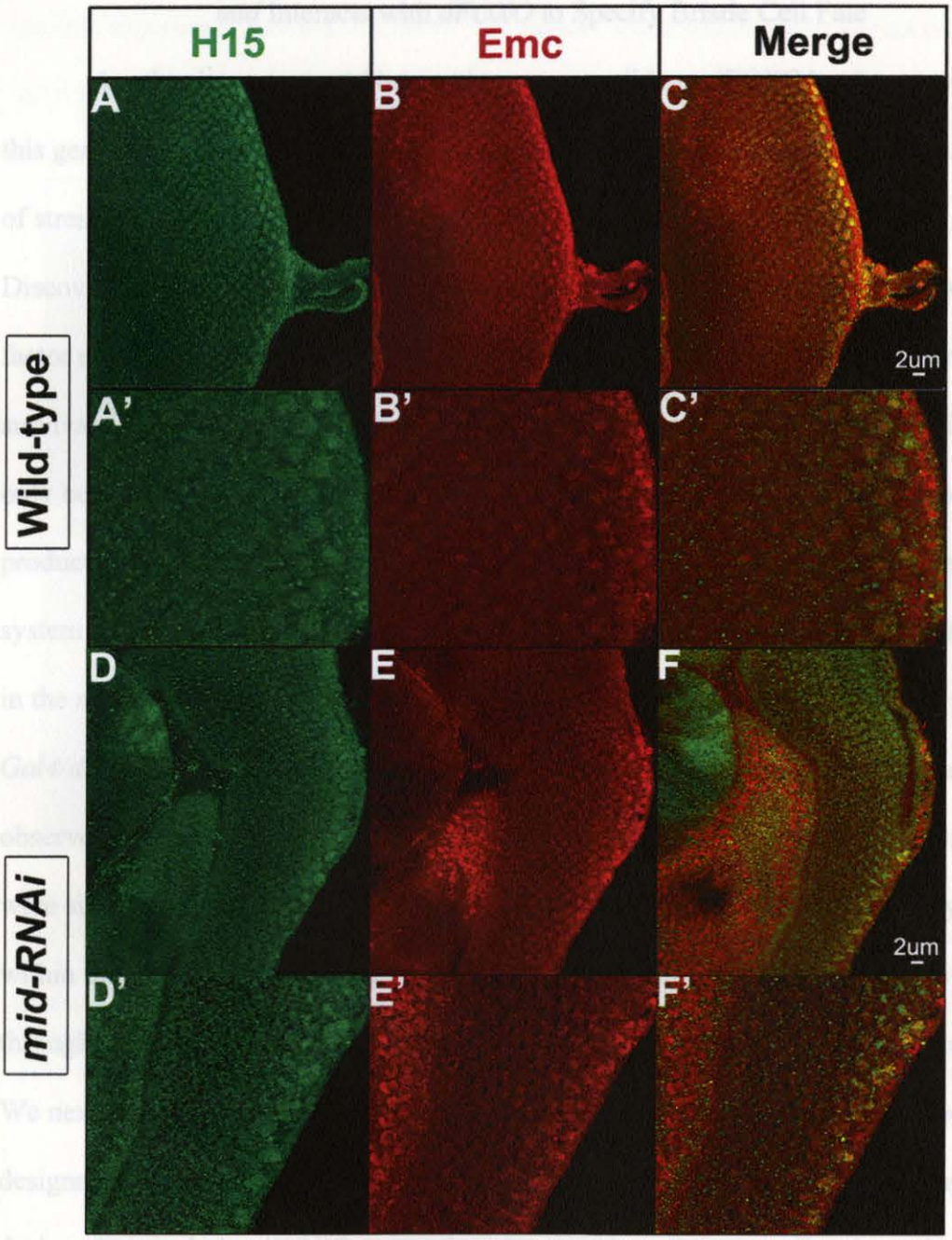

Figure 15 mid does not regulate the expression of extramacrochaetae. confocal image of a P2-staged WT pupal eye disc co-immunolabeled with (A) anti-H15 (green) and (B) anti-Emc (red) antisera shows that (C) H15 and Emc are co-expressed within numerous cells of the disc (merge). (A'-C') Higher magnification images of panels A-C. (D) A P2-staged *mid-RNAi* pupal eye disc also co-immunolabeled with (D) anti-H15 (green) and (E) anti-Emc antisera (red) depicting reduced H15 expression while (F) the level of Emc expression is unchanged (merge) (F). (D'-F') Higher magnification images of panels D-F from the boxed region shown in panel F.

mid Interacts with *dFOXO* to Specify Bristle Cell Fate

Another important *mid*-interacting gene candidate, *dFOXO* has been uncovered in this genetic modifier screen. dFOXO is a transcription factor regulated by the activation of stress-induced pathways involving the insulin receptor (InR) and Dp53 [117]. Discovering *dFOXO* as a *mid* interacting gene emphasizes that the Mid/H15 transcription factor regulatory network involves not only cell fate specification but also promotes cell survival. The latter relationship associates a novel survival function for H15/Mid that has only been reported for one T-box gene, *T-bet*, which has been shown to regulate cytokine production under conditions of stress in differentiating T-helper cells within the immune system of the mouse [118]. We placed a heterozygous mutant allele of *dFOXO*, $dFOXO^{25}$, in the *mid-RNAi* sensitized background to determine whether *UAS-mid-RNAi/+;GMR-Gal4/*$dFOXO^{25}$ flies recapitulated the suppression of the mutant eye bristle phenotype observed in *UAS-mid-RNAi/+;GMR-Gal4/Df(3R)ED5634* flies, We observed that bristles were significantly increased in *UAS-mid-RNAi/+;GMR-Gal4/*$dFOXO^{25}$ adult eyes except within the center of the eye (Figure 16G,I). The deposition of pigment was also recovered throughout the adult eyes of *UAS-mid-RNAi/+; GMR-Gal4/*$dFOXO^{25}$ flies (Figure 16G). We next placed a semi-lethal mutant allele of *dFOXO in the mid-RNAi* background designated $dFOXO^{EY16506}$. The $dFOXO^{EY1650Y}$ line is one of several enhancer trap lines designed to track the *dFOXO* expression pattern using a surrogate B-galactosidase reporter gene inserted downstream from the *dFOXO* enhancer region. *The* $dFOXO^{EY1650Y}$ P-element insertion is also located approximately 18 kb from the *dFOXO* promotor region before the coding region for the *dFOXO transcription factor* DNA-binding motif. Placing $dFOXO^{EY1650Y}$ in a heterozygous state in the *mid-RNAi* background partially recovered bristles (Figure 16 H, I) indicating that the C-terminal domain of the *dFOXO*

protein expressed from the *dFOXO*^{EY1650Y} mutant allele retained partial functional activity. These results identify *dFOXO* as a novel mid-interacting gene.

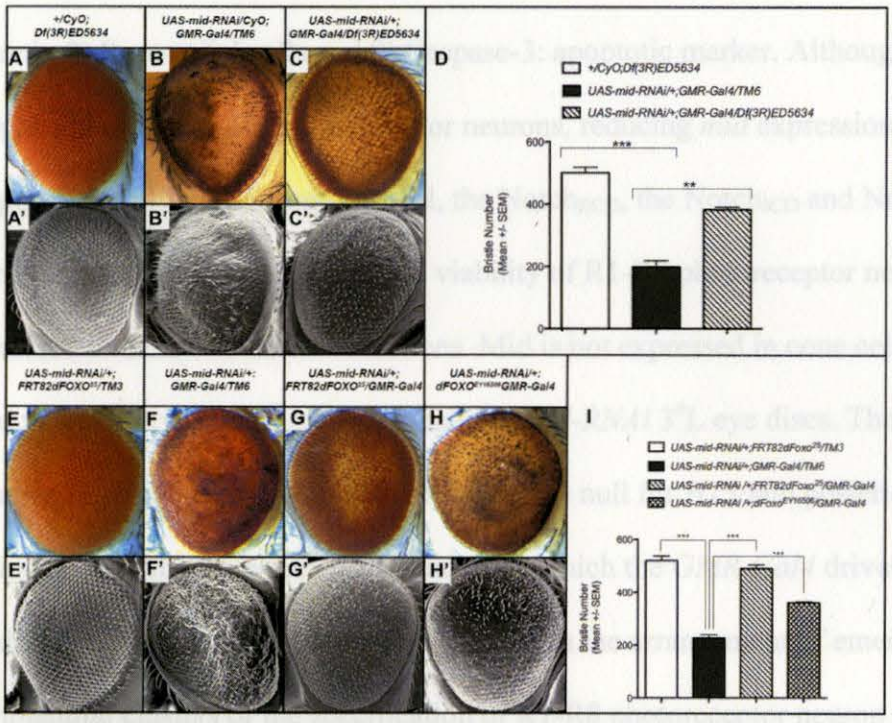

Figure 16. dFOXO collaborates with mid to regulate interommatidial bristle formation. (A) WT and (B) *mid-RNAi* compound eyes exhibit features previously described (Figure 9). (C) Placing *mid-RNAi* in a heterozygous *Df(3R)ED5634* background suppresses the mutant phenotype with a partial recovery of bristles. (D) The bar chart represents mean bristle numbers +/- SEM quantitated for 10 eyes per experimental group. Student's T-Test analyses indicated a significant decrease in bristles. The SEM images were obtained by Yan Zong.

Mid Does not Regulate the Specification, Assembly, Spacing, or Viability of Cone Cells and R1-R8 Clusters within Third-Instar Larval and Early-staged Pupal Eye Imaginal Discs

To identify specific cellular structures affected by the reduction of *mid*, we examined a wide range of antibody probes against different cytoplasmic and nuclear proteins both in WT and staged-matched *mid-RNAi* third-instar larval eye discs. Marker proteins are listed as follows: 1) Elav, Lozenge and Atonal: photoreceptor neurons,

2) Cut: cone cells, 3) D- and E-Cadherin, Armadillo: adhesion proteins, 4) Actin: the cytoskeleton, 5) Notch receptors: the Notch Extracellular Domain ($Notch_{ECD}$) and $Notch_{ICD}$, 6) Notch-specific ligands: Delta and Scabrous (Sca), 7) A Notch antagonist: Numb, 8) Repo: glial cells and 9) Caspase-3: apoptotic marker. Although Mid is expressed in the R1-R8 photoreceptor neurons, reducing *mid* expression did not affect the expression of Elav, Lozenge, Atonal, the $Notch_{ECD}$, the $Notch_{ICD}$ and Numb. The arrangement, adhesion, spacing and viability of R1-R8 photoreceptor neurons were also unaffected under *mid-RNAi* conditions. Mid is not expressed in cone cells or glial cells and these cell types developed normally in *mid-RNAi* 3°L eye discs. The co-expression studies were validated by inducing LOF clones null for *H15/mid* posterior of the MF to coincide with the developmental window in which the *GMR-Gal4* driver was activated and within the MF. We observed no changes in the arrangement of emerging pre-ommatidial clusters or the specification of R1-R8 photoreceptor neuron clusters in *mid-RNAi* 3°L eye discs (data not shown).

Under *mid-RNAi* conditions, however, we detected a minor reduction of Delta (Figure 17) and Sca expression (Figure 18) in cells posterior of the MF. We generated *H15/mid* LOF clones within and posterior of the MF and also detected minor reductions in Delta (Figure 17) and Sca expression (Figure 18). It is plausible that the Serrate ligand, also specific for Notch, may have redundantly compensated for sub-threshold levels of Delta and Sca ligands required for the specification of the R8 photoreceptor neuron under *mid-RNAi* and *H15/mid* null conditions [54,77]. *H15/mid* null clones generated in the posterior-most domains of the larval eye imaginal disc expressed normal expression levels of Delta, Notch and Numb (data not shown).

Using specific antibody probes, we repeated co-expression analyses of Mid in combination with Elav, $Notch_{ECD}$, Numb and Cut in *mid-RNAi* pupal discs at the P2 stage. The expression patterns of these proteins were unaffected in *mid-RNAi* discs compared to WT discs (data not shown). As such, reducing *mid* expression during the 3^{o}L-P2 stages can at least allow for permissive Notch signaling. A reciprocal cross-regulatory inhibition mechanism occurring between *mid* and *Notch* remains to be examined.

Recently, *cis*-regulatory modules for Tbx-16 were identified upstream of the Zebrafish *delta-c* gene [119]. Based upon this related study providing new evidence linking vertebrate T-box TF activity to the regulated expression of a *delta* homolog and from the analyses of the preliminary data we gathered from the *mid-RNAi* eye phenotype and *H15/mid* LOF studies detecting minor reductions in the expression of Delta and Sca, we next examined whether *mid* functions downstream of the *Notch-Delta* to regulate the specification of SOP cells during early pupal stages. The identification of *emc* as a *mid*-collaborating gene further catalyzed continued genetic studies to place *mid* within the *Notch-Delta* genetic hierarchy specifying SOP cell fates.

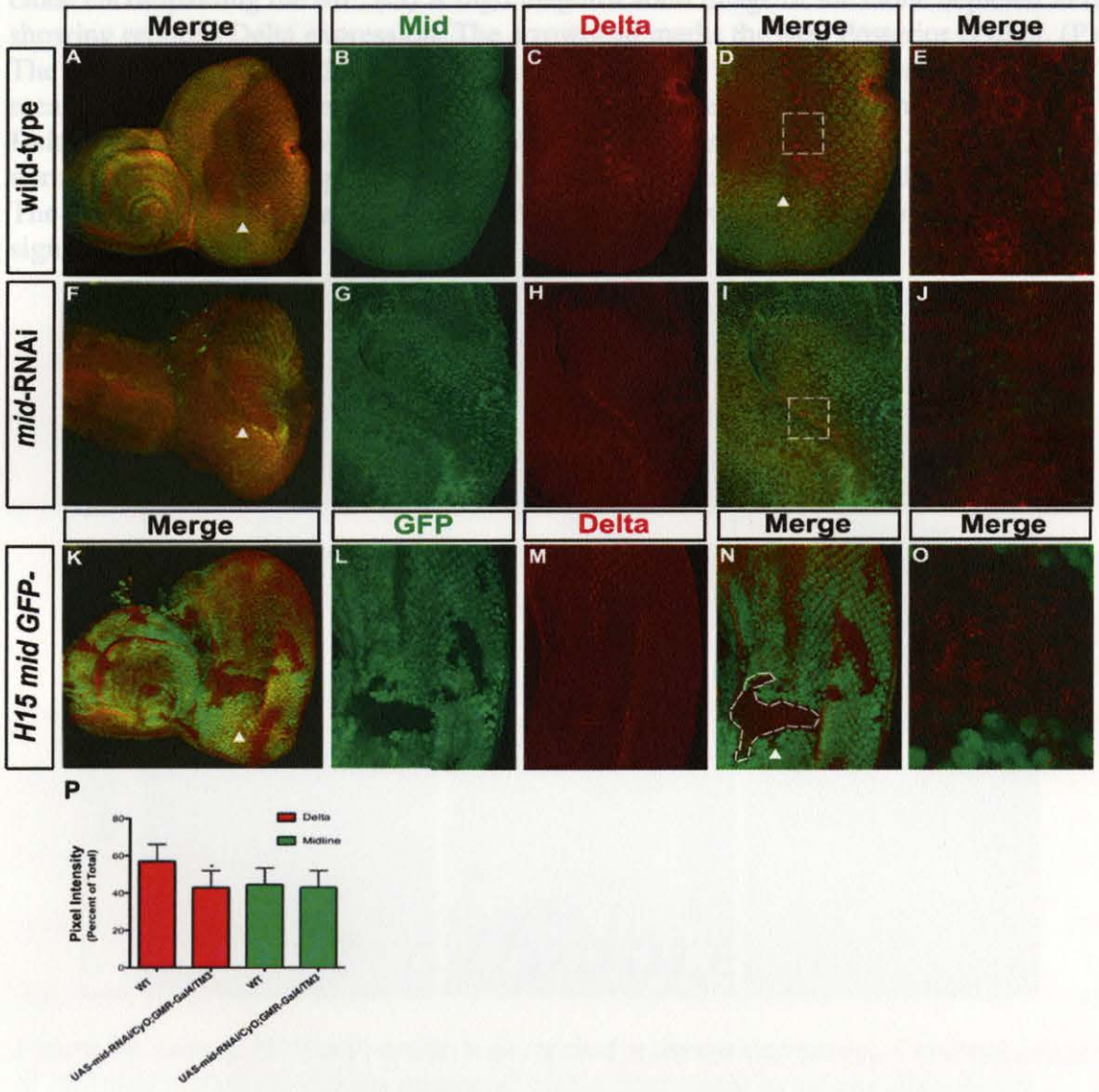

Figure 17. Loss of H15/mid results in decreased Delta expression within proneural clusters posterior of the MF. Confocal image of a (A) WT eye discs co-immunolabeled with anti-Mid and anti-Delta antisera. (B) A higher magnification depicts Mid expression (green) within photoreceptor neuron clusters posterior of the MF. (C) Delta (red) predominantly labels proneural clusters within the furrow. (D) A merged image of (B) and (C) where the *dashed white box* is magnified in (E) to show Delta expression within the plasma membranes of clustered proneural cells. (F) A *mid*-RNAi disc co-immunolabeled with anti-Mid and anti-Delta antisera. (G) A higher magnification of panel F detects non-specific Mid binding (green) to cells of the squamous epithelial cell layer. (H) Delta (red) is expressed within a narrow band of cells in vaguely defined furrow. Proneural clusters are not detected by Delta labeling. (I) A merged image of (G) and (H) where the dashed white box is magnified in (J). (K) *H15/mid* LOF clones (*-GFP*) generated within the eye disc are numerous. (L) A *H15/mid* clone (*-GFP*) immunolabeled with (M) anti-Delta antibody exhibits reduced expression of Delta (red). (N) Representation of the merged image from (L) and (M). The dashed white box outlines a

clone encompassing the MF. (O) A high magnification image of the clone depicted in (N) showing reduced Delta expression. The arrowhead marks the MF. Posterior is right. (P) The bar chart represents the mean intensity +/- the SEM of fluorophore emission measured in pixels for the 488 nm signal detecting Mid and the 594 signal detecting Delta within the MF of WT (n=3) and *mid-RNAi* eye imaginal discs (n=3). Each value is normalized as a percentage of the total signal intensity emitted from both immunofluores. The Delta signal is reduced within *mid-RNAi* eye discs with a marginal degree of significance (*$p < 0.01$).

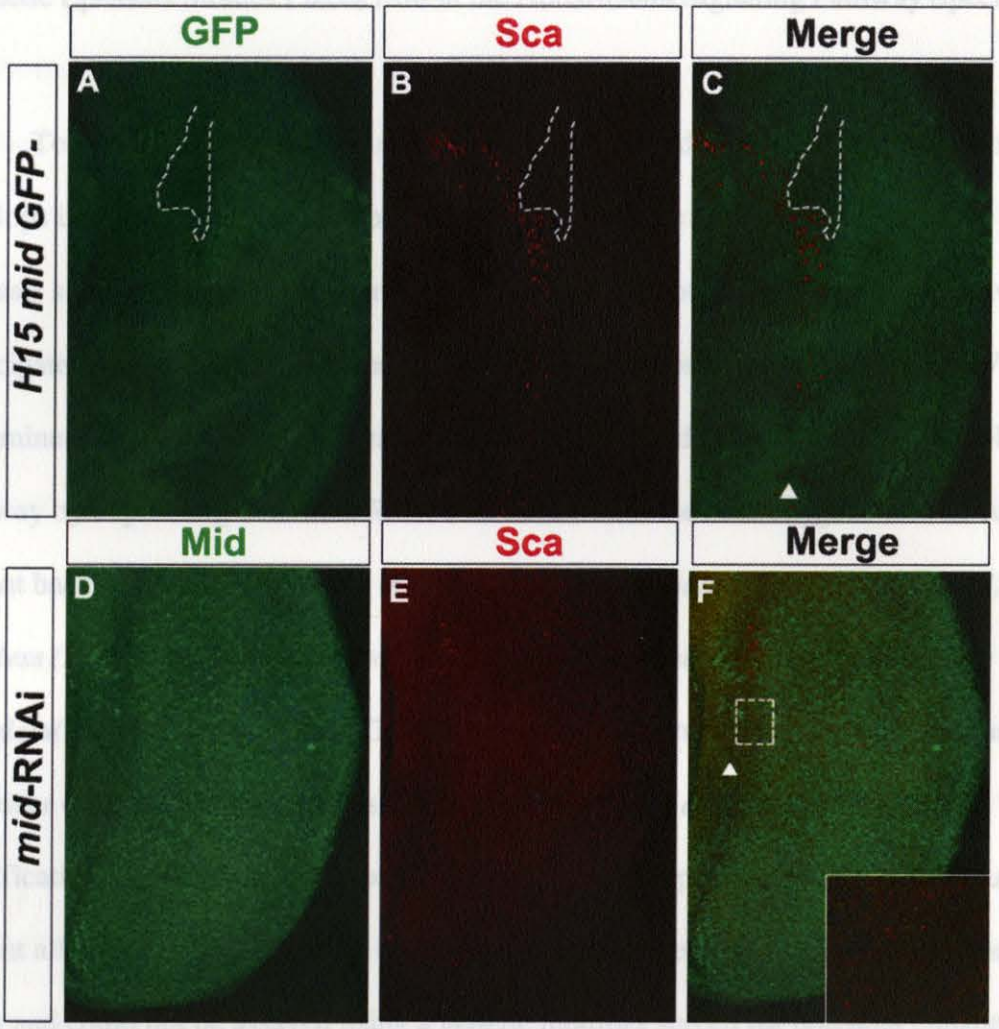

Figure 18. Loss of H15/mid results in decreased scabrous expression. Confocal images of *H15/mid* mutant conditions generated within third-instar larval eye discs depict changes in Sca expression. (A) Several large *H15/mid* LOF clones are detected (*-GFP*) and one clone spans a large region of the MF (dashed outline). (B) The discs are immunolabeled with anti-Sca (red) antibody and detect a WT expression pattern of Sca in the MF within proneural clusters as well as within R8 cells posterior of the furrow emerging from the clusters. *H15/mid* clones lack Sca expression (dashed outline). (C) A merged image of (A) and (B) depicts a clone with significantly reduced Sca expression (dashed line). A *mid-RNAi* mutant disc co-immunolabeled with (D) anti-Mid and (E) anti-Sca antisera also exhibits reduced *Sca* expression (red) within the MF depicted in the merged image (F) and within an enlarged area of the MF (inset). The arrowhead marks the MF.

Genetic Epistasis Studies Places Mid in the Notch-Delta Signaling Pathway Specifying SOP Cells

To test the hypothesis that *mid* regulates cell fates during the specification of SOP develops into an interommatidial bristle cell (IOB) complexes we initiated genetic epistasis studies. As mentioned earlier, members of the Notch-Delta signaling pathway participate in SOP cell fate decisions either as a negative or a positive influence. We determined whether there are interactions between *mid* and members of the Notch-Delta pathway by expressing *UAS-mid-RNAi* construct within the heterozygous loss-of-function mutant background of *Suppressor of Hairless Su(H)^{1}, Enhancer of Split E(Spl)-m8, Hairless (H^{1}), hairy(h^{1}), atonal(ato^{1}) , daughterless(da), achaete(ac^{1}) and senseless(sen^{E2})* driven by GMR-Gal4 in the eye tissue. The *hairy* gene functions as a repressor of proneural gene expression in the PNS [120] and *ato* functions in the specification of the R8 photoreceptor neuron [121,122]. As expected, a range of heterozygous mutant alleles of *Notch, Delta, da* and the *ac-sc* complex exhibited a significant loss of IOBs and could not be assayed using a genetic modifier screen for potential enhancement of the *mid-RNAi* mutant phenotype. However, *Su(H)^{1}*, *H^{1}*, *h^{1}*, *ato^{1}*, *da^{1}*, *ac^{1}* and *sens^{E2}* heterozygous mutant alleles exhibited normal bristle numbers compared to WT flies and were each independently crossed to *mid-RNAi* flies (data not shown). With the exception of *da^{1}* and *ac*^{1}, all other alleles represent LOF mutations; *da^{1}* and *ac^{1}* are hypomorphic alleles; (flybase.org). Of the mutant heterozygous alleles assayed, the neurogenic genes *ato^{1}* (Figure 19) and *sens^{E2}* (Figure 20) significantly suppressed the *mid-RNAi* phenotype. Placing *Su(H)^{1}*, *h^{1}*, *da^{1}* or *ac^{1}*heterozygous mutant alleles within the *mid-RNAi* background did not modify the mutant phenotype (data not shown). However, we cannot completely rule out their interaction with *mid* given the dosage constraints of the modifier

assay. As previously shown using immunolabeling methods, Ac expression was significantly reduced within SOP cells of *mid-RNAi* pupal discs (Figure 13). Taken together, the immunolabeling expression analyses and genetic studies place *mid* upstream of *E(Spl)*, in parallel with *Su(H)* and *H* and epistatic to the Notch-Delta lateral inhibition pathway specifying SOP cell fates (Figure 21A).

We must account for a contribution of bristle loss by the *GMR-Gal4* driver line. Several combinations of heterozygous mutant alleles and the *GMR-Gal4* line resulted in a ~10-18% decrease in bristles (Figures 14, 18, 19). The most significant decrease of bristles by 25% occurred in $+/H^{1}$; *GMR-Gal4/TM3* flies (Figure 22). As such, we could not assay H^{1} as a modifier of the *mid-RNAi* mutant phenotype with certainty due to this background effect although *UAS-mid-RNAi*/H^{1}; *GMR-Gal4/TM3* flies also showed a 25% reduction of bristles tentatively negating a contribution of *H* (Figure 22). The contribution of the *GMR-Gal4* transgene to bristle loss may be due to at least two biological possibilities. The *GMR-Gal4* transgene insertion site may be disrupting an enhancer region that regulates the expression of one or more genes essential for bristle formation and/or cell viability. Alternatively, the Gal4 TF may be activating endogenous enhancer regions independently of the UAS target site as reported recently in wing disc development [123]. These effects of a biological nature did not significantly impact the results or interpretation of the genetic modifier study. The suppression levels we quantified for reported mutant alleles are conservative estimates of bristle recovery. Moreover, by removing one copy of each mutant allele screened, dosage effects in the genetic modifier assay are half-maximal. In theory, null mutations would result in a greater suppression or recovery of IOBs.

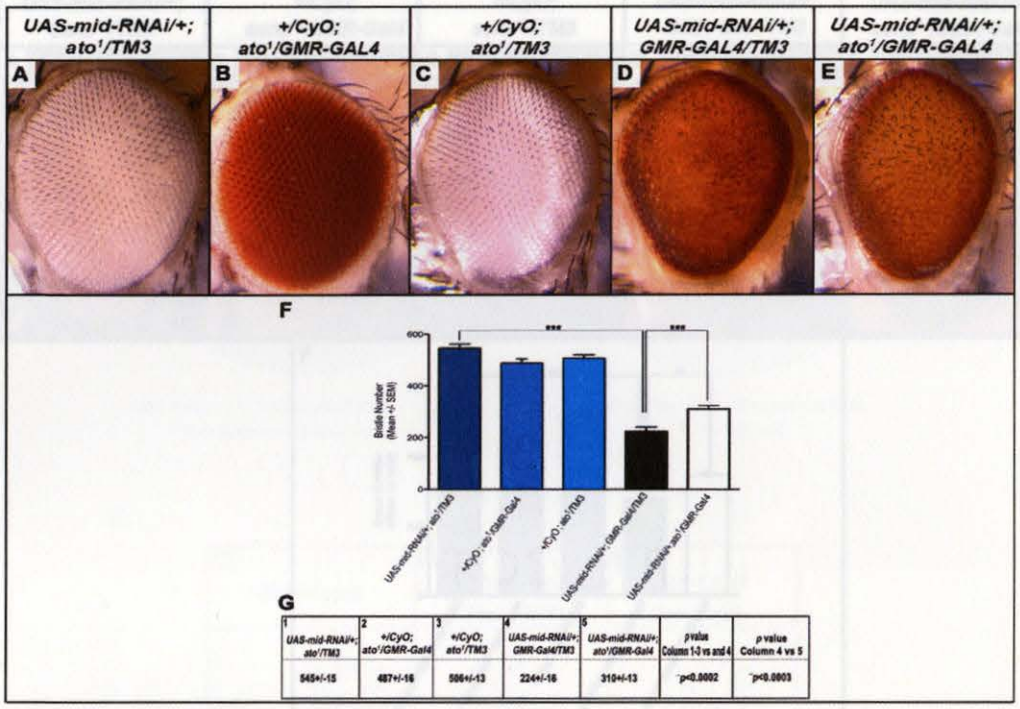

Figure 19. mid collaborates with atonal to regulate interommatidial bristle generation. (A-E) Light microscope images at 120X magnification depict (A) *UAS-mid-RNAi/+;ato^{1}/TM3*, (B) *+/CyO;ato^{1}/GMR-Gal4* and (C) *+/CyO;ato^{1}/TM3* eyes of F1 progeny exhibiting an ommatidial array and numbers of IOBs that are nearly equivalent to the WT OR eye. (D) A *UAS-mid-RNAi/+; GMR-Gal4/TM3* (*mid-RNAi*) eye exhibits a significant loss of IOBs by ~59% and disorganized ommatidia. (E) Placing the heterozygous *ato^{1}* mutant allele in the *mid-RNAi* genetic background to generate a *UAS-mid-RNAi/+; GMR-Gal4/ato^{1}* eye partially suppresses the mutant IOB phenotype with a ~16% gain of IOBs. The integrity of the ommatidial array is not restored and remaining IOBs are disorganized. (F) The bar graph represents mean bristle numbers +/- SEM quantitated for 10 eyes per each F1 genotype shown in panels A-E. Comparisons of data are indicated by *brackets* linking specific data sets. (G) A table with columns labeled 1-5 in the left top corners represents the mean IOB numbers +/- the SEM for each genotype represented in the bar graph. The inhibition of bristle numbers in *mid*-RNAi mutants was statistically significant comparing columns 1-3 versus (vs) 4 where ***$p < 0.0002$. The suppression of IOB loss observed in *mid-RNAi* eyes in the absence of one functional copy of *ato* was also statistically significant comparing column 4 vs 5 where ***$p < 0.0003$. Statistical analyses were performed using Shaprio-Wilk's test and the Student's t-test as detailed in methods.

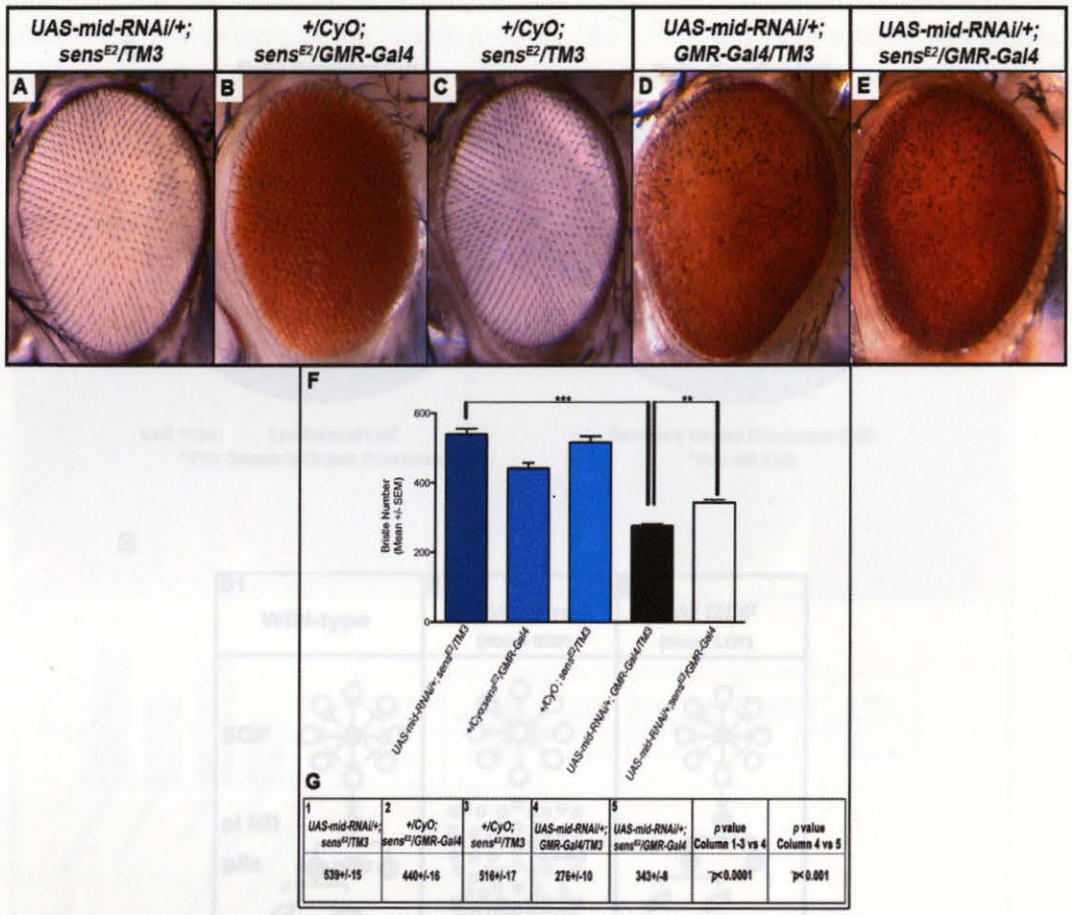

Figure 20. mid collaborates with senseless to regulate interommatidial bristle generation. (A-E) Light microscope images at 120X magnification depict (A) *UAS-mid-RNAi/+;sens^{E2}/TM3*, (B) *+/CyO;sens^{E2}/GMR-Gal4* and (C) *+/CyO;sens^{E2}/TM3* eyesF1 progeny. While eyes depicted in panels (A) and (C) exhibit an ommatidial array and numbers of IOBs that are nearly equivalent to the WT OR eye, placing a heterozygous mutant allele of (B) *sens^{E2}* in the *GMR-Gal4* background results in an ~18% loss of IOBs which is significant. (D) A *UAS-mid-RNAi/+;GMR-Gal4/TM3* (*mid-RNAi*) eye exhibits an ~49% loss of IOBs and disorganized ommatidia. (E) Placing the heterozygous *sens^{E2}* mutant allele in the *mid-RNAi* genetic background to generate a *UAS-mid-RNAi/+;GMR-Gal4/sens^{E2}* eye partially suppresses the mutant IOB phenotype exhibited by a ~14% increase in IOBs. However, the ommatidial array and remaining IOBs are disorganized. (F) The bar graph represents mean bristle numbers +/- SEM quantitated for 10 eyes per each F1 genotype shown in panels A-E. Comparisons of data are indicated by *brackets* linking specific data sets. The full genotype of the mutant *sens^{E2}* allele is *sens^{E2}red^{1}e^{1}*. (G) A table with columns labeled 1-5 in the left top corners represents the mean IOB numbers +/- the SEM for each genotype represented in the bar graph. The inhibition of bristle numbers in *mid*-RNAi mutants was statistically significant comparing columns 1-3 versus (vs) 4 where ***$p < 0.0001$. The suppression of IOB loss observed in *mid-RNAi* eyes in the absence of one functional copy of *sens* was also statistically significant comparing column 4 vs 5 where **$p < 0.001$. Statistical analyses were performed using Shaprio-Wilk's test and the Student's t-test as detailed in methods.

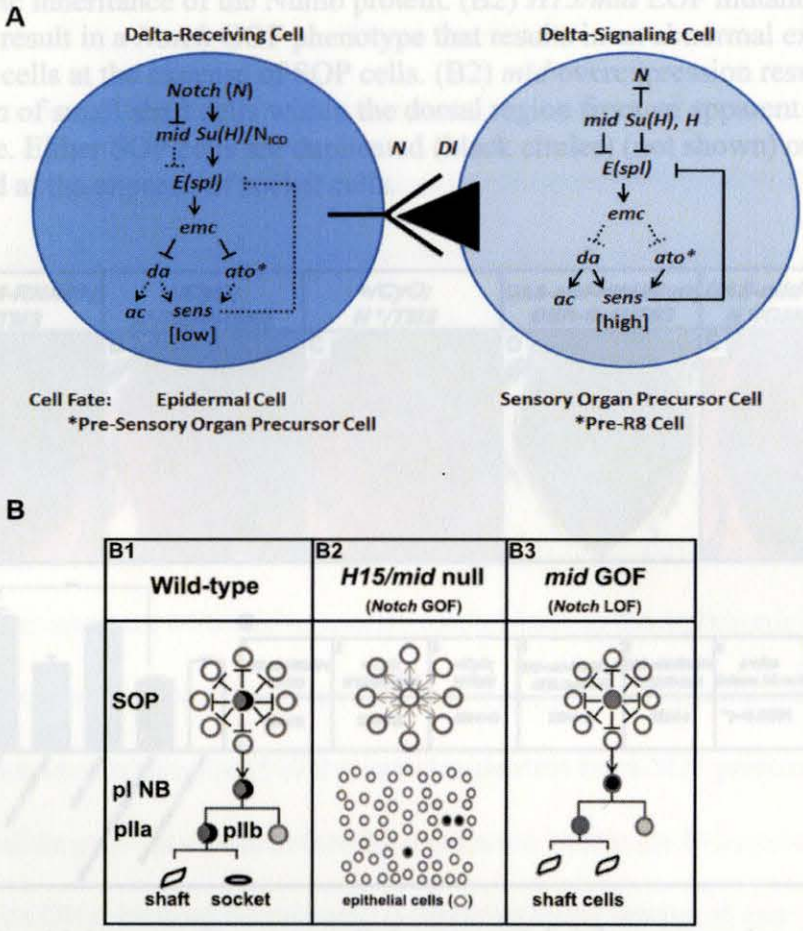

Figure 21. Schematics of the Notch-Delta genetic pathway of SOP specification and some cells of the SOP lineage. (A) Notch (N) signaling is inhibited in the sensory organ precursor cell (right) by the co-repressors Su(H) and H that inhibit *E(spl)* expression. (B) We conjecture that this leads to the potential reduction of *emc* expression or change in Emc activity. With Emc inactive, a subsequent increase in Da as well as increased *ac*, *ato*, and *sens* gene expression occurs. High levels of Sens further activate *ac* expression. *We propose that *ato* expressed in the pre-R8 cell ensures the early specification of neighboring pre-SOP cells during 3^{o}L stages in a cell non-autonomous manner where terminal specification events are later consolidated by Delta signaling during the P0-P2 stages. Conversely, in the Delta-receiving cell (left) Notch signaling is active. Su(H) and the N_{ICD} activate *E(spl)* expression. E(Spl) then positively modulates either *emc* expression or Emc activity. Emc can now physically sequester Da and Ato resulting in reduced proneural (*ac*) and neurogenic gene (*sens*) expression. Low levels of Sens also are predicted to inhibit *ac* expression. (B) A series of Notch-Delta signaling events illustrated in schematics compares WT and *mid* mutant conditions in the generation of SOPs and SOP daughter cells. (B1) Under WT conditions, lateral inhibition by Notch-Delta signaling results in the generation of a pI neuroblast from an SOP while neighboring cells assume the default epidermal fate. The pI neuroblast divides giving rise to the pIIa and pIIb cells. The pIIa cell divides to generate the shaft and socket cells. The

black crescent shown in the SOP cell, pI neuroblast and pIIa precursor cell depicts the asymmetric inheritance of the Numb protein. (B2) *H15/mid* LOF mutant conditions appear to result in a *Notch* GOF phenotype that results in an abnormal expansion of epithelial cells at the expense of SOP cells. (B2) *mid* overexpression results in the generation of small shaft cells within the dorsal region from an apparent *Notch* LOF phenotype. Either SOP cells are duplicated (black circles) (not shown) or shaft cells are duplicated at the expense of socket cells.

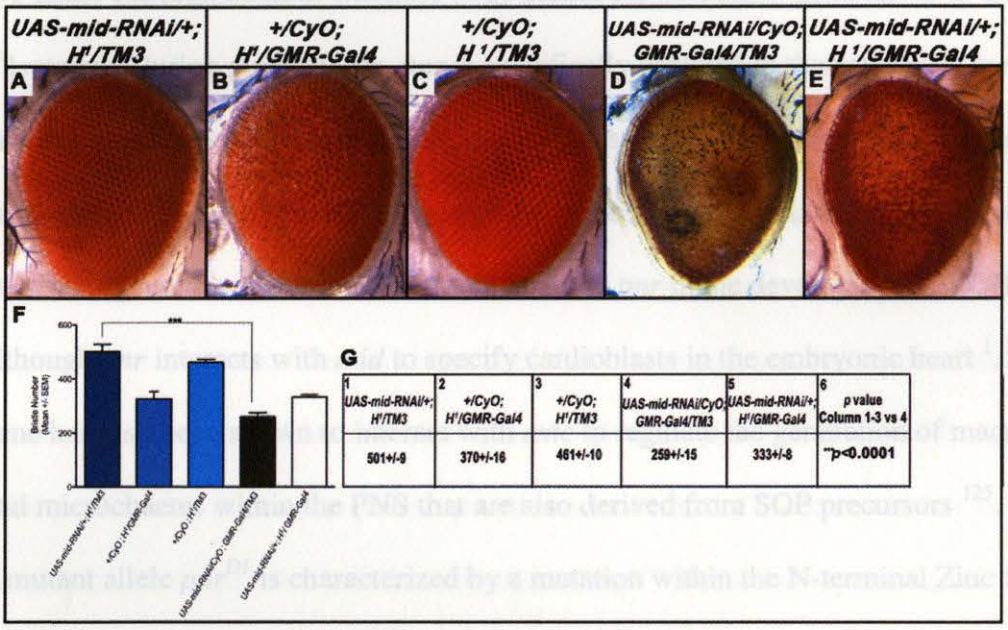

Figure 22. mid does not appear to collaborate with hairless to regulate interommatidial bristle generation. (A-E) Light microscope images at 120X magnification of WT and mutant eyes. (A) The *UAS-mid-RNAi/+;H^{1}/TM3* eye appears WT whereas the (B) *+/CyO;H^{1}/GMR-Gal4* eye appears to have lost IOBs and is exhibiting a background effect. (C) The *+/CyO;H^{1}/TM3* eye appears WT also exhibiting a normal ommatidial array and IOB numbers. (D) A *UAS-mid-RNAi/+;GMR-Gal4/TM3* (*mid-RNAi*) eye exhibits a significant loss IOBs by ~48% and disorganized ommatidia. (E) A *UAS-mid-RNAi/+;GMR-Gal4/H^{1}* eye shows that the *H^{1}* allele has no effect on the *mid-RNAi* phenotype compared with (B). (F) The bar graph represents mean bristle numbers +/- SEM quantitated for 10 eyes per each F1 genotype shown in panels A-E. Comparisons of data are indicated by brackets linking specific data sets. (G) A table with columns labeled 1-5 in the left top corners represents the mean IOB numbers +/- the SEM for each genotype represented in the bar graph. The inhibition of bristle numbers in *mid*-RNAi mutants was statistically significant: columns 1-3 versus (vs) 4 where $***p < 0.0001$. Statistical analyses were performed using Shaprio-Wilk's test and the Student's t-test as detailed in methods.

Mid Does not Collaborate with Pannier to Regulate Bristle Complex Formation in the Pupal Eye Disc

pannier (pnr) is a GATA transcription factor expressed within a narrow peripheral margin of the dorsal half of the disc and establishes the dorsal margin of the eye under the regulation of *wingless* (*wg*) during the mid third-instar larval (3^{o}L) and late 3^{o}L stages. During pupal stages, *pnr* is specifically detected in the peripodial membrane that eventually gives rise to dorsal head structures near the adult eye and is not expressed in the retina [124]. Based upon the reported *pnr* expression pattern, we did not expect to uncover a genetic collaboration between *mid* and *pnr* in the development of IOBs although *pnr* interacts with *mid* to specify cardioblasts in the embryonic heart [1]. The *pnr* gene has also been shown to interact with *emc* to regulate the generation of macrochaetes and microchaetes within the PNS that are also derived from SOP precursors [125]. The class 4 mutant allele pnr^{D1} is characterized by a mutation within the N-terminal Zinc finger region of its DNA binding domain and is sensitive to the dosage of *emc* [126]. With decreasing copies of *emc* in pnr^{D1} mutants, additional dorsocentral (DC) bristles in the notum are observed and inversely, increasing copies of *emc* results in a loss of DC bristles [125]. The class 3 dominant allele pnr^{vx4} mutation is characterized by a loss of its C-terminal α helices and reduced *ac-sc* expression resulting in the loss of bristles [126]. The pnr^{vx4} gene functions independently of *emc* [125,127,128]. We placed each of these functionally diverse *pnr* mutant alleles within the *mid-RNAi* background and IOB numbers were not significantly affected (data not shown). Conversely, we misexpressed *pnr* in the *mid-RNAi* background and did not detect a modification of the bristle phenotype (data not shown). These studies validate that *mid* does not collaborate with *pnr* to specify SOP cells, affirming the specificity of the allelic modifier screen on a *mid* LOF

mutation. Since the previous research showed that *mid* functions as a selector gene in specification of the ventral cell fate downstream of Wingless and Decapentaplegic signaling pathway in the developing leg disc of *Drosophila* [129]. Moreover our observations suggest that *mid-RNAi* mutant eye disc exhibited a more severe loss of bristle cells in the ventral part of the eye. This information indicates that *mid* might work as a ventral selector gene.

A *mid* GOF Mutation Results in Multiple Cellular Defects in the Adult Eye

Generating *mid* GOF mutants using the *GMR-Gal4* driver and the UAS-Gal4 system resulted in an excess of small, trichome-like shaft cells in the posterior-dorsal region of the adult eye. The data suggested that overexpressing *mid* resulted in a phenocopy of a *Notch* LOF mutation at the level of the pIIa cell (Figure 23). Misspecification of the pIIa precursor cells under *Notch* LOF conditions has been shown to give rise to small bristle shafts without sockets [130]. Since misexpressing *mid* caused perturbing defects in eye development including loss of bristles, bristle defects and ommatidial fusion, attempts to rescue the *UAS-mid-RNAi* mutant phenotype by overexpressing *mid* in the *mid-RNAi* background with a range of *UAS-mid* constructs were not effective given the overlap of pleiotropic phenotypes. Of the *UAS-mid* transgenes assayed, one provided a dosage of *mid* expression that, albeit incomplete, partially rescued bristle numbers to normal levels observed in WT flies (Figure 24).

We considered the possibility that a necessary co-factor or perhaps several co-factors may be required to fully rescue the *mid-RNAi* bristle phenotype. The most essential co-factor required for optimal *mid* activity would likely be its paralog, *H15*. Contrary to this hypothesis, however, overexpression of *H15* in the *mid-RNAi* genetic background resulted in pupal lethality. We did not obtain surviving *UAS-mid-RNAi/UAS-*

H15;*GMR-Gal4/+* progeny. These results indicate that the expression level and dosage-dependent activity of both *H15* and *mid* must be strictly regulated to achieve the perfect ratio of Notch-Delta signaling to induce a lateral inhibition mechanism. The effect of overexpressing *H15* alone in the eye disc also results in lethality (data not shown). However, in the embryonic CNS overexpressing *H15* in neurons with the *Elav-Gal4* driver did not effect *mid* expression or the development of cells in the ventral nerve cord [4]. Conversely *H15* mutant flies are viable, exhibiting no obvious defects in eye development or IOB bristle generation (data not shown).

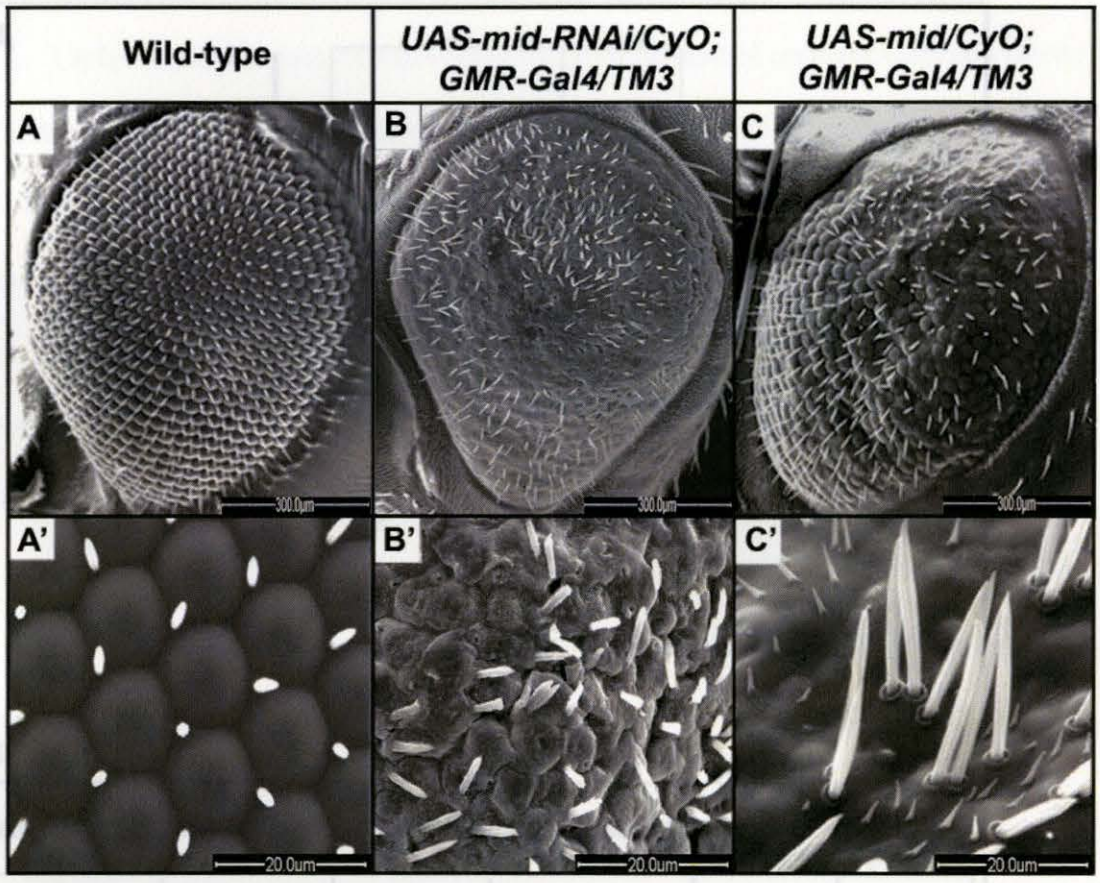

Figure 23 A mid gain-of-function mutation exhibits some features that are similar to a Notch Loss-of-Function phenotype. (A-C) Scanning electron micrographs of one-day old adult eyes depicting (A) a WT compound eye with a regular pattern of ommatidia and IOBs; Panel A' is an enlarged image. (B) A *mid-RNAi* eye showing mutant features previously described; Panel B' is an enlarged image. (C) A *UAS-mid/CyO; GMR-Gal4/TM3* mutant eye illustrates a variety of bristle defects within the dorsal-posterior region of the eye, major areas of ommatidial fusion throughout the eye field and IOB loss. (C') An enlarged image of panel B depicts an excess of socketless, small shaft cells and duplicated IOB complexes that exhibit otherwise normal features. These phenotypes are indicative of a potential *Notch* LOF phenocopy at the level of the SOP where IOBs are duplicated and the pIa daughter cell generates bristles at the expense of sockets (Figure 20C). Scale bars measure lengths in micrometers. This study was accomplished by Brandon Drescher.

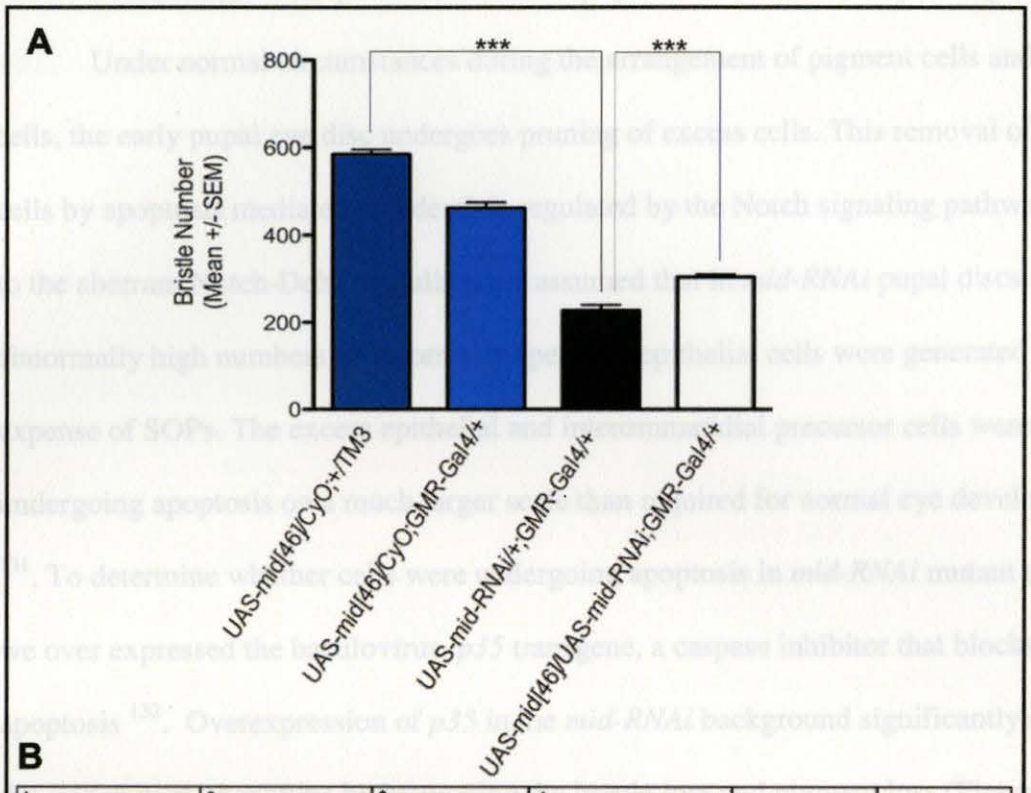

B

1 UAS-mid[46]/CyO; +/TM3	2 UAS-mid[46]/CyO; GMR-Gal4/+	3 UAS-mid-RNAi/+; GMR-Gal4/+	4 UAS-mid[46]/UAS-mid-RNAi; GMR-Gal4/+	p value Column 2 vs 3	p value Column 4 vs 5
584+/-10	461+/-14	226+/-12	303/-6	***p<0.0001	***p<0.0001

Figure 24. Overexpressing a UAS-mid transgene partially recovers the mid-RNAi mutation. (A) The bar graph represents mean bristle numbers +/- SEM quantitated for 10 eyes per each represented F1 genotype. Comparisons of data are indicated by brackets linking specific data sets. (B) A table with columns labeled 1-4 in the left top corners represents the mean IOB numbers +/- the SEM for each genotype represented in the bar graph. The inhibition of bristle numbers in *mid-RNAi* mutants was statistically significant: columns 2 vs 3 where $*p < 0.0001$. The suppression of IOB loss observed in *mid-RNAi* by overexpressing the *UAS-mid [46]* transgene is statistically significant: column 3 vs 4 where $*p < 0.0001$. Statistical analyses were performed using Shaprio-Wilk's test and the Student's t-test as detailed in methods.

Reducing *mid* Expression Induces Apoptosis within Early Pupal Stages

Under normal circumstances during the arrangement of pigment cells and bristle cells, the early pupal eye disc undergoes pruning of excess cells. This removal of excess cells by apoptosis mediated cell death is regulated by the Notch signaling pathway. Due to the aberrant Notch-Delta signaling, we assumed that in *mid-RNAi* pupal discs, abnormally high numbers of incorrectly specified epithelial cells were generated at the expense of SOPs. The excess epithelial and interommatidial precursor cells were likely undergoing apoptosis on a much larger scale than required for normal eye development [131]. To determine whether cells were undergoing apoptosis in *mid-RNAi* mutant eye discs, we over expressed the baculovirus *p35* transgene, a caspase inhibitor that blocks apoptosis [132]. Overexpression of *p35* in the *mid-RNAi* background significantly rescued the *mid* mutant phenotype by recovering the bristle loss and pigment loss (Figure 25D, E). Although bristles showed a slight degree of disorientation within the very center of the eye, a majority of bristle complexes were recovered in a radial, outward to inward pattern (Figure 25 E). The radial generation of eye bristles in WT flies has been previously described [133].

The recovery of bristles and cell viability of ommatidia by *p35* suggests that bristle loss in *mid-RNAi* eyes results in part from apoptosis. We further examined *mid-RNAi* pupal eye discs during the P2 stage of development for changes in nuclear morphology and Caspase-3 expression by co-labeling *mid-RNAi* and WT P2-staged pupal eye discs with the nuclear marker DAPI and anti-Caspase-3. We detected increased Caspase-3 expression levels in *mid-RNAi* discs compared to WT discs (Figure 25G, H). In addition, placing the *mid-RNAi* background in a heterozygous *Df(3L)H99* background deficient in the pro-apoptotic genes *grim*, *reaper* and head involution defective (*hid*),

partially suppressed the *mid* mutation (Figure 25I,M). Based upon these comprehensive studies, we conclude that IOB loss due to misspecification and apoptosis occur simultaneously under *mid-RNAi* conditions. Future studies to decipher *mid* function as a cell-fate determinant and pro-survival factor will dissect specific cell signaling pathways genetically on a "gene by gene" basis and within a narrower window of eye imaginal disc development

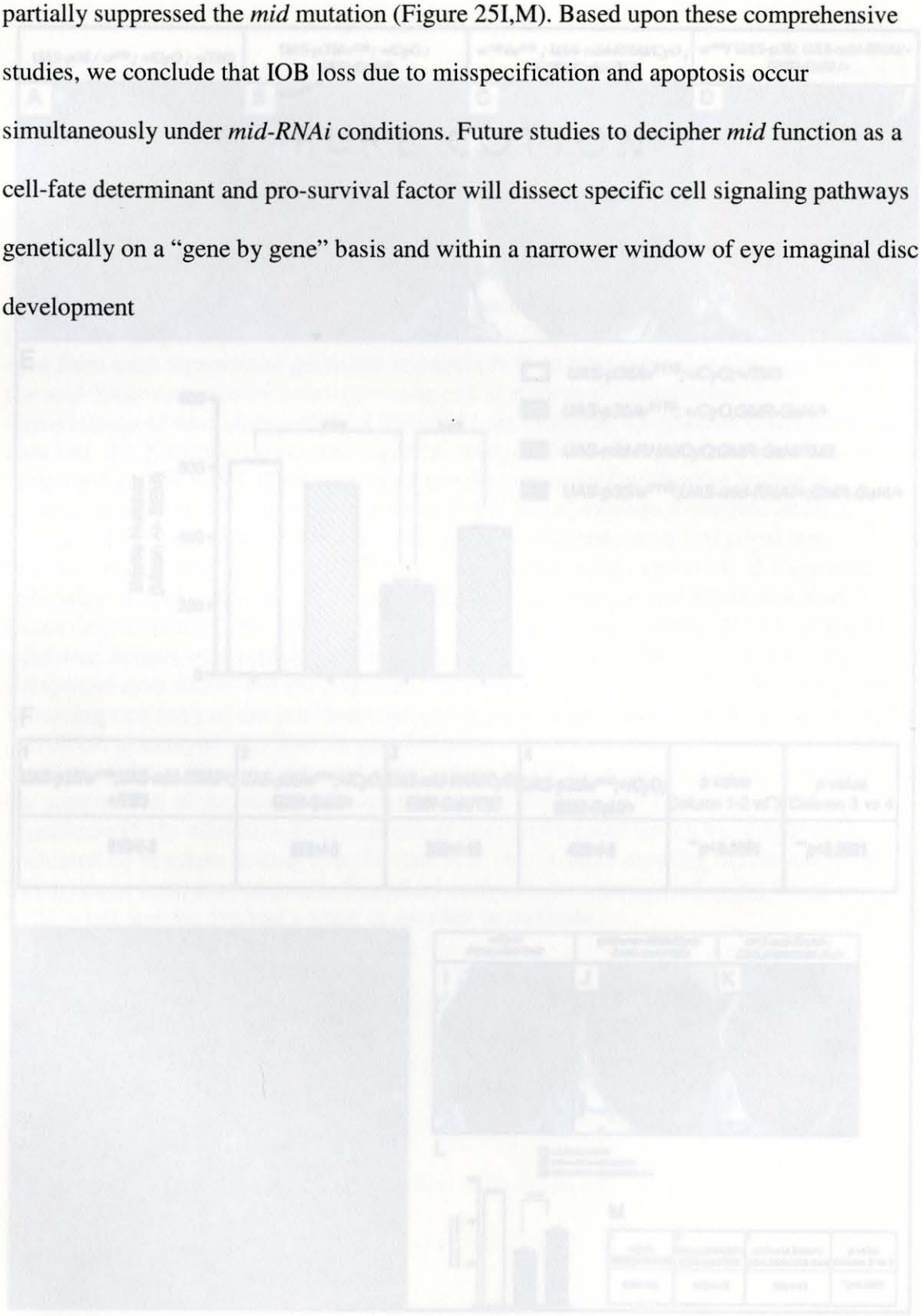

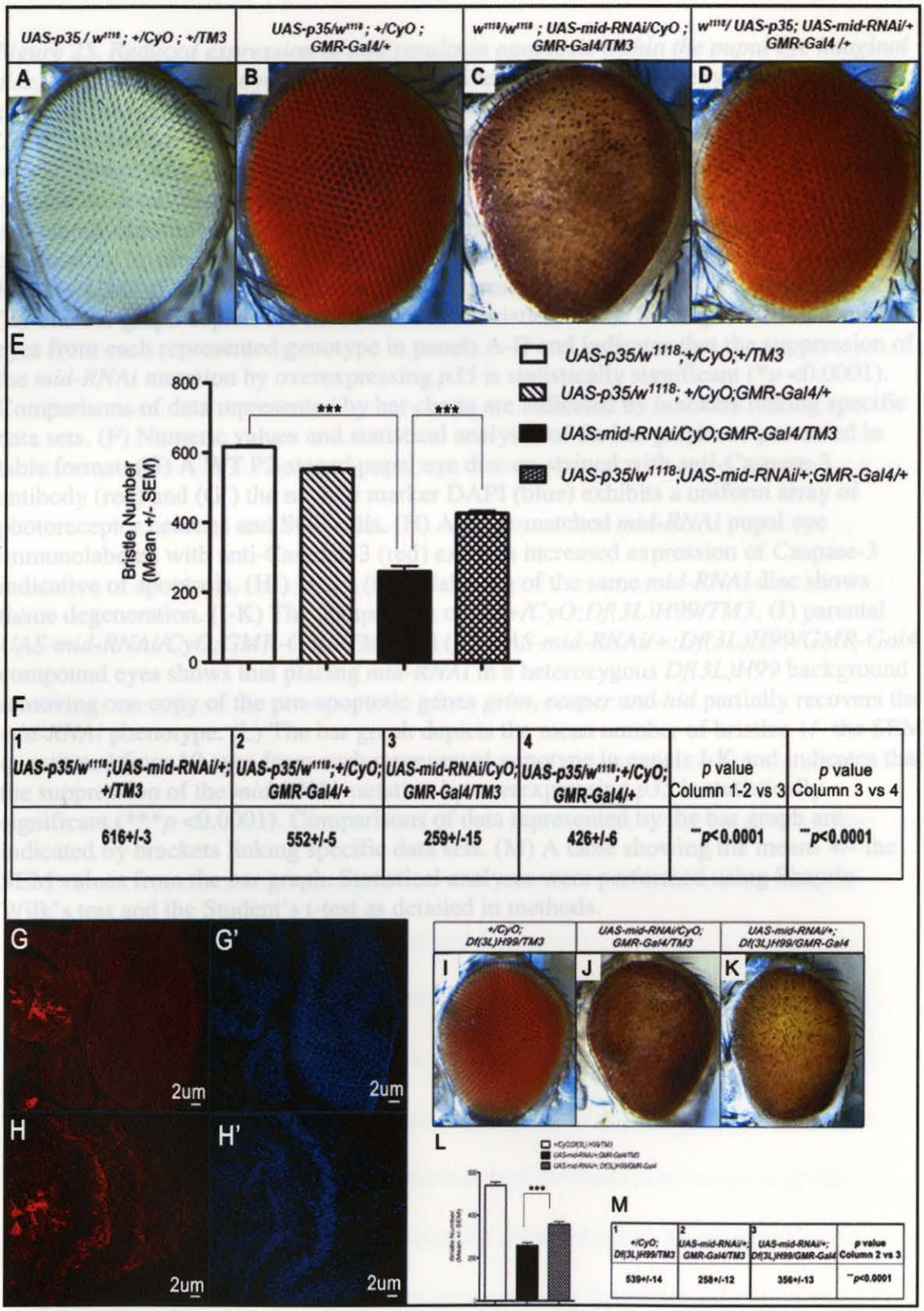
UAS-p35 / w1118 ; +/CyO ; +/TM3
UAS-p35/w1118 ; +/CyO ; GMR-Gal4/+
w1118/w1118 ; UAS-mid-RNAi/CyO ; GMR-Gal4/TM3
w1118/ UAS-p35; UAS-mid-RNAi/+ GMR-Gal4 /+
A
B
C
D
E
UAS-p35/w1118;+/CyO;+/TM3
UAS-p35/w1118; +/CyO;GMR-Gal4/+
UAS-mid-RNAi/CyO;GMR-Gal4/TM3
UAS-p35/w1118;UAS-mid-RNAi/+;GMR-Gal4/+
Bristle Number (Mean +/- SEM)
800
600
400
200
0
***
***
F
1 UAS-p35/w1118;UAS-mid-RNAi/+; +/TM3
2 UAS-p35/w1118;+/CyO; GMR-Gal4/+
3 UAS-mid-RNAi/CyO; GMR-Gal4/TM3
4 UAS-p35/w1118;+/CyO; GMR-Gal4/+
p value Column 1-2 vs 3
p value Column 3 vs 4
616+/-3
552+/-5
259+/-15
426+/-6
***p<0.0001
***p<0.0001
G
G'
H
H'
2um
+/CyO; Df(3L)H99/TM3
UAS-mid-RNAi/CyO; GMR-Gal4/TM3
UAS-mid-RNAi/+; Df(3L)H99/GMR-Gal4
I
J
K
L
M
1 +/CyO; Df(3L)H99/TM3
2 UAS-mid-RNAi/+; GMR-Gal4/TM3
3 UAS-mid-RNAi/+; Df(3L)H99/GMR-Gal4
p value Column 2 vs 3
539+/-14
258+/-12
356+/-13
***p<0.0001

Figure 25. Reduced expression of mid results in apoptosis within the pupal eye imaginal disc. (A-D) Compound eyes from representative genotypes of progeny generated from crossing *UAS-p35/Y; +/+;+/+* males to w^{1118}/w^{1118}*;UAS-mid-RNAi/CyO;GMR-Gal4/TM3* (*mid-RNAi*) females. (A) *UAS-p35/*w^{1118}*;+/CyO;+/TM3* and (B) *UAS-p35/*w^{1118}*;+/CyO;GMR-Gal4/+* flies exhibit normal numbers of bristles. (C) It was not possible to obtain female *mid-RNAi* flies from the cross because the *UAS-p35* transgene is on the X-chromosome. For this reason we used parental *mid-RNAi* female flies for quantitating bristles for comparisons with other groups. (D) w^{1118}*/UAS-p35; UAS-mid-RNAi/+;GMR-Gal4* eyes exhibit a partial suppression of the *mid-RNAi* mutant phenotype. (E) The bar graph depicts the mean number of bristles +/- the SEM quantitated from 10 eyes from each represented genotype in panels A-D and indicates that the suppression of the *mid-RNAi* mutation by overexpressing *p35* is statistically significant (**p* <0.0001). Comparisons of data represented by bar charts are indicated by brackets linking specific data sets. (F) Numeric values and statistical analyses of the bar graph are presented in table format. (G) A WT P2-staged pupal eye disc co-stained with anti-Caspase-3 antibody (red) and (G') the nuclear marker DAPI (blue) exhibits a uniform array of photoreceptor neurons and SOP cells. (H) A stage-matched *mid-RNAi* pupal eye immunolabeled with anti-Caspase-3 (red) exhibits increased expression of Caspase-3 indicative of apoptosis. (H') DAPI (blue) labeling of the same *mid-RNAi* disc shows tissue degeneration. (I-K) The comparison of (I) *+/CyO;Df(3L)H99/TM3*, (J) parental *UAS-mid-RNAi/CyO;GMR-Gal4/TM3* and (K) *UAS-mid-RNAi/+;Df(3L)H99/GMR-Gal4* compound eyes shows that placing *mid-RNAi* in a heterozygous *Df(3L)H99* background removing one copy of the pro-apoptotic genes *grim*, *reaper* and *hid* partially recovers the *mid-RNAi* phenotype. (L) The bar graph depicts the mean number of bristles +/- the SEM quantitated from 10 eyes from each represented genotype in panels I-K and indicates that the suppression of the *mid-RNAi* mutation by overexpressing *p35* is statistically significant (****p* <0.0001). Comparisons of data represented by the bar graph are indicated by brackets linking specific data sets. (M) A table showing the means +/- the SEM values from the bar graph. Statistical analyses were performed using Shaprio-Wilk's test and the Student's t-test as detailed in methods.

CHAPTER V

DISCUSSION

Determining the Function of Mid in the Development of *Drosophila* Eye

Specific knockdown of *mid* transcripts by using the gene silencing technique of *RNAi* within the developing eye disc resulted in a striking phenotype of bristle loss, ommatidial fusion, defects of bristle polarity and the generation of melanized tissue. The *mid-RNAi* genetic background is an ideal sensitized background for undertaking a genetic modifier screen. The dosage-sensitive phenotype worked as a tool to identify *mid*-interacting transcription factors toward deciphering a Mid regulatory network specifying cell fates. The severe *mid-RNAi* phenotype indicates the importance of Mid in eye development and its function to regulate cellular differentiation within the developing eye. To determine the function of Mid as a cell fate regulator we utilized genetic epistasis studies that examined the potential interaction of Mid with different classes of transcription factors which play a role in cell fate decisions in the developing eye. The current understanding of the function of Mid suggests that Mid functions within the Notch-Delta signaling pathway regulating SOP selection and specification and also indicates that Mid functions as a pro-survival factor.

Mid Functions within the Notch-Delta Regulated Signaling Pathway

The precise development of photoreceptor neurons, SOP cells and its lineage in the developing ommatidia is highly regulated in terms of spatial and temporal action of Notch signaling. An imbalance of stoichiometry of the Notch-Delta signaling causes switch in cell fate decision during neuronal cell differentiation. As an example, the temporal induction of a GOF *Notch* transgene encoding the intracellular domain ($Notch^{int}$) from 0-16 hrs after puparium formation (APF) was shown to suppress SOP

cells giving rise to IOBs while the development of ommatidia was left undisturbed [134]. A significant loss of interommatidial bristles (IOBs) observed in *mid-RNAi* mutant eyes resembled a Notch gain-of-function phenotype. Interestingly, overexpression of the full-length Notch (N^{Full}) receptor in the eye using the *GMR-Gal4* driver resulted in a nearly equivalent *mid-RNAi* phenotype with IOB loss and a rough eye (Figure 24D) [115,135]. This observation led us to hypothesize that knockdown of *mid* disrupts the stoichiometry of Notch-Delta signaling and therefore influences the IOB cell fate.

Mid Regulates SOP Cell Fate Specification in Collaboration with Members of Notch-Delta Signaling Pathway

To secure the function of Mid as a cell fate regulator during SOP selection in the early pupal stages of development, we examined genetic interactions between positive and negative regulators of SOP selection and specification in the Notch-Delta signaling pathway with *mid.* Based on the results of these genetic studies, we developed a model in which *mid* functions downstream of *Notch* and upstream of *E(spl)* in parallel with the *Su(H)* canonical pathway. This model represents the genetic hierarchy in which *mid* functions downstream of Notch to specify SOP and epidermal cells (Figure 21). As shown, the SOP cell generates the highest level of Delta expression among proneural clusters that establishes a positive feedback loop regulated by Ac-Sc. Subsequently, Notch signaling is activated in surrounding cells. Activation of the Notch signaling cascade prevents these cells from adopting neuronal cell fate and thereby they adopt default epidermal cell fates. According to our working model in the SOP cell Emc is antagonized by E(spl)-m8 and can no longer sequester Da and Ac leading to the activation of *sens* expression. Conversely, in the Delta-receiving cell, Emc sequesters Da resulting in the inhibition of *ac* and *sens* expression, where *sens* is absolutely [70,96,136-138]

required for the conversion of the SOP cell to a pI neuroblast [116,139]. Moreover, Sens has been shown to physically interact with Ac and Sc to function as a co-activator in the regulation of proneural gene expression [140].

Senseless acts as a binary switch to restrict the proneural field from which an SOP cell is selected [139]. In a model proposed by Jafar-Nejad et al. [139], low levels of *sens* repress proneural gene expression within cells of a proneural field while increased expression of *sens* upregulates proneural gene expression. In addition, the transition of the Delta-signaling cell to the SOP cell fate is secured by the repression of Notch signaling where Su(H) and Hairless as well as other corepressors inhibit *E(spl)* expression. The binary switch model is partly incorporated within the illustrated *Notch-Delta* genetic pathways (Figure 21A) [139]. These pathways show that *mid* plays a role in the Notch-Delta signaling pathway mediating SOP selection and cell fate specification by genetically collaborating with *emc*, *ato* and *sens*.

How do *mid* and *emc* Collaborate to Specify SOP Cell Fate?

We examined the genetic interaction of ac^1 and *mid* by placing an ac^1 heterozygous mutant allele in the *mid-RNAi* sensitized background and observed no change in the *mid-RNAi* mutant phenotype. We also examined other heterozygous mutation alleles of *ac-sc* but were unable to use these in the allelic modifier screen because they showed a significant amount of IOB loss. Despite this, it was previously shown that *ac* and *sc* are not absolutely required for the specification of SOP cells giving rise to IOB complexes within the eye [116]. Although *ac* and *sc* are not essential for the specification of SOP cells, proneural clusters are endowed with the ability to achieve the neuronal fate by expressing *ac* and *sc* .The expression of *ac–sc* genes throughout development is maintained by autoregulation mediated by Ac-Da heterodimers that bind

to E boxes within the *ac-sc* promoters [141]. The bHLH repressor Hairy binds directly to the *ac* promoter sequences. The HLH repressor Emc represses *ac* indirectly by preventing Da from forming heterodimers with Ac-Sc; this blocks both regulation of downstream genes and autoregulation [96,120]. This interaction largely determines whether *sens* proneural gene expression will be enhanced or suppressed (Figure 20A) [142]. In contrary to the genetic studies, immunolabeling of *mid-RNAi* mutant pupal eye discs (0-6 hrs APF) with anti-Ac and anti-Sens detected a significant reduction of *ac* and *sens* expression. This observation suggests that ubiquitous expression of Emc sets a negative threshold for proneural cells. Now a single cell will be able to overcome this negative threshold by expressing higher levels of delta and creating a positive feed-back loop to express proneuronal *ac* and *sens*. Since Emc and Da are expressed ubiquitously during third- instar larval and early pupal stage of development, we did not detect changes in Emc expression during either larval or pupal stages of development under *mid-RNAi* conditions (Figure15). However, the genetic data suggest that Mid and Emc collaborate either directly or indirectly to regulate IOB cell fate [142,143]. In addition, immunofluorescent analyses showed that H15 expression overlapped with Emc in most cells of the P2-staged pupal eye imaginal disc (Figure 15). Comparative studies have shown that Tbx20 and a vertebrate homolog of Emc, Inhibitor of DNA binding (Id-1), are expressed in the neural retina during early mammalian embryogenesis [6,7].

A Cross Regulatory Induction of Atonal on the Mid Expressing SOP Cells

The genetic modifier screen identified *ato* as a *mid* interacting gene candidate in the specification of the SOP cell fate. Interestingly, Ato is the proneural transcription factor first expressed in a band of cells anterior of the furrow and within an approximate 20-cell large intermediate group of cells emerging from the furrow during the 3°L stage

and its expression endows the proneural cells with the ability to acquire neural cell fates. Later, Ato expression is refined only in the R8 photoreceptor cell which is the founder cell that differentiates first from the MF and recruits other photoreceptor cells in a sequential manner [144,145]. As observed, Mid expression is not prominent at the furrow. As such, we did not detect coexpression of Ato and Mid at the furrow while Mid is largely expressed in photoreceptor neurons posterior of the furrow during the 3°L and P0-P1 stages of development. Under *mid-RNAi* conditions, it was difficult to discern whether the level of Ato expression was affected although the 20-cell clusters seemed disorganized (data not shown). These observations indicate that Ato might interact with the Mid in a cell non-autonomous or cross regulatory manner.

In support of this hypothesis, a cross-regulatory loop of *ato* expression epistatic to Notch-Delta was proposed to occur between the femoral chordotonal organ SOP and committed SOPs [146]. The chordotonal organ expresses *ato* leading to increased Delta expression. The Delta-bound Notch receptor of the neighboring SOP cell activates E(Spl) downstream of Notch. E(Spl), in turn, inhibits *ato* expression to complete a cross-regulatory negative loop between both cells. We predict that a similar mechanism may be taking place between the *ato*-expressing R8 cell and pre-SOP cells of the neural field during late 3°L stages. In this corresponding scenario, the R8 *ato*-expressing cell inhibits *ato* expression within neighboring pre-SOP cells to prevent them from competing to assume the R8 cell fate. Subsequently, both cell types progress independently along separate pathways of neuronal specification and differentiation. This would assume that pre-R8 cells are physically close to pre-SOP cells. P2-staged pupae immunolabeled with antibody markers specifically detecting the R8 photoreceptor neurons and SOP cells

show both of these cell types are in close proximity, a position likely unchanged since 3°L stages [116].

Mid Functions as a Pro-Survival Factor in Developing Pupal Discs

The knockdown of *mid* by *RNAi* resulted in multiple defects in the adult eye of the *mid-RNAi* flies. One of the major *mid-RNAi* phenotypes was the increased level of apoptosis. This observation was confirmed directly by a significant recovery of IOBs under *mid-RNAi* conditions when we overexpressed the caspase inhibitor p35 or removed one copy of the pro-apoptotic genes *grim*, *reaper* and *hid* using the *Df(3L)H99* line. Moreover, increased levels of Caspase-3, a marker identifying apoptosis in the *mid-RNAi* early pupal eye disc has also been observed. A significant interaction between *emc* and *mid* supports this observation since specific mammalian isoforms of Emc known as Id (Id1-4) have been shown to regulate cell proliferation and changes in their activity are implicated in the etiology of gastric cancer, prostate cancer and medulla blastoma [123,147,148]. Thus, when we reduced the dose of *emc* in the *mid-RNAi* background, it not only salvaged IOBs, but also improved overall tissue viability (Figure 14E) and rescued accessory cells that degenerated during later pupal stages of development (data not shown). This relationship of *mid* with *emc* supports the hypothesis that reduction of *mid* expression during SOP cell fate specification causes misspecification of neuronal cells. These misspecified cells adopt epidermal cell fates. The expansion of epidermal cells triggers the apoptosis mediated removal of excess cells. In addition, *sens* has been also shown to inhibit pro-apoptotic pathways by repressing *reaper* in the salivary gland [149].

Interestingly, in a genetic modifier screen of a *Hairless* GOF apoptotic mutant phenotype, *emc* was not identified as an enhancer or suppressor of *Hairless* [150]. Thus, it follows that *emc* does not function within a *Notch* LOF genetic pathway. Rather, our data indicate that *emc* is activated under permissive Notch signaling when levels of *mid* are reduced and Emc activity is increased as a GOF effect in the developing eye disc ultimately resulting in fewer SOP cells (Figure 20A). The *H* GOF apoptotic phenotype driven specifically by the *GMR-Gal4* driver line was further utilized in a cell death assay to uncover novel regulators of *H* and *Notch* [150]. Placing a heterozygous *Df(2L)sc19-4* chromosomal deficiency within the *GMR-Gal4/+;UAS-H/CyO* background led to an enhancement of the apoptotic phenotype [150]. Since *mid* and *H15* are deleted from this interval they represent viable gene candidates deleted within the deficiency that function as pro-survival factors in addition to *thickveins* (*tkv*), a receptor classified as a member of the Transforming Growth Factor-β receptor family [151]. Decapentaplegic (Dpp) is a specific ligand for Tkv and Dpp has been shown to cooperate with Mid to specify cardioblast cell fates in the embryonic heart [1]. Based on our results and those of the reported genetic modifier screen of a *H* GOF apoptotic phenotype [150], *mid* functions as a pro-survival factor that surveys cellular homeostasis downstream of the Notch receptor during early stages of imaginal eye disc development.

dFOXO a New Member of the *H15/Mid* Regulatory Network Specifying Cell Fate and Survival

We have shown that *dFOXO* and *mid* collaborate to regulate the generation of intermommatidial bristles as well as the survival of ommatidial cells within developing *Drosophila* eye tissues (Figure 16). The *dFOXO* transcription factor functions downstream of the Insulin receptor (InR) to secreted insulin-like peptides released from

neurosecretory cells in the brain. Under normal metabolic conditions, nuclear dFOXO is a specific substrate for the Akt/PKB kinase and when phosphorylated at specific phosphorylation sites by Akt/PKB, exits the nucleus in association with the chaperone protein 14-3-3 to reside within the cytoplasm. Under conditions of metabolic stress, cytoplasmic dFOXO is hypophosphorylated and translocates back into the nucleus to regulate the expression of several target genes known to regulate metabolism including *myc, 4e-bp* and *InR* [152-154].

dFOXO activity is also affected by the induction of other stress pathways. Under conditions of oxidative stress, c-Jun N-terminal kinase (JNK) phosphorylates cytoplasmic dFOXO on specific target sites to recruit the 14-3-3 chaperone protein. The 14-3-3/dFOXO complex then translocates into the nucleus. Subsequent phosphorylation of 14-3-3 by JNK leads to the dissociation of the complex and the release of dFOXO enabling it to target gene expression related to cell cycle arrest, DNA repair, differentiation, cell death and detoxification [117]. The genetic collaboration of *mid* and *dFOXO* suggests that T-box genes including the conserved vertebrate homolog of *mid, Tbx-20,* have the potential to function downstream of endocrine signaling induced by metabolic and oxidative stress. Specific to our studies, we assume that a stress signal induced by *mid-RNAi* conditions triggers the surveillance activity of dFOXO which upregulates gene expression essential for inhibiting progression of the cell cycle resulting in stunted bristles (Figure 16B'-C'). Concomitant with inhibiting cell cycle progression, dFOXO increases the activity of the translational inhibitor *d4E-BP* leading to decreased protein synthesis. This cascade of signaling events alerts Dp53, which in turn, activates the apoptotic pathway to kill deleterious cells with the potential to compromise the development and survival of the organism.

The Path toward Deciphering Mid TF Regulatory Networks

Identification of transcription factors that collaborate with Mid to specify neuronal cell fates was the primary goal of the project. We utilized the *Drosophila* eye as a model system to pursue a genetic modifier screen to uncover Mid collaborating transcription factors. This genetic modifier screen identified several transcription factors of the Notch-Delta signaling pathway which showed a significant genetic interaction with Mid in specifying of the SOP cells which give rise to IOB cells of the adult eye. The transcription factor genes include *ato, emc and senseless* show a significant interaction with *mid.* Identification of such a diverse range of transcription factors collaborating with *mid* suggesting that Mid is a member of several combinatorial codes that specify cell fate specification of diverse cells including the SOP, heart and neuronal cells. This study also uncovered a new function of Mid in the regulation of cell survival. During early pupal stages of *Drosophila* eye development, Mid participates in the maintenance of cellular homeostasis. The identification of transcription factors collaborating with Mid within a cell survival pathway requires further investigation. The role of *dp53*, a *Drosophila* homolog of the mammalian tumor suppressor gene *p53* (reviewed by Rutkowski et al., 2010) [155] may be a member of a Mid transcription factor regulatory network maintaining cell survival and proliferation which can establish a link between apoptotic and oncogenic pathways in *Drosophila.* Effector caspases downstream of Dp53 have been shown to reduce cellular proliferation rates. Thus, the interaction between Mid and dp53 can expand our understanding of the function of T-box transcription factors beyond cell fate specification during development. Post-developmentally, T-box TFs may play essential physiological role to respond to unique stresses.

We observed another important aspect of Mid. Under *mid-RNAi* conditions, we detected a greater bristle loss in the ventral compartment of the eye compared with dorsal compartment of the adult (Figure 9). This compartmentalization effect of Mid supports the idea that during the early 3°L stage and prior to IOB formation *pnr* may collaborate with *mid* to establish the dorsal compartment of the imaginal eye disc downstream of *dpp*, *wg*, and/or *hedgehog* (*Hh*) [125,127]. Pannier, a GATA transcription factor functions as a dorsal selector in establishing dorsal fate in eye imaginal disc which begins to develop with a default ventral fate. The ability of *mid* to function as a selector gene has been shown in the developing leg disc where *mid* collaborates with *pnr* to establish the ventral compartment [94].

CHAPTER VI

CONCLUSION

This study is significant in establishing the role of Mid in eye development. Although the vertebrate homolog of Mid Tbx-20 has been shown to be expressed in mouse and human retinal cells, the function of this transcription factor in regulating eye development is entirely unknown. Thus identification of Mid regulatory transcription factor networks in the developing eye tissue is the first attempt towards understanding Mid function. Mid regulates cell fate specification in different tissues in collaboration with different classes of transcription factors. Thus identification of the tissue-specific Mid transcription factor regulatory networks is highly important. This current study uncovered a Mid regulatory transcription factor network that plays a significant role in the specification of IOB cell fate during the early pupal stage of *Drosophila* eye development. Based on the genetic studies, *mid* collaborates with transcription factor coding genes such as *emc, ato* and *senseless* within the Notch-Delta signaling pathway to regulate the SOP cell fate specification. Determination of the genetic interaction between Mid and the Notch-Delta signaling pathway contributed to the understanding of the role of Mid to regulate neuronal cell fates in eye development. Whether Mid regulates IOB cell fate by physically interacting with members of the Notch-Delta pathway requires further investigation. Since, *RNA*-induced *mid* silencing resulted in multiple cellular defects during the 3°L and early pupal stage of eye morphogenesis which included loss of IOBs through the apoptotic pathway and also, since *mid* collaborates with *dFOXO,* Mid functions as a prosurvival factor. Thus, this study showed two key functions of Midline in the *Drosophila* eye development, cell fate specification and regulation of cellular homeostasis.

REFERENCES

(1) Qian, L.; Liu, J. D.; Bodmer, R. *Developmental Biology* **2005**, *279*, 509.

(2) Ryu, J. R.; Najand, N.; Brook, W. J. *Developmental Dynamics* **2011**, *240*, 86.

(3) Buescher, M.; Tio, M.; Tear, G.; Overton, P. M.; Brook, W. J.; Chia, W. *Developmental Biology* **2006**, *292*, 418.

(4) Leal, S. M.; Qian, L.; Lacin, H.; Bodmer, R.; Skeath, J. B. *Developmental Biology* **2009**, *325*, 138.

(5) Nüsslein-Volhard, C.; Wieschaus, E.; Kluding, H. *Development Genes and Evolution* **1984**, *193*, 267.

(6) Meins, M.; Henderson, D. J.; Bhattacharya, S. S.; Sowden, J. C. *Genomics* **2000**, *67*, 317.

(7) Kraus, F.; Haenig, B.; Kispert, A. *Mechanisms of Development* **2001**, *100*, 87.

(8) Reim, I.; Frasch, M. *Development* **2005**, *132*, 4911.

(9) Wolpert, L. *Journal of Theoretical Biology* **1969** *25*, 1.

(10) Leptin, M. *The EMBO Journal* **1999**, *18*, 3187.

(11) Pomar, R. R.; Jackle, H. *Trends Genet.* **1996**, *12*, 478.

(12) Kavka, A. I.; Green, J. B. *Biochim Biophys Acta.* **1997**, *1333*, F73.

(13) Papaioannou, V. E.; Silver, L. M. *BioEssays* **1998**, *20*, 9.

(14) Smith, J. *Trends in Genetics* **1999**, *15*, 154.

(15) Chesley, P. *J. Exp. Zool.* **1935**, *70*.

(16) Herrmann, B. G.; Labeit, S.; Poustka, A.; King, T. R.; Lehrach, H. *Nature Genet.* **1990**, *343*, 617.

(17) Conlon, F. L.; Sedgwick, S. G.; Weston, K. M.; Smith, J. C. *Development* **1996**, *122*, 2427.

(18) Habets, P.; Moorman, A. F. M.; Clout, D. E. W.; van Roon, M. A.; Lingbeek, M.; van Lohuizen, M.; Campione, M.; Christoffels, V. M. *Genes & Development* **2002**, *16*, 1234.

(19) Hoogaars, W. M. H.; Barnett, P.; Moorman, A. F. M.; Christoffels, V. M. *Cellular and Molecular Life Sciences* **2007**, *64*, 646.

(20) Wilkinson, D.; Bhatt, S.; Herrmann, B. G. *Nature* **1990**, *343*, 657

(21) Pflugfelder, G.; Roth, H.; Poeck, B. *Biochem Biophys Res Commun.* **1992**, *186*, 918.

(22) Pflugfelder, G. O.; Roth, H.; Poeck, B.; Kerscher, S.; Schwarz, H.; Jonschker, B.; Heisenberg, M. *Proceedings of the National Academy of Sciences of the United States of America* **1992**, *89*, 1199.

(23) Li, Q. Y.; Newbury-Ecob, R. A.; Terrett, J. A.; Wilson, D. I.; Curtis, A. R. J.; Yi, C. H.; Gebuhr, T.; Philip J. Bullen; Stephen C. Robson; Tom Strachan; Damien Bonnet; Stanislas Lyonnet; Ian D. Young; J. Alexander Raeburn; Alan J. Buckler; David J. Law; Brook, J. D. *Nature Genet.* **1997**, *15*, 21.

(24) Bamshad, M.; Lin, R. C.; Law, D. J.; Watkins, W. S.; Krakowiak, P. A.; Moore, M. E.; Franceschini, P.; Lala, R.; Holmes, L. B.; Gebuhr, T. C.; Bruneau, B.; Schinzel, A.; Seidman, J. G.; Seidman, C. E.; Jorde, L. B. *Nature Genet.* **1998**, *19*, 102.

(25) Poeck, B.; Hoibauer, A.; Pflugfelder, G. *Development* **1993**, *117*, 1017.

(26) Singer, M. A.; Penton, A.; Twombly, V.; Hoffmann, F. M.; Gelbart, W. M. *Development* **1997**, *124*, 79.

(27) Porsch, M.; Hofmeyer, K.; Bausenwein, B. S.; Grimm, S.; Weber, B. H. F.; Miassod, R.; Pflugfelder, G. O. *Gene* **1998**, *212*, 237.

(28) Reim, I.; Lee, L. H.; Frasch, M. *Development* **2003**, *130*, 3187.

(29) Buescher, M.; Svendsen, P. C.; Tio, M.; Miskolczi-McCallum, C.; Tear, G.; Brook, W. J.; Chia, W. *Current Biology* **2004**, *14*, 1694.

(30) Madej, T.; Addess, K. J.; Fong, J. H.; Geer, L. Y.; Geer, R. C.; Lanczyck, C. J.; Liu, C.; Lu, S.; Marchler-Bauer, A.; Panchenko, A. R.; Chen, J.; Thiessen, P. A.; Wang, Y.; Zhang, D.; Bryant, S. H. *Nucleic Acids Res.* **2012**.

(31) Showell, C.; Binder, O.; Conlon, F. L. *Dev Dyn* **2004**, *229*, 201.

(32) Bruneau, B. G.; Nemer, G.; Schmitt, J. P.; Charron, F.; Robitaille, L.; Caron, S.; Conner, D. A.; Gessler, M.; Nemer, M.; Seidman, C. E.; Seidman, J. G. *Cell* **2001**, *106*, 709.

(33) Hiroi, Y.; Kudoh, S.; Monzen, K.; Ikeda, Y.; Yazaki, Y.; Nagai, R.; Komuro, I. *Nature Genet.* **2001**, *28*, 276.

(34) Stennard, F. A.; Costa, M. W.; Elliott, D. A.; Rankin, S.; Haast, S. J. P.; Lai, D.; McDonald, L. P. A.; Niederreither, K.; Dolle, P.; Bruneau, B. G.; Zorn, A. M.; Harvey, R. P. *Developmental Biology* **2003**, *262*, 206.

(35) Takeuchi, J. K.; Koshiba-Takeuchi, K.; Suzuki, T.; Kamimura, M.; Ogura, K.; Ogura, T. *Development* **2003**, *130*, 2729.

(36) Plageman, T. F.; Yutzey, K. E. *Journal of Biological Chemistry* **2004**, *279*, 19026.

(37) Reim, I.; Mohler, J. P.; Frasch, M. *Mechanisms of Development* **2005**, *122*, 1056.

(38) Akam, M. *Development* **1987**, *101*, 1.

(39) Bate, C. M.; Grunewald, E. B. *J. Embryol. Exp. Morphol.* **1981**, *67*, 317.

(40) Taghert, P.; Bastiani, M.; Ho, R. K.; Goodman, C. S. *Dev. Biol.* **1982**, *94*, 391.

(41) Goodman, C. S.; Bastiani, M. J. *Sci. Am.* **1985**.

(42) Doe, C. Q. *Development* **1992**, *116*, 855.

(43) McDonald, J. A.; Holbrook, S.; Isshiki, T.; Weiss, J.; Doe, C. Q.; Mellerick, D. M. *Genes & Development* **1998**, *12*, 3603.

(44) Skeath, J. B.; Thor, S. *Curr. Opin. Neurobiol.* **2003**, *13*, 8.

(45) Ready, D. F.; Hanson, T. E.; Benzer, S. *Developmental Biology* **1976**, *53*, 217.

(46) Roignant, J. Y.; Treisman, J. E. *Int. J. Dev. Biol.* **2009**, *53*, 795.

(47) Kumar, J. P. *Developmental Dynamics* **2012**, *241*, 136.

(48) Tomlinson, A.; Ready, D. F. *Dev Biol.* **1987**, *120*, 366.

(49) Wigglesworth, V. B. *Q. J. Microsc. Sci.* **1953**, *94*, 93.

(50) Waddington, C. H.; Perry, M. M. *Proc. R. Soc. Biol. Sci.* **1960**, *153*, 155.

(51) Silver, J. S.; Rebay, I. *Development* **2005**, *132*, 3.

(52) Wolff, T.; Ready, D. F. *Development* **1993**, *113*, 841.

(53) Jarman, A. P.; Grell, E. H.; Acherman, L.; Jan, L. Y.; Jan, Y. N. *Nature* **1994**, *369*.

(54) Baker, N. E.; Zitron, A. E. *Mechanisms of Development* **1995**, *49*, 173.

(55) Cavodeassi, F.; Diez del Corral, R.; Campuzano, S.; Domínguez, M. *Development* **1999**, *126*, 4933.

(56) Heberlein, U.; Wolff, T.; Rubin, G. M. *Cell* **1993**, *75*, 913.

(57) Ma, C.; Zhou, Y.; Beachy, P. A.; Moses, K. *Cell* **1993**, *75*, 927.

(58) Domínguez, M.; Hafen, E. *Genes Dev. 1997 Dec 1;11(23):* **1997**, *1*, 3254.

(59) Borod, E. R.; Heberlein, U. *Developmental Biology* **1998**, *197*, 187.

(60) Dominguez, M. *Development* **1999**, *126*, 2345.

(61) Blackman, R.; Sanicola, M.; Raftery, L.; Gillevet, T.; Gelbart, W. *Development* **1991**, *111*, 657.

(62) Greenwood, S.; Struhl, G. *Development* **1999**, *126*, 5795.

(63) Brown, N. L.; Sattler, C. A.; Paddock, S. W.; Carroll, S. B. *Cell* **1995**, *80*, 879.

(64) Baonza, A.; Casci, T.; Freeman, M. *Current Biology* **2001**, *11*, 396.

(65) Frankfort, B. J.; Mardon, G. *Development* **2002**, *129*, 1295.

(66) Dambly-Chaudiere, C.; Ghysen, A.; Jan, L. Y.; Jan, Y. N. *Roux's Arch. Dev. Biol.* **1988**, *197*, 419.

(67) Campuzano, S.; Modolell, J. *Trends Genet.* **1992**, *8*, 202.

(68) Murre, C.; McCaw, P. S.; Baltimore, D. *Cell* **1989**, *56*, 777.

(69) Cabrera, C. V.; Alonso, M. C. *EMBO J.* **1991**, *10*, 2965—2973.

(70) van Doren, M.; Ellis, H. M.; Posakony, J. W. *Development* **1991**, *113*, 245.

(71) Singson, A.; Leviten, M. W.; Bang, A. G.; Hua, X. H.; Posakony, J. W. *Genes & Development* **1994**, *8*, 2058.

(72) Bailey, A. M.; Posakony, J. W. *Genes & Development* **1995**, *9*, 2609.

(73) Kopan, R.; Turner, D. L. *Curr. Opin. Neurobiol.* **1996**, *6*, 594.

(74) Artavanis-Tsakonas, S.; Matsuno, K.; Fortini, M. E. *Science* **1995** *268*, 225.

(75) Schroeter, E. H.; Kisslinger, J. A.; Kopan, R. *Nature* **1998**, *393*, 382.

(76) De Strooper, B.; Annaert, W.; Cupers, P.; Saftig, P.; Craessaerts, K.; Mumm, J. S.; Schroeter, E. H.; Schrijvers, V.; Wolfe, M. S.; Ray, W. J.; Goate, A.; Kopan, R. *Nature* **1999**, *398*, 518.

(77) Ligoxygakis, P.; Yu, S. Y.; Delidakis, C.; Baker, N. E. *Development* **1998**, *125*, 2893.

(78) Nagel, A. C.; Maier, D.; Preiss, A. *Mechanisms of Development* **2000**, *94*, 3.

(79) Bukharina, T. A.; Furman, D. P. *Russian Journal of Developmental Biology* **2011**, *42*, 63.

(80) Guo, M.; Jan, L. Y.; Jan, Y. N. *Neuron* **1996**, *17*, 27.

(81) Blochlinger, K.; Bodmer, R.; Jan, L. Y.; Jan, Y. N. *Genes Dev.* **1990**, *4*, 1322.

(82) Schweisguth, F. *Curr. Biol.* **2004**, *14*, R129.

(83) Lieber, T.; Kidd, S.; Alcamo, E.; Corbin, V.; Young, M. W. *Genes Dev.* **1993**, *7*, 1949.

(84) Schweisguth, F.; Posakony, J. W. *Development* **1994**, *120*, 1433.

(85) Doherty, D.; Jan, L. Y.; Jan, Y. N. *Development* **1997**, *124*, 3881.

(86) Wang, S. W.; Younger-Shepherd, S.; Jan, L. Y.; Jan, Y. N. *Development* **1997**, *124*, 4435.

(87) Rebeiz, M.; Miller, S. W.; Posakony, J. W. *Development* **2011**, *138*, 215.

(88) Thomas, G. H.; Kiehart, D. P. *Development* **1994**, *120*, 2039.

(89) Rozan, L. M.; El-Deiry, W. S. *Cell Death Differ* **2007**, *14*, 3.

(90) Hay, B. A.; Wolff, T.; Rubin, G. M. *Development* **1994**, *120*, 2121.

(91) Brand, A. H.; Perrimon, N. *Development* **1993**, *118*, 401.

(92) Nakao, K.; CamposOrtega, J. A. *Neuron* **1996**, *16*, 275.

(93) Shiga, Y.; TanakaMatakatsu, M.; Hayashi, S. *Development Growth & Differentiation* **1996**, *38*, 99.

(94) Svendsen, J. M.; Smogorzewska, A.; Sowa, M. E.; O'Connell, B. C.; Gygi, S. P.; Elledge, S. J.; Harper, J. W. *Cell 138:* . **2009**, *138*, 63.

(95) Xu, T.; Rubin, G. M. *Development* **1993**, *117*, 1223.

(96) Ellis, H. M.; Spann, D. R.; Posakony, J. W. *Cell* **1990**, *61*, 27.

(97) Bainbridge, S. P.; Bownes, M. *J Embryol. Exp. Morph.* **1981**, *65*, 57.

(98) Carroll, S. B.; Whyte, J. S. *Development* **1989**, *3*, 905.

(99) Frankfort, B. J.; Pepple, K. L.; Mamlouk, M.; Rose, M. F.; Mardon, G. *Genesis* **2003**, *38*.

(100) Walther, R. F.; Pichaud, F. *Nature Protocols* **2006**, *1*, 2635.

(101) Skeath, J. B.; Carroll, S. B. *Genes Dev.* **1991**, *5*, 984.

(102) Melicharek, D.; Shah, A.; DiStefano, G.; Gangemi, A. J.; Orapallo, A.; Vrailas-Mortimer, A. D.; Marenda, D. R. *Genetics* **2008**, *180*, 2095.

(103) Younger-Shepherd S.; Vaessin H.; Bier E.; Jan L.Y.; Y.N., J. *Cell* **1992**, *70*, 911.

(104) Skeath, J. B.; Doe, C. Q. *Development* **1998**, *125*, 1857.

(105) Nolo, R.; Abbott, L. A.; Bellen, H. J. *Cell* **2000**, *102*, 349.

(106) Riggleman, B.; Schedl, P.; Weischaus, E. *Cell* **1990**, *63*, 549.

(107) Oda, H.; Uemura, T.; Harada, Y.; Iwai, Y.; Takeichi, M. *Developmental Biology* **1994**, *165*, 716.

(108) O'Neill, E. M.; Rebay, I.; Tijan, R.; Rubin, G. M. *Cell 78* **1994**, *78*, 137.

(109) Qi, H. L.; Rand, M. D.; Wu, X. H.; Sestan, N.; Wang, W. Y.; Rakic, P.; Xu, T.; Artavanis-Tsakonas, S. *Science* **1999**, *283*, 91.

(110) Diederich, R. J.; Matsuno, K.; Hing, H.; Artavanistsakonas, S. *Development* **1994**, *120*, 473.

(111) Fehon, R. G.; Kooh, P. J.; Rebay, I.; Artavanis-Tsakonas, S. *J. Cell Biol.* **1991**, *113*, 657.

(112) Jones, B. W.; Fetter, R. D.; Tear, G.; Goodman, C. S. *Cell* **1995**, *82*, 1013.

(113) Lee, E. C.; Hu, X.; Yu, S. Y.; Baker, N. E. *Mol. Cell. Biol.* **1996**, *16*, 1179.

(114) Nagaraj, R.; Banerjee, U. *Development* **2007**, *134*, 825.

(115) Hagedorn, E. J.; Bayraktor, J. L.; Kandachar, V. R.; Bai, T.; Englert, D. M.; Chang, H. C. *J. Cell Bio.* **2006**, *173*, 443.

(116) Frankfort, B. J.; Pepple, K. L.; Mamlouk, M.; Rose, M. F.; Mardon, G. *Genesis* **2004**, *38*, 182.

(117) Greer, E. L.; Brunet, A. *Acta Physiologica* **2008**, *192*, 19.

(118) Rockwell, C. E.; Zhang, M.; Fields, P. E.; Klaassen, C. D. *J Immunol.* **2012**, *188*, 1630.

(119) Jahangiri, L.; Nelson, A. C.; Wardle, F. C. *Dev. Biol.* **2012**, *371*, 110.

(120) Ohsako, S.; Hyer, J.; Panganiban, G.; Oliver, I.; Caudy, M. *Genes & Development* **1994**, *8*, 2743.

(121) Jarmen, A. P.; Grell, E. H.; Acherman, L.; Jan, L. Y.; Jan, Y. N. *Nature* **1994**, *369*, 398.

(122) Jarmen, A. P.; Sun, Y.; Jan, L. Y.; Y.N., J. *Development* **1995**, *121*, 2019.

(123) Li, W.; Zhang, C. H.; Hong, Y. L.; Li, J.; Hu, Y. M.; Zhao, C. F. *Molecular Biology Reports* **2012**, *39*, 3009.

(124) Oros, S. M.; Tare, M.; Kango-Singh, M.; Singh, A. *Developmental Biology* **2010**, *346*, 258.

(125) Heitzler, P., Bourouis, M., Ruel, L., Carteret, C. Simpson, P. 1996a. *Genetics.* **1996b**, *143*, 1271.

(126) Ramain, P.; Heitzler, P.; Haenlin, M.; Simpson, P. *Development* **1993**, *119*, 1277.

(127) Maurel-Zaffran, C.; Treisman, J. E. *Development* **2000**, *127*, 1007.

(128) Ramain, P.; Khechumian, R.; Khechumian, K.; Arbogast, N.; Ackermann, C.; Heitzler, P. *Molecular Cell* **2000**, *6*, 781.

(129) Maves, L.; Schubiger, G. *Development* **1998**, *125*, 115.

(130) Lai, E. C.; Orgogozo, V. *Developmental Biology* **2004**, *269*, 1.

(131) Wolff, T.; Ready, D. F. *Development* **1991**, *113*, 825.

(132) LaCount, D. J.; Hanson, S. F.; Schneider, C. L.; Friesen, P. D. *Journal of Biological Chemistry* **2000**, *275*, 15657.

(133) Cagan, R. L.; Ready, D. F. *Dev. Biol.* **1989b**, *136*, 346.

(134) Lyman, D. F.; Yedvobnick, B. *Genetics* **1995**, *141*, 1491.

(135) Go, M. J.; Eastman, D. S.; Artavanis-Tsakonas, S. *Development* **1998**, *125*, 2031.

(136) Garrell, J.; Modolell, J. *Cell* **1990**, *61*, 39.

(137) Cadigan, K. M.; Nusse, R. *Development* **1996**, *122*, 2801.

(138) Cadigan, K. M.; Jou, A. D.; Nusse, R. *Development* **2002**, *129*, 3393.

(139) Jafar-Nejad, H.; Acar, M.; Nolo, R.; Lacin, H.; Pan, H.; Parkhurst, S. M.; Bellon, H. J. *Genes and Dev.* **2003**, *17*, 2966.

(140) Acar, M.; Jafar-Nejad, H.; Giagtzoglou, N.; Yallampalli, S.; David, G.; He, Y.; Delidakis, C.; Bellen, H. J. *Development* **2006**, *133*, 1979.

(141) Martínez, C.; J., M. *Science* **1991**, *251*, 1485.

(142) Bhattacharya, A.; Baker, N. E. *Cell* **2011**, *147*, 881.

(143) Brown, N. L.; Paddock, S. W.; Sattler, C. A.; Cronmiller, C.; Thomas, B. J.; Carroll, S. B. *Dev. Biol.* **1996**, *179*, 65.

(144) Cagan, R. L.; Ready, D. F. *Genes Dev.* **1989a**, *3*, 1099.

(145) Baker, N. E.; Yu, S.; Han, D. *Current Biology* **1996**, *6*, 1290.

(146) zur Lage, P.; Jarman, A. P. *Development* **1999**, *126*, 3149.

(147) Sharma, P.; Chinaranangari, S.; Patel, D.; Carey, J.; Chaudhary, J. *Cancer Med.* **2012**, *1*, 176.

(148) Snyder, A. D.; Dulin-Smith, A. N.; Houston, R. H.; Durban, A. N.; Brisbin, B. J.; Oostra, T. D.; Marshall, J. T.; Kahwash, B. M.; Pierson, C. R. *Pathol. Oncol. Res. Epub.* **2013**.

(149) Chandrasekaran, V.; Beckendorf, S. K. *Development* **2003**, *130*, 4719.

(150) Muller, D.; Kugler, S. J.; Preiss, A.; Maier, D.; Nagel, A. C. *Genetics* **2005**, *171*, 1137.

(151) Affolter, M.; Nellen, D.; Nussbaumer, U.; Basler, K. *Development* **1994**, *120*, 3105.

(152) Jünger, M.; Rintelen, F.; Stocker, H.; Wasserman, J.; Végh, M.; Radimerski, T.; Greenberg, M.; Hafen, E. *J Biol.* **2003**, *2*, 20.

(153) Puig, O.; Marr, M. T.; Ruhf, M. L.; Tjian, R. *Genes & Development* **2003**, *17*, 2006.

(154) Mattila, J.; Omelyanchuk, L.; Nokkala, S. *Int. J. Dev. Biol.* **2004**, *48*, 343.

(155) Rutkowski, R.; Hofmann, K.; Gartner, A. *Cold Spring Harbor Perspectives in Biology* **2010**, *2*.